

TECHNIQUES FOR FORMING SUPERPLASTIC ALLOYS

TECHNIQUES FOR FORMING
SUPERPLASTIC ALLOYS

By

KAMAL KUMAR JAIN, B.Tech. (Hons.)

A DISSERTATION
SUBMITTED TO THE FACULTY OF GRADUATE STUDIES
IN PARTIAL FULFILMENT OF THE REQUIREMENTS
FOR THE DEGREE
MASTER OF ENGINEERING
(Production)

McMaster University

July 1972

MASTER OF ENGINEERING (1972)
(Production)

McMASTER UNIVERSITY
Hamilton, Ontario

TITLE: TECHNIQUES FOR FORMING SUPERPLASTIC ALLOYS
AUTHOR: Kamal Kumar Jain, B.Tech. (Hons.)
 (Indian Institute Of Technology, Delhi, India)
SUPERVISOR: Dr. J.L. Duncan
NUMBER OF PAGES: x , 125

SCOPE AND CONTENTS:

The field of superplasticity is reviewed, with particular reference to the mode of deformation and viability for industrial application.

Superplastic and conventional Zn-Al eutectoid alloys are compared with regard to the pressures and time required and the problems associated with the production of shaped hollow components from billet material, using extrusion followed by pressure forming.

A possible industrial process is suggested and economically assessed in a Supplement to the Dissertation.

ACKNOWLEDGEMENTS

I wish to record my indebtedness to Dr. J.L. Duncan for his assistance, guidance and above all, encouragement throughout this work.

The help extended by Dr. T.W. Watson of COMINCO Limited in providing the test material is sincerely appreciated.

Thanks are due to Mr. R.W. Young of the McMaster University Engineering Workshop and his staff for fabrication of the equipment and to Mr. A.R. Ragab for helping with the experiments.

The financial support granted by the National Research Council is gratefully acknowledged.

A final word of thanks to Mrs. Lynne Smith for typing the manuscript.

TABLE OF CONTENTS

CHAPTER		PAGE
	List of Figures	vii
	List of Symbols	ix
1	Introduction	1
1.1	Superplasticity	1
1.2	Historical Background	1
1.3	Superplastic vs conventional Metals	1
2	Conditions for Superplasticity	7
2.1	Types of superplasticity	7
2.2	Necessary criteria for micrograin superplasticity	9
2.3	Constitutive equation	14
3	Mechanism of Superplastic Deformation	17
3.1	Stress-strain rate curve	17
3.2	Proposed mechanisms	17
3.2.1	Vacancy diffusion creep model	19
3.2.2	Grain boundary sliding model	22
3.2.3	Dynamic recovery, recrystallisation and grain boundary migration model	25
4	Developing a stable ultra-fine micro- structure	28
4.1	Development of microstructure	28

4.1.1	Breakdown of grain structure	28
4.1.2	Synthesis of alloy	31
4.2	Stability of microstructure	32
5	Exploitation of superplasticity	33
5.1	Scope of application	33
5.2	Commercial alloys	34
5.3	Forming of superplastic metals	37
5.3.1	Conventional processes	37
5.3.2	Unconventional processes	40
5.4	Industrial usage of superplasticity	45
6	Scope of Present Investigation and Equipment Design and Fabrication	46
6.1	Scope of present work	46
6.2	Component size	47
6.3	Equipment design and fabrication	47
6.3.1	Backward extrusion rig	47
6.3.2	Expansion rig	56
6.3.3	Heating arrangement	61
6.3.4	Press	62
6.3.5	Auxiliary Equipment	62
6.3.6	Modifications	62
7	Extrusion Tests	63
7.1	Preparation of specimens	63
7.2	Test procedure	63

7.3	Lubricant	66
7.4	Results and discussion	69
7.4.1	Quantitative results	69
7.4.2	Qualitative aspects	76
7.5	Theoretical analysis	83
7.6	Conclusions	87
8	Macro and Micro Forming	90
8.1	Rubber plug forming	90
8.1.1	Choice of rubber	90
8.1.2	Preparation of plug	90
8.1.3	Test and results	90
8.2	Internal pressurisation	91
8.2.1	Additional equipment	91
8.2.2	Test procedure	91
8.2.3	Results and discussion	94
8.3	Conclusions	97
9	General Conclusions	98
	Supplement	99
	References	106
	Appendix I	109
	Appendix II	110
	Appendix III	111

LIST OF FIGURES

<u>NUMBER</u>		<u>PAGE</u>
1.	The effect of m on the growth of a neck in a tensile test piece	4
2.	Growth of non-uniformity with total elongation for test pieces having an initial non-uniformity of 1%	5
3.	Dependence of m on grain size, temperature, and strain rate	11
4.	Variation in flow stress with temperature for superplastic eutectoid Zn-Al alloy at a strain rate of 10^{-2} per sec.	13
5.	Zn-Al phase diagram	15
6.	Schematic log stress vs. log strain rate plot for a superplastic alloy (S) and conventional alloy (C)	18
7.	Mechanism of (a) Vacancy Diffusion (b) Grain Boundary Shear and (c) Dislocation Climb	20
8. (a)	Superplastic structure of quenched Zn-Al eutectoid.	
(b)	Lamellar microstructure of slow cooled alloy	29
9.	Stamping die made from superplastic Zn-Al	39
10.	Deep drawing of cup	39
11.	Pressure augmented deep drawing of cup	41
12.	Die-less drawing	42
13.	Vacuum formed refrigerator door inner panel	42
14.	Pressure forming of superplastic materials	44
15.	Design of backward extrusion rig	48 to 54
16.	Backward extrusion equipment assembly	57
17.	Exploded view of extrusion equipment	58

LIST OF FIGURES (cont'd)

NUMBER	PAGE
18. (a) Expansion split die segment	59
(b) Expansion die bottom	60
19. Removal of extruded cup from ram	65
20. Backward extruded cup	67
21. L to R-- (a) Cup extruded using graphite as lubricant. (b) Cup prior to modification of guide. (c) Effect of guide inclination. (d) Fully extruded cup with flash	68
22. (a) Ram travel vs. time for as cast material	70
(b) Ram travel vs. time for heat treated Zn-Al.	71
23. Microstructures of as cast and heat treated material	74
24. Microstructure of superplastic Zn-Al	77
25. Load-Velocity characteristics for	
(a) As cast material	78
(b) Heat treated material	79
(c) As cast and superplastic material	80
26. Effect of misalignment of guide	82
27. 'Deformation zone' and 'reduction' defined for backward extrusion through a conical die	86
28. Plug for sealing and application of air pressure in expansion experiments	92
29. Pressure forming equipment	93
30. Pressure formed cup-- 250 psi, 5 minutes	95
31. Rubber plug formed and other expanded specimen	96
32. Preliminary design of Production Machine	100
33. Development of shaped hollow component from billet	101

LIST OF SYMBOLS

T_m	- melting point on Absolute Scale
σ	- true stress
ϵ	- true strain
n	- strain hardening index
m	- strain rate sensitivity index
$\dot{\epsilon}$	- strain rate
L	- grain size
Q	- activation energy for superplastic deformation
V	- atomic volume
D_l	- lattice diffusion constant
D_{gb}	- grain boundary diffusion constant
σ_0	- threshold stress
\bar{m}	- true strain rate sensitivity
R.A.	- reduction in area
V_d	- drawing speed
V_c	- speed of travel of heated zone
R	- V_d/V_c
p	- extrusion pressure
$\bar{\gamma}$	- mean yield stress in uniaxial compression
$\bar{\epsilon}$	- equivalent strain
r	- reduction
v	- ram velocity
A_2	- cross section area at indenting end of punch

- V_1 - volume of material entering deformation zone/time
- V - volume of deformation zone
- t - time for material to pass through deformation zone
- $\dot{\epsilon}_{av}$ - mean strain rate
- A_0 - container area
- A_1 - orifice area

CHAPTER 1

INTRODUCTION

1.1 Superplasticity

Superplasticity is defined as the unusual ability of a metal to flow with the fluid-like characteristics of hot polymers and glasses⁽¹⁾.

This property is most dramatically exhibited in the tensile test where superplastic metals undergo very large elongations, sometimes more than 1000%, with anomalously low flow strength.

1.2 Historical Background

The phenomenon of superplasticity was first noticed by Rosenhein⁽²⁾ in 1920 who observed that the cold-rolled Zn-Cu-Al tertiary eutectic alloy 'behaved differently from ordinary crystalline materials such as Aluminium but very similarly to ---- pitch, glass, etc.' This was followed by Pearson's⁽³⁾ work and Russian work⁽⁴⁻⁶⁾ published between 1944 and 1961. Modern interest in the subject was sparked by a review by Underwood⁽⁷⁾ and a series of papers by Backofen and his co-workers^(1,8,9) who gave it a well characterized phenomenology.

1.3 Superplastic vs Conventional Metals

A ductile material, when stretched by a tensile force, can deform uniformly only while stable flow occurs. The limit of stable flow is marked by the onset of geometrical instability. Thus after a certain uniform extension, the load bearing capacity of one section of the specimen falls below that of others and deformation is concentrated in this section, ceasing elsewhere. This rapidly leads to fracture.

At temperatures below $0.3 T_m$ (melting temperature) instability occurs by the material exhausting its capacity for strain-hardening and the true strain ϵ at this point may be shown to be numerically equal to the strain hardening index n defined in the relation

$$\sigma = K\epsilon^n \quad (1)$$

where σ is the true stress and K is a constant, referred to as the strength coefficient.

n usually lies between 0.1 to 0.6 and hence normally, elongation varies from a few percent for hardened materials to 60-70% for very ductile materials like copper.

At higher temperatures ($0.5 T_m$ and above), however, materials often exhibit larger deformations than at low temperatures. The rate of strain hardening decreases, but the 'strain rate sensitivity' becomes the controlling factor in enhancing stability. Rossard⁽¹⁰⁾ has shown that a generalized relation of the form

$$\sigma = K' \epsilon^n \dot{\epsilon}^m \quad (2)$$

seems to hold where $\dot{\epsilon}$ is the strain rate, m is the strain rate sensitivity index and K' is a constant.

n is very small for high temperature processes and zero for viscous materials.

When $n = 0$, eqn. (2) reduces to

$$\sigma = K\dot{\epsilon}^m \quad (3)$$

where K is a constant.

This equation of viscous flow was first applied to superplastic behaviour by Backofen et al⁽¹⁾ and is now employed widely.

In conventional metals, even at temperatures up to $0.9 T_m$, the strain rate sensitivity 'm' is always less than 0.2. In hot polymers, depending on temperature and strain rate, 'm' values ranging from 0.3 to 1.0 are found. Superplastic materials at temperatures above $0.5 T_m$, exhibit 'm' value between 0.4 and 0.9.

This realization of high strain rate sensitivity provides an explanation for the most remarkable feature of superplastic alloys --- a large tensile elongation without local fracture.

The effect of m on the stretching behaviour is indicated in fig. 1. (11). Here two materials are considered, each exhibiting zero strain hardening but with $m = 0.1$ and $m = 0.6$, corresponding to hot working and superplasticity respectively. In a tensile bar of such materials, fig. 1 (a), necking will commence instantly though this does not imply that the total elongation will be zero. Within the neck, the stress will increase by an amount $d\sigma$ due to the difference in cross-section area at the neck. For equal differences in area, the difference in stress will be the same for both materials, but the increase in strain rate $d\dot{\epsilon}$ in the neck will be different. Figs. 1(b) and (c) show that this depends on the slope of the $\log \sigma | \log \dot{\epsilon}$ curve - that is, on m. Where m is small - as in normal hot working - $d\dot{\epsilon}$ is large, the neck develops quickly and failure occurs with very little overall elongation. In the superplastic material the increase in strain-rate in the neck is small and the specimen as a whole strains with only small variations in strain-rate along the length. The neck therefore develops very slowly and large total elongations are obtained before failure.

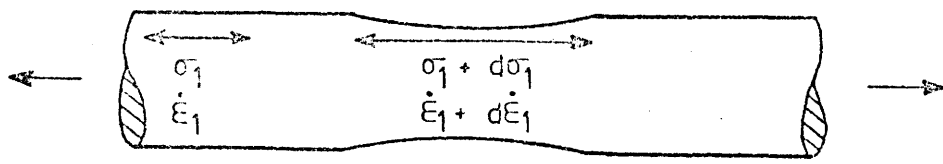


Fig 1 (a)

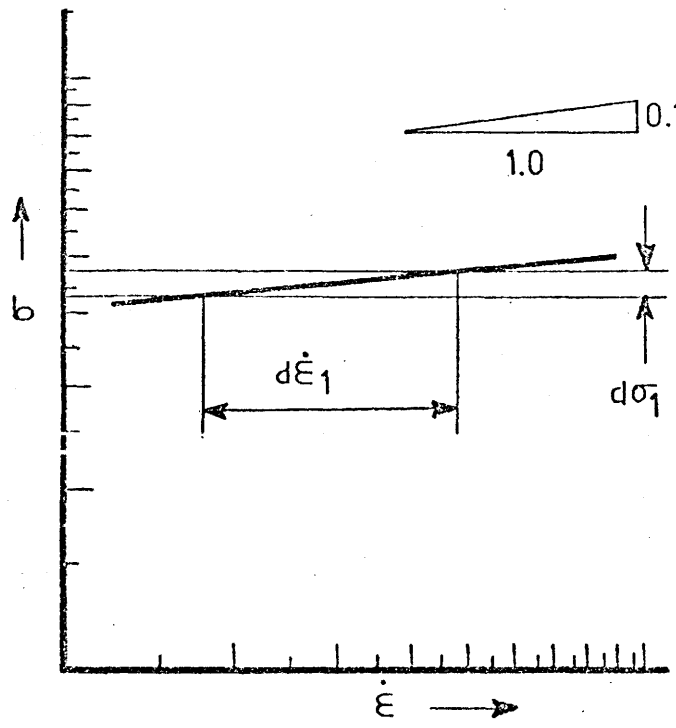


Fig. 1 (b)

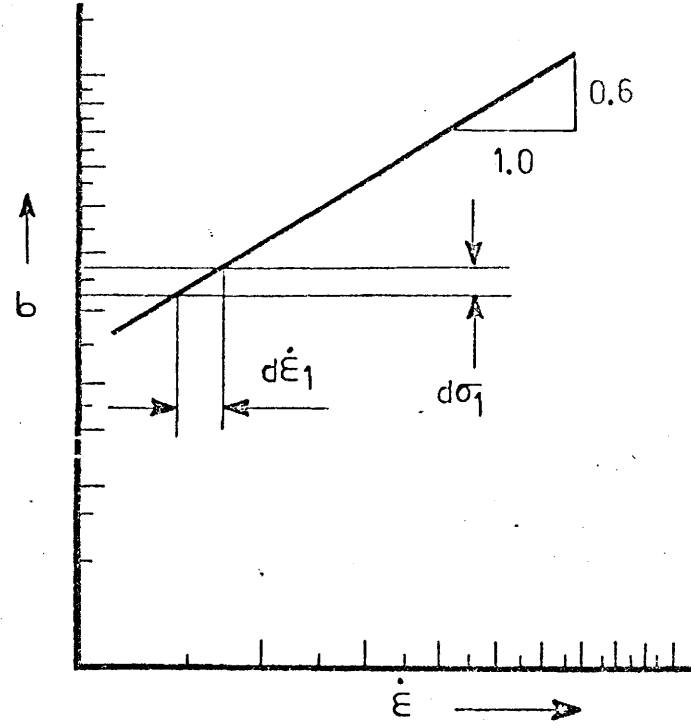


Fig. 1 (c)

Figure 1 - The effect of m on the growth of a neck in a tensile test-piece (Ref. 11).

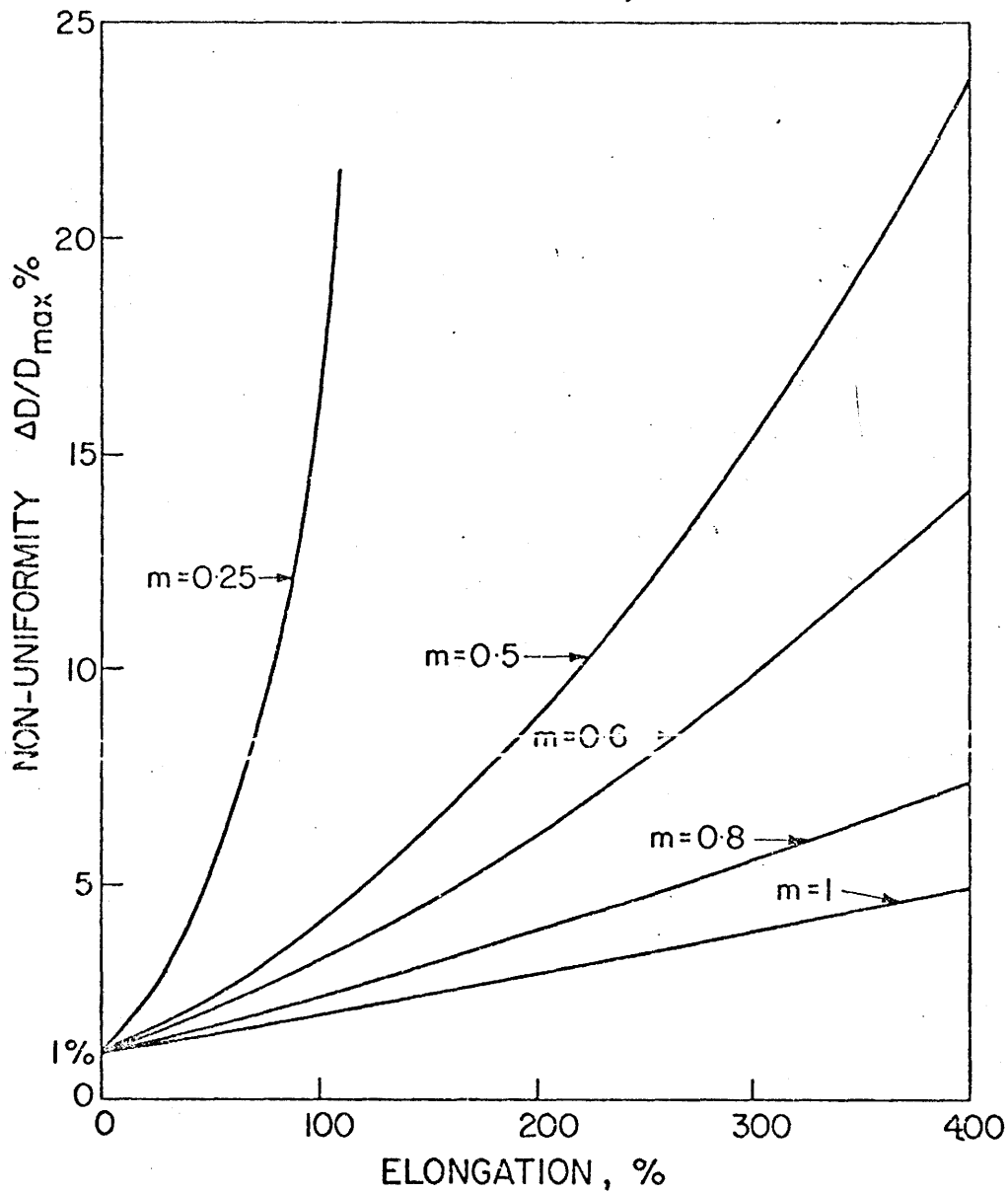


Figure 2 - Growth of non-uniformity with total elongation for test pieces having an initial nonuniformity of 1% (Ref. 12).

In all superplastic tensile processes non-uniformities similar to those in the neck in fig. 1 will develop continuously during the process, but their rate of growth depends on m . Ragab and Duncan (12) have theoretically derived the increase in non-uniformity for different values of m for tensile test pieces having an initial non-uniformity of 1% (Fig. 2).

' m ' depends on a number of factors such as strain-rate, etc.

(to be discussed in the next chapter). It is defined by the relation

$$m = \frac{\dot{\epsilon}}{\sigma} \frac{d\sigma}{d\dot{\epsilon}} \quad \left(= \frac{d(\log \sigma)}{d(\log \dot{\epsilon})} \right) \quad (4)$$

CHAPTER 2

CONDITIONS FOR SUPERPLASTICITY

2.1 Types of Superplasticity

Superplastic behaviour can broadly be divided into two types:

a) Environmental Superplasticity

Thermal cycling of a material about an allotropic phase transformation temperature, neutron irradiation or temperature cycling of a thermally anisotropic material makes some materials 'spontaneously plastic' by generating intergranular stresses. When a small external stress is applied to a material in this condition it behaves superplastically^(13,14).

This is called environmental or phase change superplasticity and a number of steels have been shown to exhibit this behaviour. Large extensions (>500%) have been produced in several plain carbon steels by repeating the ferrite/austenite transformation⁽¹³⁾.

b) Micrograin Superplasticity

The second type, known as 'Micrograin' or 'Isothermal' superplasticity is associated with alloys in which the structure has been broken down to an aggregate of small (<10 microns) equiaxed grains stable at temperatures above half the absolute melting point. Deformation is at a constant temperature above $0.5 T_m$ and the microstructure remains basically unaltered during the process.

A list of some typical superplastic materials is given in Table 1⁽¹⁵⁾.

Industrially, micrograin superplasticity is much more important

TABLE 1 Superplastic Alloys

Base Metal	Alloy wt%	Temp. °C	Grain size (microns = 10 ⁻⁶ metres)	"m"
Aluminum	33 Cu	440-530	1-2	0.9
	12 Si 4 Cu	500	-	0.4
Cadmium	26 Zn	20	1-2	0.5
Chromium	27.5 Co	1200	-	-
Cobalt	10 Al	1200	0.4	0.3
Copper	10 Mg	700	-	-
	10-12 Al	500 - 700	3	0.6
	10 Al 1-4 Fe	800	10	0.8
	38-50 Zn	450 - 550	3	0.5
	40 Zn	600	3	0.7
	38 Zn Ti	600	5	0.7
	38 Zn 2 Fe	600	-	-
	2.8 Al 1.8 Si	550	1	0.4
	0.4 Co			
Iron	0.14 C 1.2 Mn	900	2	0.6
	0.1 V			
	0.34 C 0.47 Mn	900	2	0.5
	2.8 Al			
	0.42 C 1.9 Mn	730	1-2	0.6
	26 Cr 6.5 Ni) 30 Cr 6.0 Ni)	870 - 980	2	0.5
Lead	20 Sn	20	3	0.5
	5 Cd	0-100	1-10	0.6
Magnesium	0.5 Zr	500	20	0.3
	6 Zn 0.6 Zr	270 - 310	0.5	0.5
	23 Ni	450	-	-
	30 Cu	450	-	-
	33 Al	400	-	-
Nickel	nil	820	8	-
	39 Cr 8 Fe 2 Ti	980	2	0.5
Tin	5 Bi	20	1	0.5
	2-38 Pb	20	1-2	0.5
	33 Cd	20	1-2	0.5
Titanium	6 Al 4V	900 - 980	6	0.9
	5 Al 2.5 Sn	1000	18	0.7
Zinc	nil	0-20	1-2	-
	0.5 Al	20	1-2	-
	5 Al	200 - 360	1-2	0.7
	22 Al	200 - 260	1-2	0.5
	40 Al	250	1-10	0.5
Zirconium	-	900	12	0.5

than the phase change type because of the obvious inconvenience involved in applying temperature cycling to the material.

2.2 Necessary Criteria for Micrograin Superplasticity

A number of criteria have to be satisfied if superplasticity is to occur:

a) Small, Equiaxed grains

The microstructure of the material must consist of extremely fine equiaxed grains (or a microduplex structure) which remains stable at the temperature of deformation. Thus grain size and shape are important structural parameters. At constant strain rate and temperature,

$$\sigma \propto L^b \quad (5)$$

where L is the grain size, taken to be the metallographic mean free path. The value of the exponent b is not very well agreed upon in literature and has been reported as lying between 0.7 to 1.2^(16,17).

The strain rate corresponding to a given flow stress and temperature has been shown to vary with grain size as:

$$\dot{\epsilon} \propto 1/L^a \quad (6)$$

Again, the exponent a has been given as 2 and also as 3. Packer and Sherby⁽¹⁶⁾ have suggested that a can only be considered to lie within the above limits.

These relations are quite different from those governing the deformation of conventional metals which follow the Petch relation⁽¹⁸⁾

$$\sigma \propto \frac{1}{\sqrt{L}} \quad (7)$$

which implies that plastic strength is increased as grain size becomes smaller.

b) High Strain Rate Sensitivity

As mentioned earlier, the strain rate sensitivity (SRS) has to be high for superplasticity to occur. The SRS, m , is primarily a function of strain rate, grain size and the temperature of deformation. A large enough m for substantial necking resistance can be expected only when the strain rate is in the range of 10^{-4} to 10^{-1} sec^{-1} , T/T_m is above 0.5 and L is not much more than 5 microns ⁽¹⁹⁾. In general, m increases with decreasing grain size on increasing temperature but goes through a maximum with increasing strain rate. (fig. 3).

c) Low Strain Rate

Full benefits of superplastic behaviour are obtained only at strain rates in the range of 10^{-4} sec^{-1} to 10^{-1} sec^{-1} which are rather low as compared to normal metal working processes. Table 2 gives a comparison of superplastic strain rates with those achieved in other processes.

d) Temperature above $0.5 T_m$

Superplastic deformation occurs at temperatures above half the absolute melting point.

The flow stress would normally decrease with increasing temperature unless some intrinsic transformation occurs to inhibit superplasticity. The superplastic zinc-aluminium eutectoid alloy for instance, shows a marked decrease in flow stress as temperature rises till about 260°C after which it starts increasing (fig 4)⁽²⁰⁾. As may be seen from

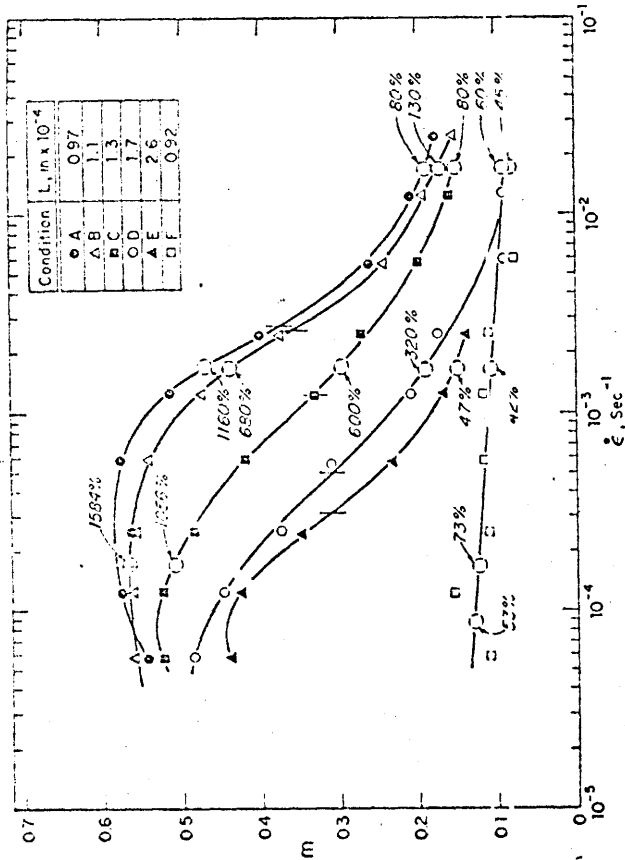


Figure 3 (a) - The dependence of strain-rate sensitivity on strain rate of lead-tin eutectic specimens with different grain size, L . (Ref. 9).

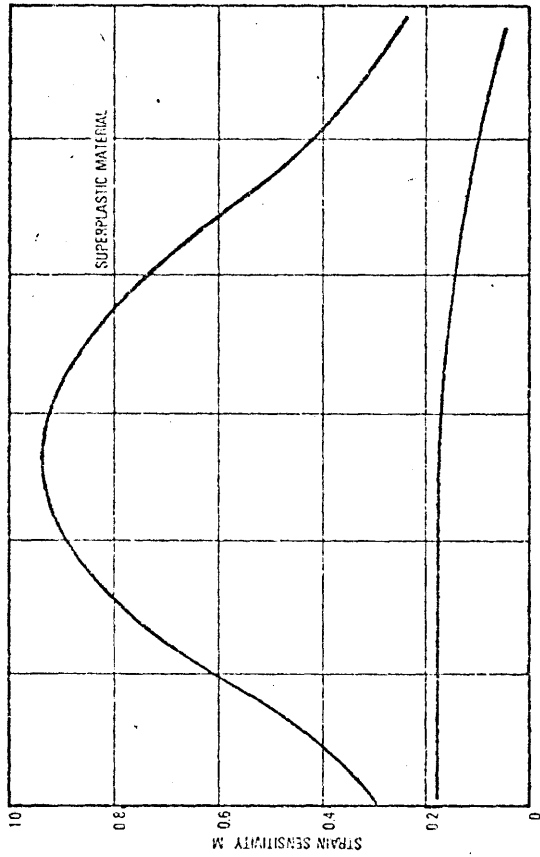


Figure 3 (c) - Schematic variation of m with strain rate.

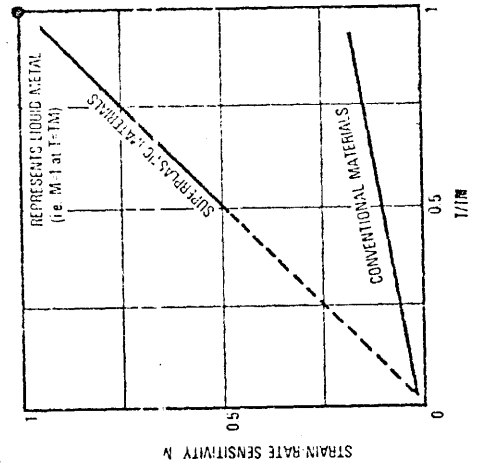


Figure 3 (b) - Schematic variation of m with temperature.

Figure 3 - Dependence of m on grain size, temperature and strain rate.

TABLE 2

Strain Rates in Metalworking Processes

PROCESS	STRAIN RATE (per sec.)
Superplastic deformation	10^{-4} to 10^{-1}
Creep	10^{-10} to 10^{-5}
Normal hotworking processes	1 to 10^2
Machining (cutting speed 80 ft/sec.)	10^4
Explosive forming	10 to 10^2
Explosive welding	10^5

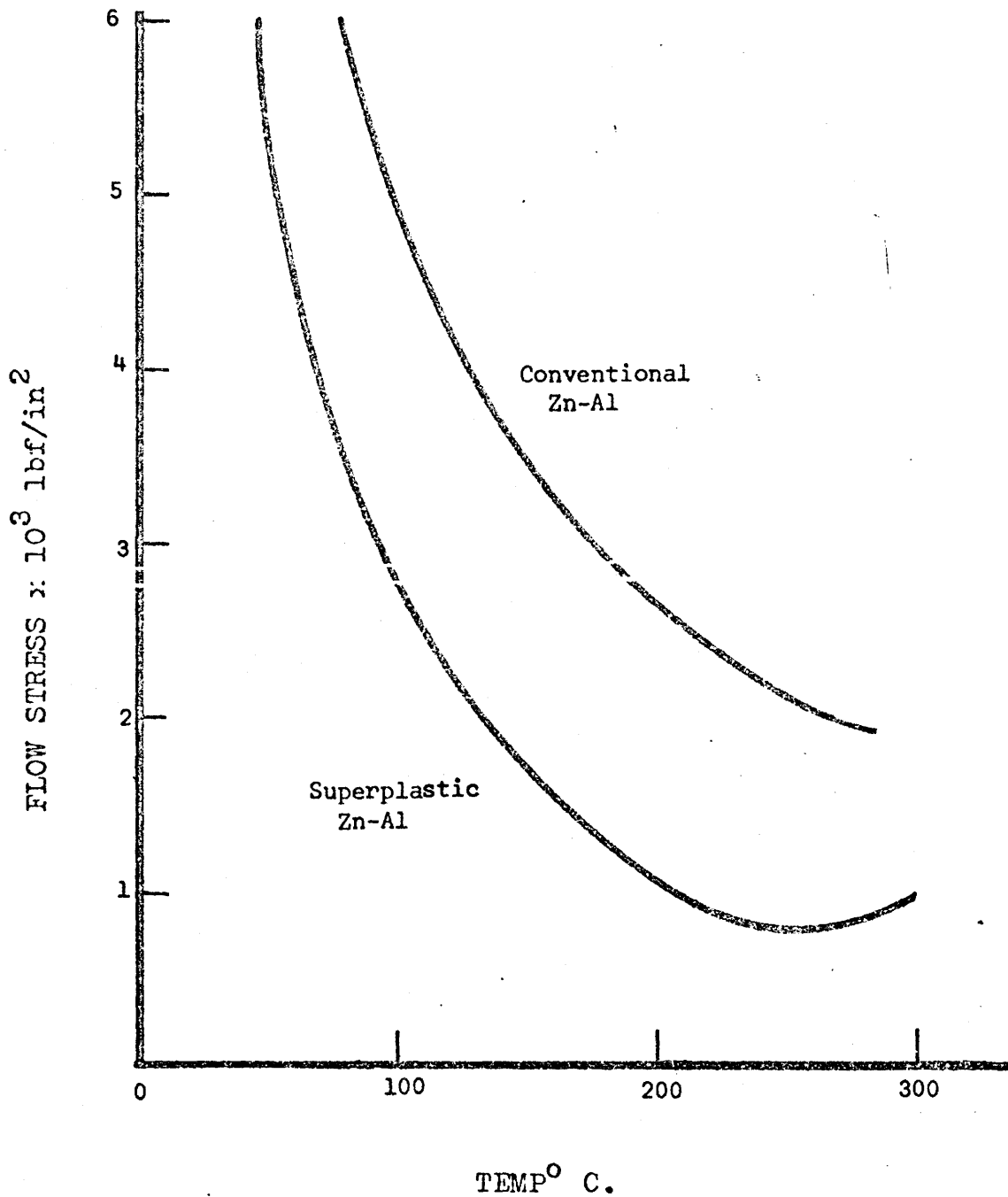


Figure 4 - Variation in flow stress with temperature for superplastic eutectoid Zn-Al alloy at a strain rate of $10^{-2}/\text{sec}$. (After Ref. 20).

the Zn-Al phase diagram (fig. 5), 275°C is the eutectoid temperature above which the two phase alloy transforms into a single phase system.

e) Appropriate Constituent Phase Properties

While single phase materials also show superplastic properties, those exhibiting increased stability and optimum extensibility are more commonly multiphased. It appears that the phases should have approximately the same ductility and be present in nearly equal proportions by volume. Many superplastic materials are therefore based on eutectic or eutectoid systems between phases having similar melting temperatures (22). Also, there is some indication that the diffusion rates in both phases of a duplex alloy should be similar at the temperature of deformation if superplasticity is to occur. For instance, while the Zinc-Aluminium eutectoid alloy can be made superplastic, the aluminium-silicon eutectic cannot (23).

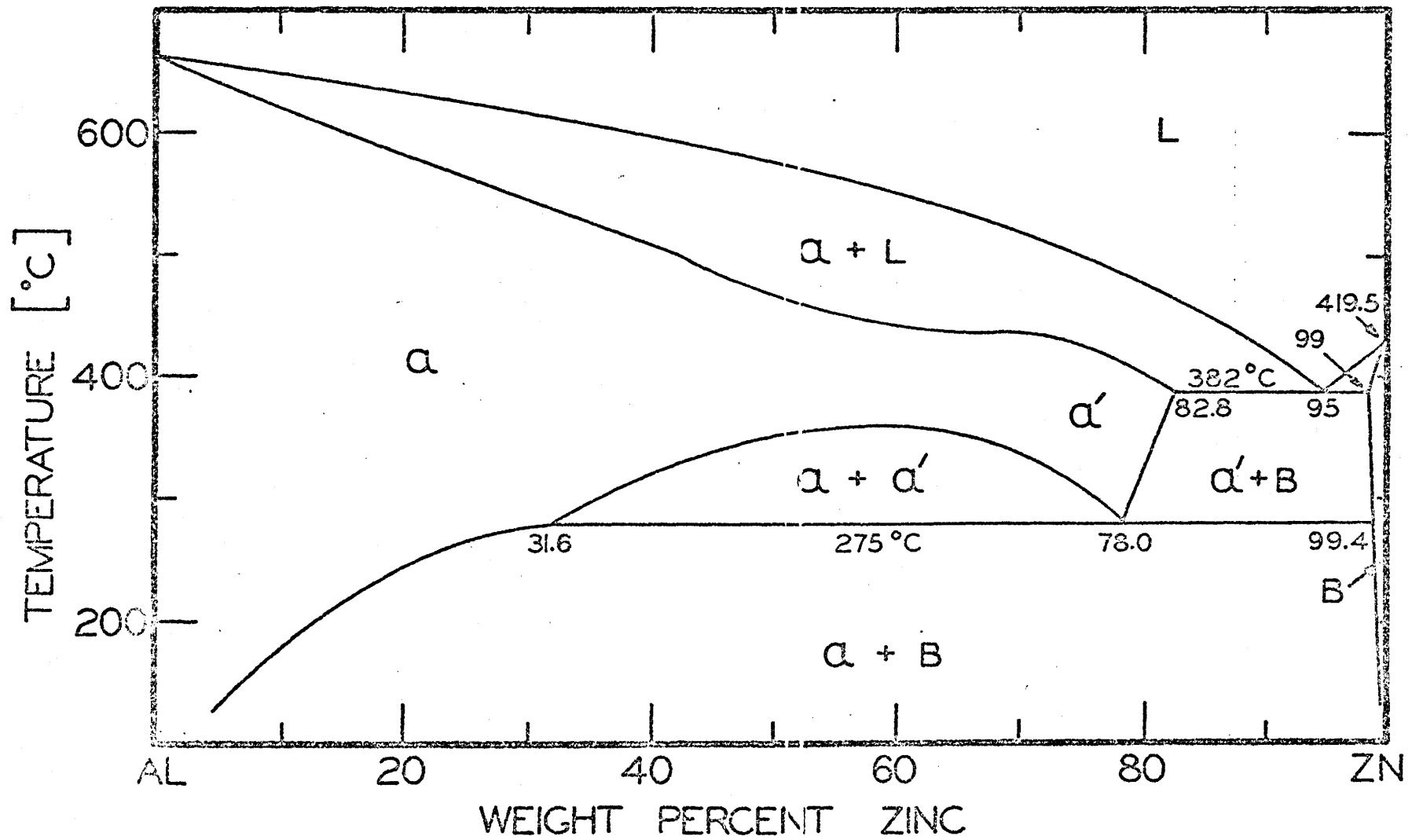
2.3 Constitutive Equation

In alloys satisfying the above criteria, it has been found experimentally that an activation energy Q for the deformation process may be found from the relation

$$\dot{\epsilon}_{\sigma,L} \propto \exp\left(\frac{-Q}{kT}\right) \quad (8)$$

where k is the Boltzmann constant. For the Zinc-Aluminium eutectoid alloy the activation energy is about 14.5 K cal/mole, which is of the same order of magnitude as the activation energy for grain boundary diffusion.

Combining equations 5, 6 and 8, the general dependence of strain rate during superplastic deformation on stress level, grain size and temperature may be expressed as



ALUMINUM - ZINC PHASE DIAGRAM.

$$\dot{\epsilon} = \text{constant} \cdot \frac{\sigma^n}{L^a} \exp\left(\frac{-Q}{kT}\right) \quad (9)$$

where $n = a/b$ and lies in the range of 1.6 to 4.2; $n \approx \frac{1}{m}$, the strain rate sensitivity index.

CHAPTER 3

MECHANISM OF SUPERPLASTIC DEFORMATION

3.1 Stress-Strain Rate Curve

Most superplastic materials exhibit a sigmoidal stress/strain rate curve in a logarithmic diagram, (fig. 6). The region of maximum strain rate sensitivity (Region II) with slope >0.3 delineates the superplastic region. Both regions I and III exhibit values of $m \sim 0.1 - 0.2$ and correspond to conventional plasticity and creep.

Many alloy systems, eg. lead-tin⁽⁹⁾, Aluminium-copper⁽⁸⁾, etc. show all three regions. In contrast, some materials, eg. zinc-aluminium only show regions II and III.

3.2 Proposed Mechanisms

Any deformation mechanism proposed for the superplastic region II must also account for the low values of m in region I and II.

The important experimental observations are:

- a) equiaxed grains and absence of defect substructures in region I and lower end of region II, and
- b) elongated grains, grain boundary sliding, dislocation tangles and cell formation in the high strain rate region⁽¹⁵⁾.

A number of mechanisms have been proposed but only three of them provide an explanation of all three regions of the stress-strain curve.

- (a) diffusional creep model^(9,19,25)
- (b) grain boundary sliding model^(8,26,27,28)
- (c) dynamic recrystallisation model⁽²⁹⁾

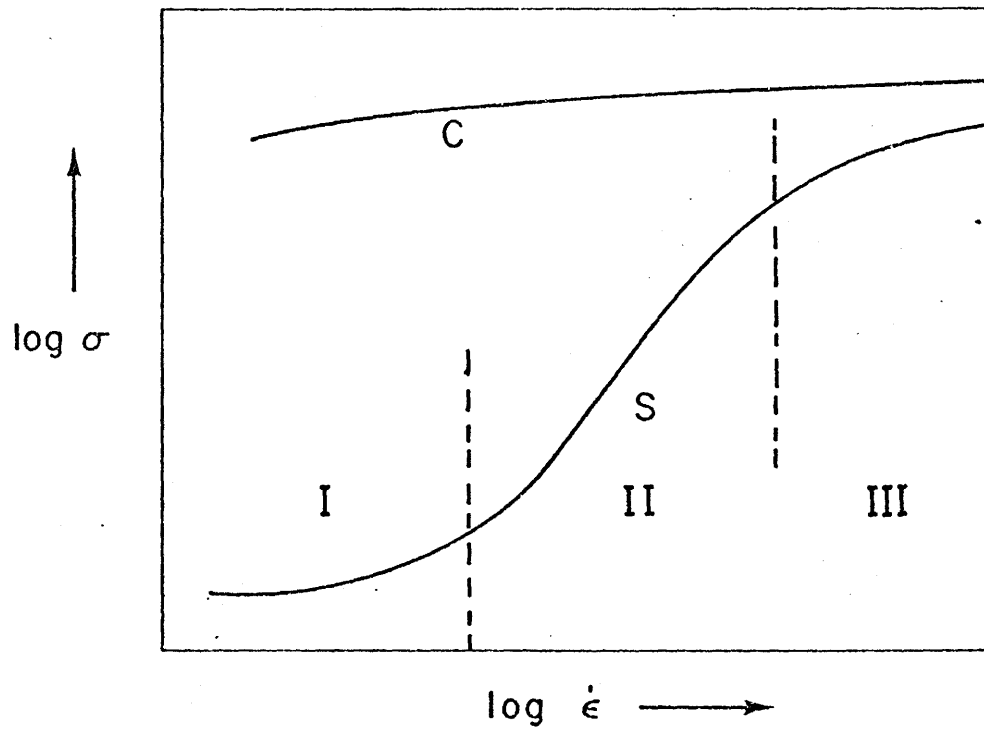


Figure 6 - Schematic log stress vs. log strain-rate plot for a superplastic alloy (S) and conventional alloy (C).

Which of the above mechanisms is the dominant one in a particular condition is not, however, very clear. It is conceivable that different materials may be following different deformation modes, or that more than one mechanism might be operating simultaneously or at different stages of deformation.

Each of these are discussed below.

3.2.1 Vacancy Diffusion Creep Model

Fig 7(a) shows the mechanism of vacancy diffusion creep. Under an applied tensile stress, the upper and lower grain boundary facets experience a tensile stress which aids formation of vacancies. The grain boundary facets on the side experience a compressive stress, resulting in a vacancy concentration level below the equilibrium value. As a result, there is a movement of vacancies from the top and bottom facets to the sides and atom migration in the opposite direction.

Vacancy migration, either through the lattice (Nabarro-Herring Creep) or along the grain boundaries (Coble Creep) have been suggested as the rate controlling mechanisms for superplastic behaviour because in each case the theoretical strain rate dependence on stress and grain size shows some similarity with that observed in superplastic deformation.

The creep relations governing the rates of deformation are as follows: (30,31)

$$\text{N-H Creep : } \dot{\epsilon} = (B_1 | L^2) (V\sigma/RT) D_l \quad (10)$$

$$\text{Coble Creep: } \dot{\epsilon} = (B_2 | L^3) (V\sigma/RT) D_{gb} \quad (11)$$

where B_1 and B_2 are constants, L the grain size, V the atomic volume and D_l and D_{gb} are the lattice and grain boundary diffusion constants

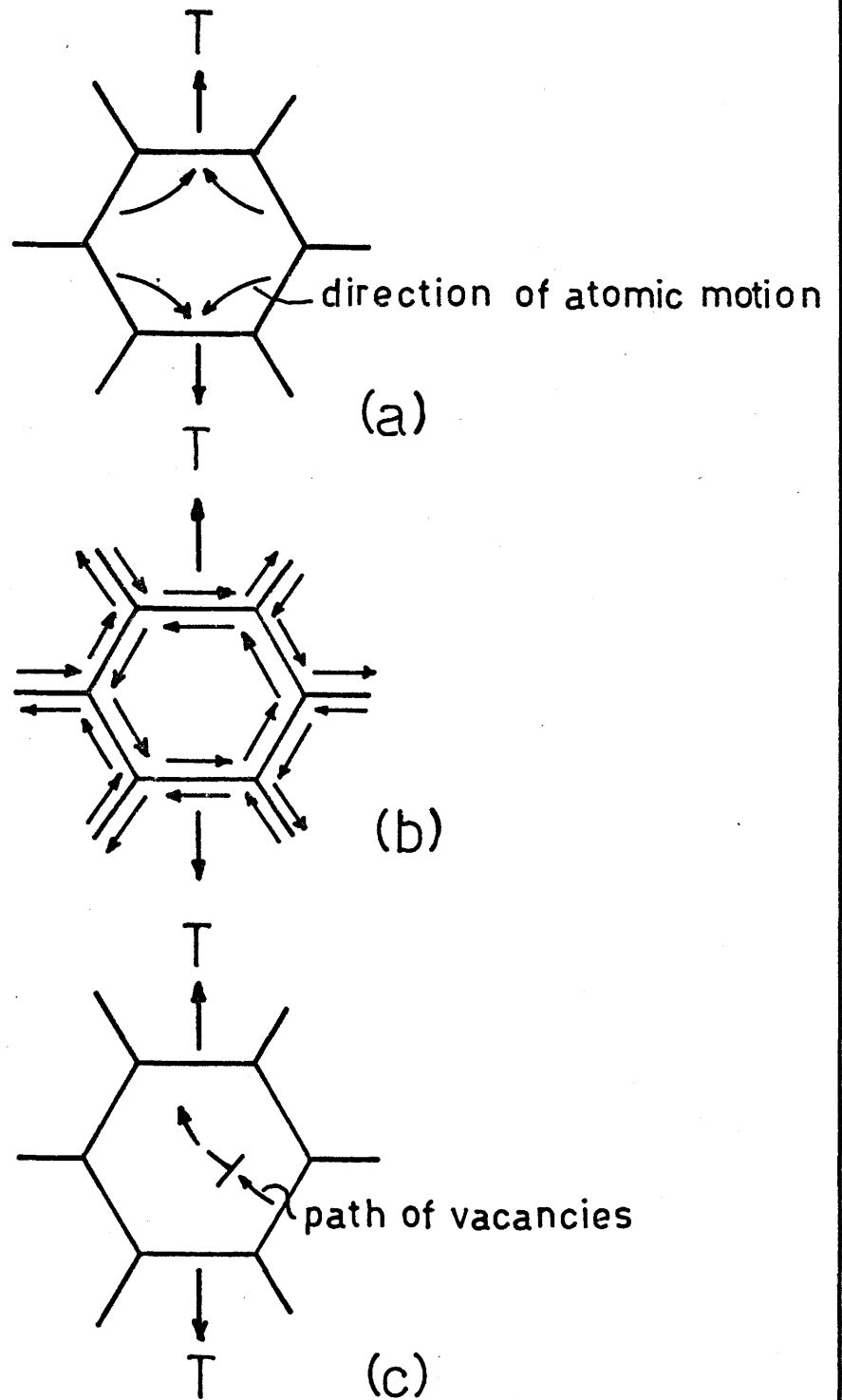


Figure 7 - (a) Mechanism of Vacancy Diffusion. (b) Grain Boundary Shear Mechanism. (c) Mechanism of Dislocation Climb.

respectively.

These relations predict a strain rate sensitivity of 1. However, it is well known that superplastic flow is non-Newtonian and that m passes through a maximum value with strain rate.

Further, both lattice and grain boundary diffusion predict the formation of elongated grains, which is in conflict with experimental observation except at high strain rates.

It has since been suggested by Backofen et al⁽²⁵⁾ that the behaviour of superplastic alloys is more like that of a Bingham solid, with a 'threshold' or 'creep yield' stress of σ_0 below which the strain rate is zero. This would modify the stress-strain relation to

$$\sigma = \sigma_0 + K \dot{\epsilon}^m \quad (12)$$

where σ_0 has been included to account for the low strain rate sensitivity of Region I.

Karim⁽³²⁾ adds that the genuine rate sensitivity should be defined as

$$\bar{m} = \frac{\sigma}{\sigma - \sigma_0} m \quad (13)$$

$m \rightarrow 1$ only when $\sigma_0 \mid \sigma \rightarrow 0$ but long before that the imposed stress would become so high that the other non-Newtonian processes (like the non-conservative motion of dislocations) will take over and m will start falling. The value of m , however, is always unity so long as diffusion is significant.

Ashby⁽³³⁾ has shown that grain boundaries act as perfect vacancy sources and sinks (as required for N-H or Coble creep) only if the

dislocation-like line defects in them are free to climb. If these become pinned by precipitates on or near grain boundaries, they can no longer be perfect sources or sinks. This supports the theory that there is a 'threshold stress' σ_0 required to initiate climb and hence diffusion creep in superplastic materials.

Further research into the existence and nature of σ_0 is likely. Recently Burton⁽³⁴⁾ has measured a 'creep yield stress' in the eutectic Pb-Sn alloy by replotting the low strain rate region of the $\log \sigma$ vs $\log \dot{\epsilon}$ curve on a linear scale and measuring the stress at zero strain rate as the intercept on the stress axis. He found σ_0 to be 270 lbf/in².

Karim and Backofen⁽³⁵⁾ have very recently given 'direct evidence' for existence of diffusional flow in superplastic deformation in the form of denuded (ie. precipitate free) zones along grain boundaries subjected to the algebraically largest normal stress and in the form of solute profiles across these zones which show them to consist only of the diffusing species.

However, Lee⁽³⁶⁾ has pointed out that denuded zones could well arise from grain boundary migration, and not necessarily only from diffusive creep. He has also reported⁽²⁶⁾ the observation of extensive grain rotation at the intermediate strain rates where m is a maximum. This is not compatible with the diffusion creep model. Secondly the strain across transverse grain boundaries is not maximum at these strain rates as might be expected from the diffusion creep model.

3.2.2 Grain Boundary Sliding Model

Grain boundary sliding (GBS) is the relative movement of adjacent

grains by a shear translation along their common interface (fig. 7b)

The fact that the grains remain unchanged in shape after deformation in most SP materials has led a number of workers^(8,26,27) to suggest that grain boundary sliding is the chief mechanism in superplastic flow, with diffusion creep, grain boundary migration or dislocation motion by glide/climb acting as accomodation processes.

A large amount of evidence has been presented in favour of grain boundary shear. Alden⁽²⁷⁾, for instance, in his experiments on Sn-Bi eutectic superplastic alloy, has shown that scratches remaining from metallographic polishing are offset at grain boundaries and remain relatively straight within each grain. A few percent strain was found enough to transform an initially polished surface into one with an intense granular appearance. Further, the grains remained equiaxed after deformation. All these phenomena are a well-documented part of the process of high temperature creep, which is believed to be greatly facilitated by grain boundary sliding.

Under conditions of pure grain boundary sliding in small grain size systems, the rate of straining would be given by⁽³⁷⁾:

$$\dot{\epsilon} = B_3 \frac{\sigma V}{kT} D_l \quad (14)$$

where B_3 is a constant.

However, even the most avid exponents of the grain boundary shear model agree that such an ideal situation is not possible as sliding cannot occur continuously on all boundaries without some accompanying deformation within the grains themselves. Without this added deformation mode the polycrystalline aggregate as a whole cannot be plastically

deformed to any appreciable degree without porosity⁽²⁶⁾ which has generally been found to be absent in superplastic elongation (except in some copper based alloys).

GBS by itself would lead to a low strain rate sensitivity because grain boundaries are not smooth, and after some shear, sliding may be obstructed where ledges and such obstacles along the boundary interlock. There is additional interference at triple junctions.

Thus, for highly strain rate sensitive boundary shear to occur, resistance to sliding must be lowered by smoothening out the ledges and making the stress concentration triple junctions mobile.

Nevertheless, it is argued that at least 60-70% of the total elongation is accounted for by grain boundary sliding.

Lee⁽²⁶⁾ has proposed that at low strain rates at least 50% of the deformation occurs by GBS, whereas either GBS or diffusion creep could account for the rest. In the intermediate strain rate, where m is maximum, accommodation is achieved by grain deformation and recovery. Grain rotation is one means of relieving localised stresses, distributing the stress uniformly throughout the grain. The migration of grain boundaries followed by GBS is another means of eliminating stress concentrations.

Holt and Backofen⁽⁸⁾ also suggest that recrystallisation and dynamic recovery are the accommodation modes. Grain boundary migration, which is enhanced by shearing, helps in eliminating the mechanical barriers. Recrystallisation rate also increases with strain rate. These explanations could well account for the higher value of m at higher strain rates.

Dunlop and Taplin⁽³⁸⁾ have postulated that at low strain rates accommodation is by vacancy diffusion while at high strain rates the glide/climb movement of dislocations acts in parallel with GBS. They have presented evidence from thin foil electron microscopy that dislocation movement does take place at high strain rates.

Backofen and associates^(19,25,39) have proposed a 'dashpot model' in which both Newtonian diffusion creep and non-Newtonian grain boundary shear contribute to the deformation. At low strain rates grain boundary shear might be the rate controlling mechanism whereas diffusion creep could be rate-controlling under conditions of maximum m . They conclude that the elongated grains created by diffusional creep experience a shape relaxation during straining, through direct grain boundary migration and recrystallisation, and thus tend to revert to equiaxed.

3.2.3 Dynamic Recovery, Recrystallisation and Grain Boundary Migration Model

It has generally been observed that after deformation, the superplastic material is essentially in a fully recovered state. The dislocation density is low, there is little work hardening and dislocation tangles and cells are not formed, except in the higher strain rate region. This has led to the idea that processes of dynamic recovery or recrystallisation could be rate controlling mechanisms.

Dislocation climb (fig 7(c)) is one of the processes of recovery during both creep and hot forming. In deformation of coarse-grained materials dislocations usually become entangled, forming dislocation cells or sub-grains in the stable sub-structure. These dislocation cells

are regions of relatively perfect crystal bounded by a wall of tangled dislocations. Flow in such a case is controlled by dislocation climb and the non-conservative motion of jogs in screw dislocations. Theory predicts a value of 0.2 for m , well substantiated by experiments. Ball and Hutchinson⁽⁴⁰⁾ propose that because of the microfine grains in superplastic materials, the stable subgrain size is larger than the actual grain size. In such a case, dislocations can move within the grains (as there are no subcells in the grains to block dislocation movement) and climb into the grain boundary with the aid of vacancies supplied by grain boundary diffusion. This model, however, does not satisfactorily account for the distinct stages of the stress-strain curve.

Packer, Johnson and Sherby⁽²⁹⁾ have suggested a model involving slip and continuous recovery by grain boundary migration or recrystallisation.

Dynamic recrystallisation is regarded as the operative softening mechanism in metals at large strains during hot working. It has also been observed in creep at high stresses. Grain boundary migration or subgrain coalescence are perhaps responsible for the formation of recrystallised grains. Dynamic recrystallisation is initiated at regions of high local lattice strain.

It has been observed that round tensile specimens of zinc-aluminium superplastic material become elliptical after deformation. It is proposed that this is consistent with basal slip in the zinc matrix. The lack of change in grain shape after deformation suggests that recrystallisation or grain boundary migration is required to continuously regenerate the morphology.

The type of recrystallisation envisaged for superplasticity is different from that responsible for high ductilities in hot working. It is suggested that in superplastic materials, crystallographic slip in the matrix phase is accompanied by grain boundary shearing and both processes are complementary in leading to distortion of the lattice in the vicinity of the grain boundary where a recrystallisation process could be initiated. It is more likely that the original grain boundary migrates rather than a new boundary being created and migrating. The necessary movement of boundaries to recreate regions capable of further slip is then largely controlled by the abundant pinning points provided by the second phase.

To explain the regions of the stress-strain curve, it is suggested that the recovery properties of the matrix are dependent on stress and may be related to the observed changes in metallographic structure in each range.

Nevertheless, clear experimental evidence for the occurrence of dynamic recrystallisation is lacking. Further, the periodic cycles of flow stress observed in dynamic recrystallisation during hot working have not been observed in superplastic deformation.

3.2.4 Summary

This brief account of the various mechanisms proposed gives an idea of the existing confusion in this field. Much more work is required to gain complete understanding of what actually happens inside the material during superplastic deformation.

CHAPTER 4

DEVELOPING A STABLE ULTRA-FINE MICROSTRUCTURE

4.1 Development of Micro-Structure

The ultra-fine grain size required for superplasticity may be achieved either by breakdown of the normal coarse-grained structure or by synthesis of the alloy from its basic constituents.

4.1.1 Breakdown of Grain Structure

The existing structure of the alloy may be broken down by thermo-mechanical processing. This includes one or more of the processes of hot-working, cold-working, recrystallisation, precipitation, etc.

Three different alloys, the Zinc-Aluminium Eutectoid, the Lead-Tin Eutectic and the Nickel-Chromium-Iron system are considered below to demonstrate the various thermo-mechanical processes used.

(i) Zn-Al

The Zn-22Al eutectoid alloy is made superplastic by solution treating it at about 320°C and then quenching at 0°C.

Phase transformation in the solid state is an important phenomenon in Zn-Al alloys. The phase diagram (fig. 5) shows that when the eutectoid alloy is heated above 275°C, the invariant temperature, it is transformed from a two phase mixture to a single solid phase. If this heated alloy is suddenly cooled to 0°C it results in a supercooled, unstable solid solution which, when brought up to room temperature, decomposes into two phases with the required microduplex structure (fig 8(a)).

The same alloy, however, if cooled slowly from the invariant,

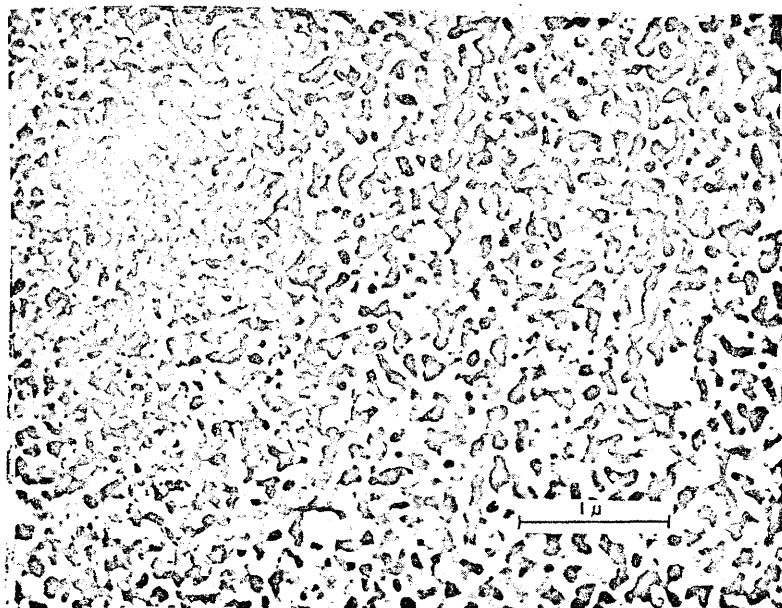


Figure 8 (a)
Superplastic structure of quenched Zn-Al eutectoid.
(Ref. 24).



Figure 8 (b)
Lamellar microstructure of slow cooled alloy

yields a typical lamellar eutectoid structure (fig. 8(b)).

A possible interpretation of these effects may be made in terms of the process of spinodal decomposition⁽²⁴⁾. The eutectoid alloy has a spinodal temperature in the range of 0°C - 100°C. The slow-cooled alloy would thus decompose by the normal eutectoid decomposition processes of cellular growth whereas in the quenched alloy, the supercooled single phase would be prevented from decomposing by this process by the prior spinodal decomposition.

(ii) Pb-Sn

The lead-tin phase diagram⁽²¹⁾ shows that the eutectic alloy consists of two solid phases at all temperatures below the eutectic temperature. This alloy can be given a micro duplex structure by drastic extrusion, which has the effect of reducing the cross-sectional area of the grains. As a grain is squeezed, its length is initially increased to maintain constant volume and then the energy put into the system by extrusion is dissipated to a large extent by recrystallisation. Recrystallisation breaks up the individual long, narrow and heavily strained grains into several short strain-free ones.

(iii) Ni-Cr-Fe

These alloys fall in the class where superplasticity may be introduced by an appropriate combination of working and heating and cooling.

The phase diagram for this system indicates that some mixtures of these metals will have a single phase equilibrium structure when heated to quite high temperatures (1200-1300°C). At lower temperatures

(from room temperature to about 1,100°C) the equilibrium structure consists of two phases.

The material is heated into the single phase region and then hot worked by rolling or forging. Hot working is continued till the temperature of the workpiece decreases well into the two phase region.

During deformation and cooling, there is simultaneous occurrence of recrystallisation and precipitation. Recrystallisation helps form smaller grains. Precipitation consists of a second phase forming from within a primary phase. The second phase preferentially precipitates at the grain boundaries of the fine grained primary phase, and by its very presence, retards the process of grain growth.

These are only a few of the various processes used to break the structure into microfine grains. In general, the processing steps have to be adapted to any given alloy system.

4.1.2 Synthesis of Alloy

Backofen and others^(25,41) have produced 'artificial' fine-grained Sn-Pb alloys by pack rolling of alternate sheets of tin and lead as also by alternate electroplating of the two metals - with good superplastic properties in both cases. The standard commercial alloy Mg-6% Zn-0.6% Zr was made superplastic by extrusion of fine grained pellets.

These synthetic methods open up many interesting possibilities. Alloys can be made from specific proportions of immiscible or nearly immiscible phases designed for maximum grain size stability at the optimum temperature without regard for the limitations imposed by the relevant phase diagram. Considerable advantages might accrue from the

use of 4,-5-or even 6 component phase systems rather than the conventional binary phase systems⁽⁴²⁾.

4.2 Stability of Microstructure

The stability of the fine grained structure in superplastic alloys at high temperatures in comparison with conventional metals arises from the fact that eutectic solidification or eutectoid decomposition leads to the production of a mechanical mixture of two phases, one rich in one element and the other rich in the second. Grain growth would then require massive solute transport over distances of the order of the grain size rather than the normal migration of a grain boundary by atom movement across it⁽²⁴⁾. Thus one phase effectively pins the grain boundaries of the other, inhibiting grain growth.

CHAPTER 5

EXPLOITATION OF SUPERPLASTICITY

5.1 Scope of Application

The behaviour of materials in the superplastic state is more like that of plastics than metals. Superplasticity occurs only under special conditions - which implies that this property may be "switched on and off" at will. It thus offers designers a new class of materials which form like plastics but perform like metals and opens up interesting scope for innovation in the metalworking field.

It has often been argued that strain rates in superplastic metals are low and such elongations as 2000% are far in excess of normal requirements. However, these materials, even under practical straining rates, will often possess a level of ductility which is significantly greater than that obtainable in the non-superplastic condition .

Moreover, in the aircraft industry and other advanced areas of manufacturing, there is an increasing requirement for normally difficult to form metals. A good example is the titanium alloys presently being introduced in supersonic aircraft. For such projects, the slow rate characteristic of superplasticity is not a factor limiting its application provided it replaces otherwise complex and expensive fabrication techniques.

Furthermore, if suitable techniques could be perfected to synthesize superplastic alloys from their basic constituents, the grain size could be reduced still further. As the strain rate is inversely proportional to the square or cube of the grain diameter (Eqⁿ 6), a smaller

grain would enable us to use far larger straining rates, reducing work loads at rates typically used in rolling, extrusion, etc.

Only 20% of all metals are cast directly to shape, the remainder requiring some working operation to obtain the final shape. It is estimated that more than half the capital in the manufacturing industry is associated with the tools for working materials.^(43,44) So unless circumstances justify high unit costs large production runs are required. With superplastic materials, because of their ability to flow readily under low stresses, lighter and less expensive machinery can be used and the material is attractive for short production runs.

If the superplastic temperature for an alloy is low and service temperatures are likely to be high, a grain-coarsening treatment may have to be applied after processing to ensure that superplasticity does not return during use. In the case of zinc-aluminium this may be done simply by heating the formed part above the eutectoid temperature and cooling it in air. However, in case of high melting point materials - such as alloys of copper, iron, titanium - the service temperatures are well below the superplasticity range, and the fine grained structure remaining after deformation can be retained to provide excellent mechanical properties in the finished product. The small grain size is also advantageous in that it leads to the production of very smooth surfaces ideal for polishing or plating.

5.2 Commercial Alloys

(a) Zn-22Al

The eutectoid zinc-aluminium alloy is, perhaps, the most attrac-

tive superplastic alloy known today. It is relatively easy to cast and roll into sheet and simple heat treatment produces the required fine grain size in an unusually stable microstructure. Its SRS is not greatly strain-rate dependent and remains at a reasonably high level to strain rates up to 10%/sec, which are within a technologically useful range. Maximum m for this material is observed in the range of 250°C - 270°C which is above normal service temperatures and yet not high enough to present any difficulty in actual forming.

The binary zinc-aluminium eutectoid alloy has low creep resistance at room temperature; however, this problem has been successfully reduced^(20,45) with small additions of other metals which reduce creep rates to acceptable levels without affecting the superplastic behaviour.

Its room temperature strength is comparable to that of 70/30 brass. The alloy may be joined by soldering and spot welding, and its resistance to corrosion under atmospheric conditions and in steam is much better than that of mild steel.

Considerable academic and industrial attention is focussed on this alloy, and it is the most common superplastic material available commercially. Typical service properties for one such commercial form are shown in Table 3⁽⁴⁶⁾.

It presently sells for 75¢/lb in North America in the superplastic state.

(b) Aluminium Bronzes

Some superplastic aluminium bronzes have recently been placed on the market. Two such alloys, CDA 619 and CDA 638 have room tempera-

TABLE 3
New Jersey Zinc Data Sheet on Super ZTM 300

TYPICAL MECHANICAL PROPERTIES

	<u>As Rolled</u>	<u>Annealed and*** Air Cooled</u>
Tensile strength,* psi	45,000	58,000
Yield strength, psi (0.2% offset)	37,000	51,000
% Elongation	27	11
Modulus, psi	11.6×10^6	9.8×10^6
Hardness (Rockwell 15-T)	70	84
Creep strength,** psi	3,000	6,000-7,000
Impact strength, ft. lb., 68° F. (See Fig. 1)	25	18

PHYSICAL PROPERTIES

	<u>As Rolled</u>	<u>Annealed and Air Cooled</u>
Thermal expansion, 68°-212° F., in./in./°F x 10 ⁻⁶	with grain: 12.2 across grain: 12.9	with grain: 14.8 across grain: 14.9
Density, lb./cubic in.	0.188	0.188
Electrical conductivity, % IACS	32	28

TYPICAL SUPERPLASTIC PROPERTIES

m.....	0.42-0.47
K (psi—minutes).....	1,200-1,500

*Tension test conducted in accordance with ASTM E8-69 with a cross head speed of 0.25 in./min.

**Stress to produce a creep rate of 0.01% per 1,000 hours (1% in 11.4 years).

***Annealed at 660° F. and air cooled.

ture tensile strength of 40-50 tons /sq.in. and yield strength of 20-25 tons/sq. in. After simple heat treatment, CDA 619 has a yield strength of 50-60 tons/sq. in.⁽¹¹⁾. Their resistance to corrosion, oxidation and abrasion is excellent and conductivity is good.

5.3 Forming of Superplastic Metals

The applicability of various forming processes to superplastic metals is best discussed by classifying these processes as

- (a) Conventional (normal metal working techniques) and
- (b) Unconventional (special forming techniques which become viable due to the peculiar properties of superplastic materials)

5.3.1 Conventional Processes:

i) Rolling:

In rolling, any reduction in the roll separating force would be advantageous and in theory superplasticity would allow this if the strain rate during rolling were not too high. If the rolling mills had to be slowed down to accommodate superplasticity, a suitable balance must be achieved. The rolling of uncommon, and difficult to work alloys which are fortuitously superplastic under rolling conditions could be carried out to advantage. The Ti/6Al/4V alloy, commonly used in the aircraft industry, is such an example. It has been suggested that reductions of 10:1 can be effected in roll separating forces during plastic deformation⁽⁴⁴⁾.

(ii) Forging

Low flow stresses required for superplastic flow permit lower loads in press forging. This is particularly beneficial in parts in which intricate detail and sharp corners must be obtained. In these parts high forging loads are required with conventional materials to

achieve complete die filling. With superplastic alloys the material will continuously flow into the interstices under a moderate load applied for a longer period and excellent detail is obtained. Saller and Duncan⁽⁴⁷⁾ demonstrated this by making an excellent Zn-Al stamping die using a coin as pattern. They then used this die at room temperature to strike an impression on a copper slug (fig.9). The dynamic strength of Zn-Al at room temperature is much higher than that of copper and the die was found satisfactory for short production runs.

The superplastic copper alloy CDA 638 is being used on an experimental basis for computer memory discs⁽¹¹⁾. These can easily be forged from this material in one furnace flattening operation with little or no further machining. Gauge control and flatness are two important requirements in these discs and conventionally they are made by numerous cycles of furnace flattening and extensive surface machining.

Yet another practical example of superplastic forging is the production of a salt shaker with fine surface detail in five operations (4 cents labour cost) instead of 22 operations (18 cents labour cost)⁽⁴⁴⁾.

(iii) Drawing Processes

In conventional cold-working of sheet where deep shaped parts are required, it is usual to start with a sheet considerably longer than the plan area of the final part. The material is drawn into the die and deep parts are produced without excessive thickness variation. The process is typified by the deep drawing of a cylindrical cup as shown in fig. 10. The ram presses on the bottom of the cup and the

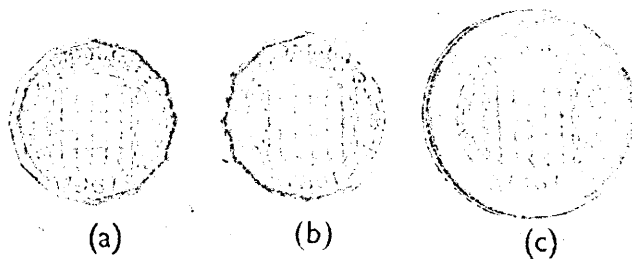


Figure 9 - Stamping die made from superplastic Zn-Al. (Ref. 47).
 (a) Coin used as pattern. (b) Superplastic die. (c) Impression struck in copper in the die.

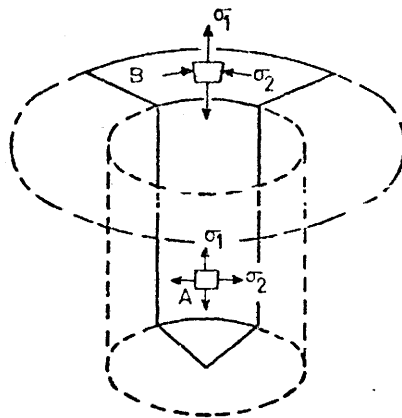


Figure 10 (a) - Stress situation in deep drawing.

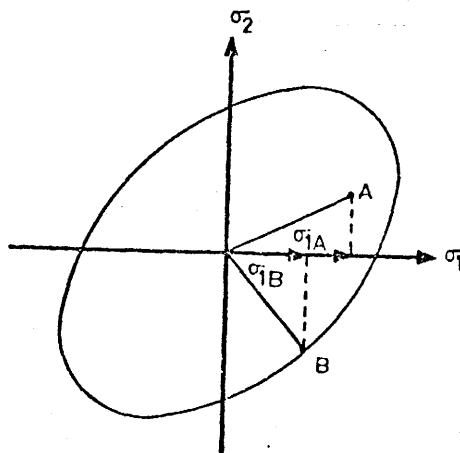


Figure 10 (b) A rigid-plastic material.

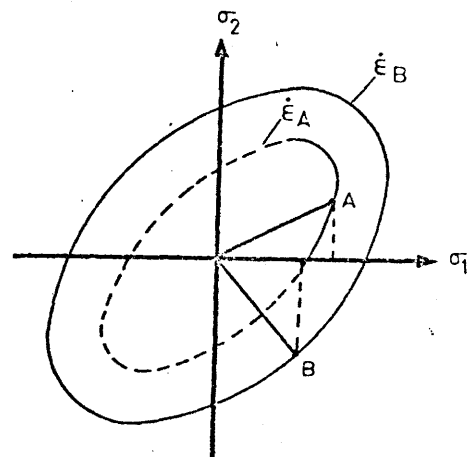


Figure 10 (c) A superplastic material

Figure 10 - Deep drawing of cup (Ref. 11)

forming force is transmitted through the wall in order to deform the flange and draw it inwards. It can be shown that the stress required to cause yielding in the flange is much less than that required in the cup wall so that the flange can be deformed inwards while the cup wall remains rigid. But in superplastic alloys, deformation occurs under the action of any stress and the cup wall deforms and progressively thins if drawing is attempted (11). Al Naib and Duncan⁽⁴⁸⁾ have however, used a modification of the Fuchs process to 'draw' deep parts (fig. 11).

(iv) Extrusion

Since extrusion is another compressive process, most of the discussion on rolling and forging would apply here as well.

Further, alloys which are difficult to extrude in the normal coarse-grained state may possibly become extrudable in the fine-grained superplastic condition.

5.3.2 Unconventional Processes

(i) Dieless drawing and 'roll-less' rolling

The resistance to necking of superplastics has been used to devise a method of dieless drawing⁽⁴³⁾.

On applying tension, size reduction may be achieved in a locally heated region (induction heating is used) which is at the superplastic temperature (fig. 12). A good degree of conformity to the original shape is possible and reproducibility to within .0005 inch can sometimes be achieved.

Reduction in area (R.A.) obtainable by this process is related to the ratio R of the drawing speed V_d to the speed of travel of the heated

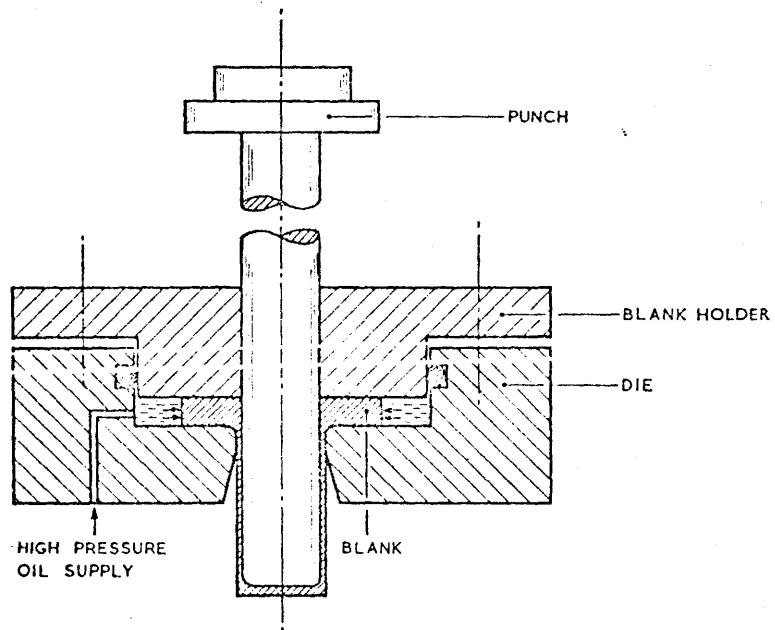


Figure 11 - Pressure augmented 'deep drawing of cup. (Ref. 48).

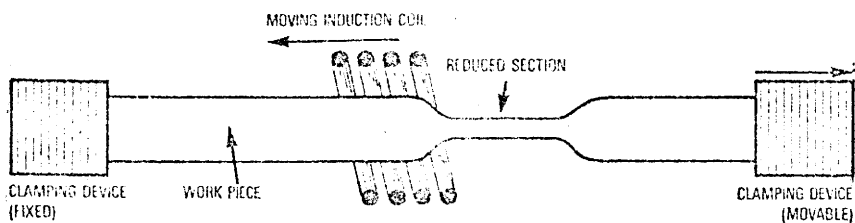


Figure 12 (a) Die-less drawing process.

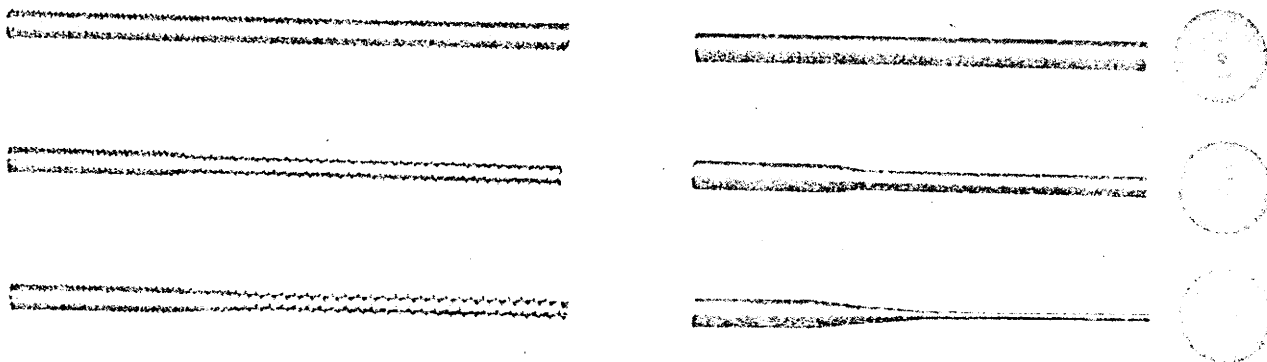


Figure 12 (b) Complex cross-sections and fine bore tubes drawn in a die-less process

Figure 12 - Die-less drawing. (Ref. 43).

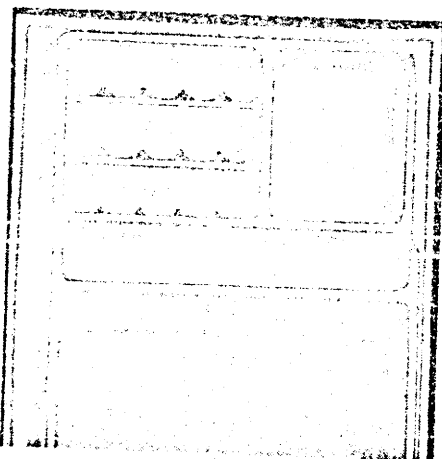


Figure 13 - Vacuum formed refrigerator door inner panel.

zone, V_c by the expression

$$\text{R.A. \%} = (100R)/(1+R) \quad (15)$$

With $R=5$, the reduction in area is 83% which exceeds the maximum reduction of 63 percent theoretically possible in conventional die drawing with an ideal plastic material, friction and redundant deformation being neglected. There is obviously no die wear or die lubrication.

This method can also be used to produce controlled tapered or stepped lengths of complex shapes.

A process of 'roll-less rolling' based on the same principle can be envisaged.

(ii) Stretch Forming

Superplastic alloys may be treated as high strength, high modulus, heat treatment sensitive thermoplastics. The plastics industry uses a wide variety of techniques for forming common thermoplastics such as ABS or polypropylene-vacuum forming (drape forming, plug assisted forming, etc.) and pressure forming (blow moulding, trapped sheet forming, and so on). Most of these processes have been successfully tried with superplastic sheet on tubular preforms.

Fig. (13) shows a refrigerator door inner panel vacuum formed from Zn-Al sheet. It would be impossible to make such a panel from conventional metals in a single operation. The British car industry has investigated the possibility of using Zn-Al sheet for producing automobile body panels. Normally a large number of different panels are individually pressed-many of them requiring complicated sequences of operations-and then assembled

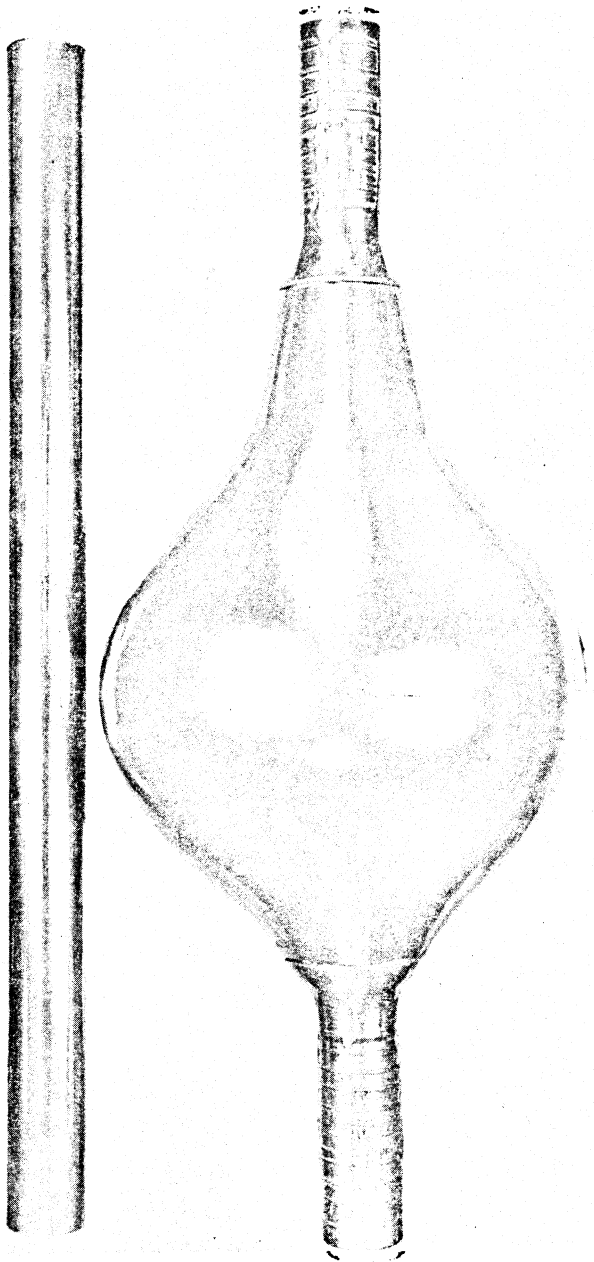


Figure 14 (a) Free expansion of Pb-Sn superplastic tube by internal

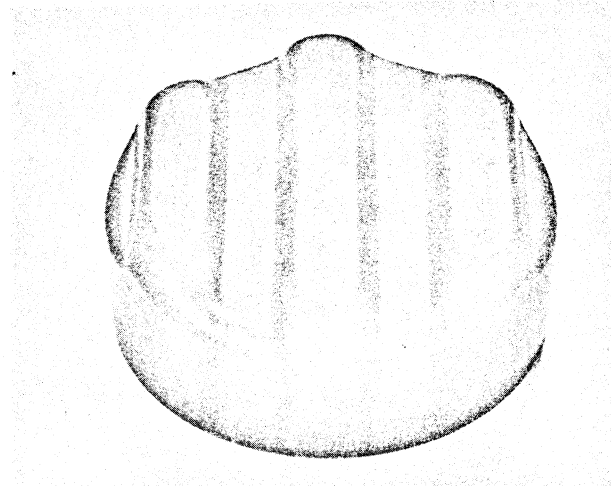


Figure 14 (b) Cup formed from superplastic stainless steel sheet, using female die only (Ref. 49).

Figure 14 - Pressure forming of superplastic materials.

together. With zinc-aluminium, quite complicated panels can be vacuum-formed in one operation.

A number of workers^(48,49,50) have demonstrated the applicability of pressure forming techniques to superplastic material (fig. 14). The pressure and time required are highly dependent on the thickness of the sheet.

The advantages of using superplastic alloys in these processes include reduction of tooling and labour costs, elimination of interstage annealing, and less variation in thickness across the formed part than with conventional metals.

5.4 Industrial Usage of Superplasticity

Some of the components today being manufactured from superplastic alloys include jet engine turbine and compressor discs, aircraft nose wheels, Concorde passenger amenities panels, air to air heat exchanger cores, pulleys and gears used in electronic equipment, etc.⁽⁵⁰⁾

CHAPTER 6

SCOPE OF PRESENT INVESTIGATION AND EQUIPMENT DESIGN AND FABRICATION

6.1 Scope of Present Work

This project was undertaken to study some forming techniques for superplastic alloys and their viability for industrial application. The Zn-Al eutectoid alloy was chosen as it appears to have more industrial potential than any other superplastic material known today.

In particular, it was decided to investigate the following areas:

- a) Extrusion: Though some theoretical studies have been made on the extrusion of superplastic alloys, little experimental work has been reported in the literature. Experiments were devised to obtain some data on the extrusion of conventional and superplastic Zn-Al. Specifically, it was planned to obtain load vs extrusion rate characteristics for the material in its as cast and superplastic form and to study the qualitative aspects of extrusion.
- b) Rubber Plug Forming: The possibility of using a rubber plug to expand a tubular specimen into a complex shape was investigated.
- c) Pressure Forming: Most pressure forming work has been done with thin sheets, <.040 inch. Investigation into the time and pressure required for macroforming (overall shape change) and microforming (forming into small grooves; reproduction of surface detail) thicker sheet, using air pressure, was planned.

These processes were studied by producing a hollow component in a two-stage process:

- a) Backward extrusion of a cylindrical cup from billet material, and,

b) Expansion of this preform in a shaped moulding die using a rubber plug or internal pressure.

6.2 Component Size

The following cup dimensions were decided on for extrusion:

Length..... 3.875"

I.D. 2.000"

Wall thickness..... 0.066"

Thickness of base 0.100"

It was planned to form a 0.5" wide, 0.040" thick flange on the top of the cup for holding in the expansion die.

For the second part, it was decided to expand the cup to approximately double its internal volume.

6.3 Equipment Design and Fabrication

6.3.1 Backward Extrusion Rig

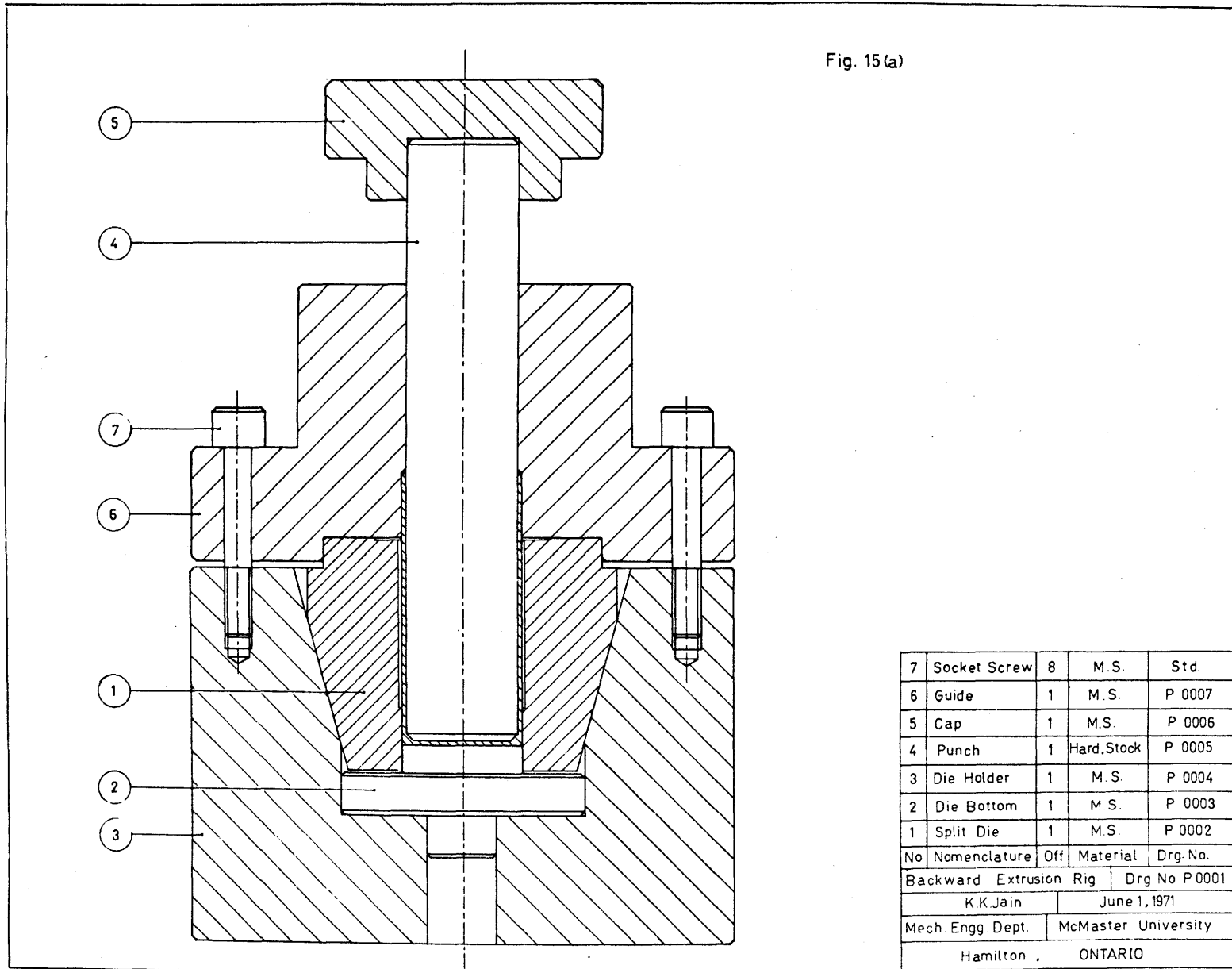
A complete design of the extrusion rig is given in fig. 15.

It essentially consists of a four-piece split die and a 'die bottom' resting in a cavity in the die holder. The 'guide', which is bolted down on the die holder, serves the dual purpose of guiding the punch in centrally and locating the die.

All parts were made of mild steel except the punch which was made from hardened and ground steel stock.

The various parts of the rig are described below:

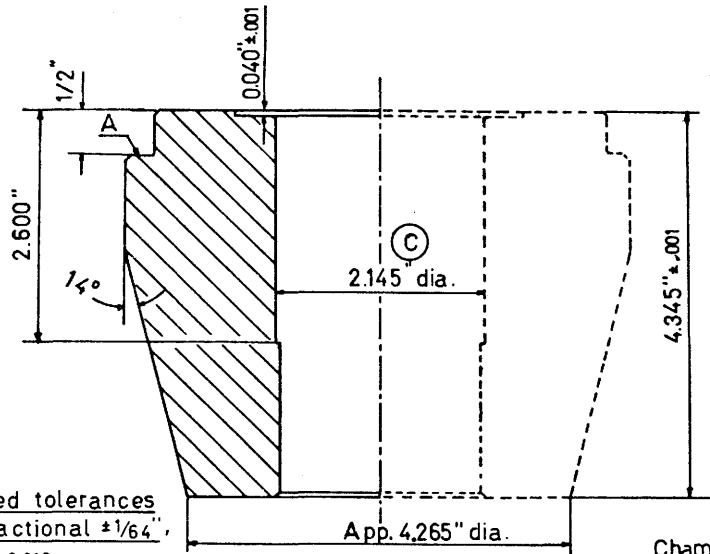
a) Die The die was split in order to facilitate removal of the extruded



7	Socket Screw	8	M.S.	Std.
6	Guide	1	M.S.	P 0007
5	Cap	1	M.S.	P 0006
4	Punch	1	Hard Stock	P 0005
3	Die Holder	1	M.S.	P 0004
2	Die Bottom	1	M.S.	P 0003
1	Split Die	1	M.S.	P 0002
No	Nomenclature	Off	Material	Drg.No.
Backward	Extrusion Rig		Drg No	P 0001
	K.K.Jain		June 1, 1971	
Mech. Engg. Dept.	McMaster University			
	Hamilton		ONTARIO	

Figure 15 - (a) to (g) - Design of Backward extrusion rig.

Date	Sym.	Revision
Dec.15'71	C	Dimn 2.132 changed to 2.145



Unspecified tolerances to be Fractional $\pm 1/64$, Decimal ± 0.010

Chamfer all corners $1/16 \times 45^\circ$

NOTE Split die to be made from 4 3/4 sq. blocks of mild steel soft-soldered together as shown

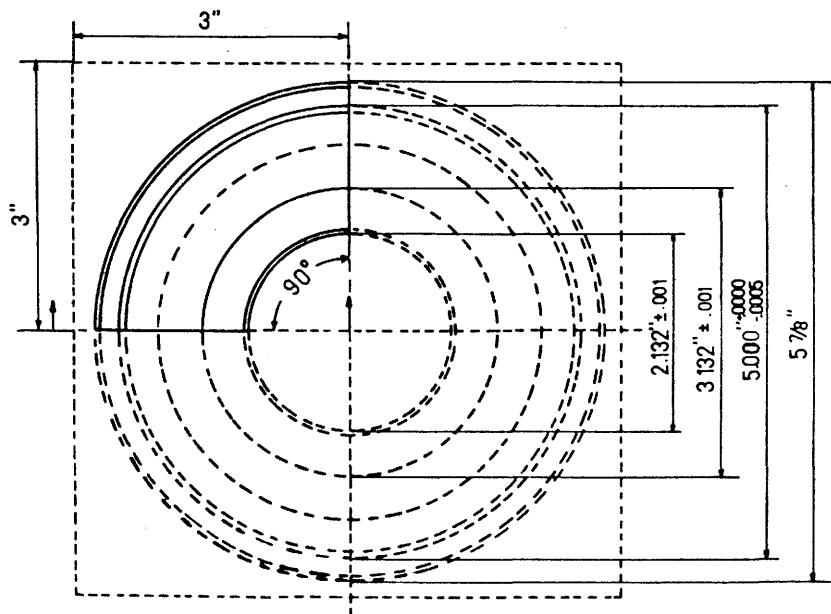
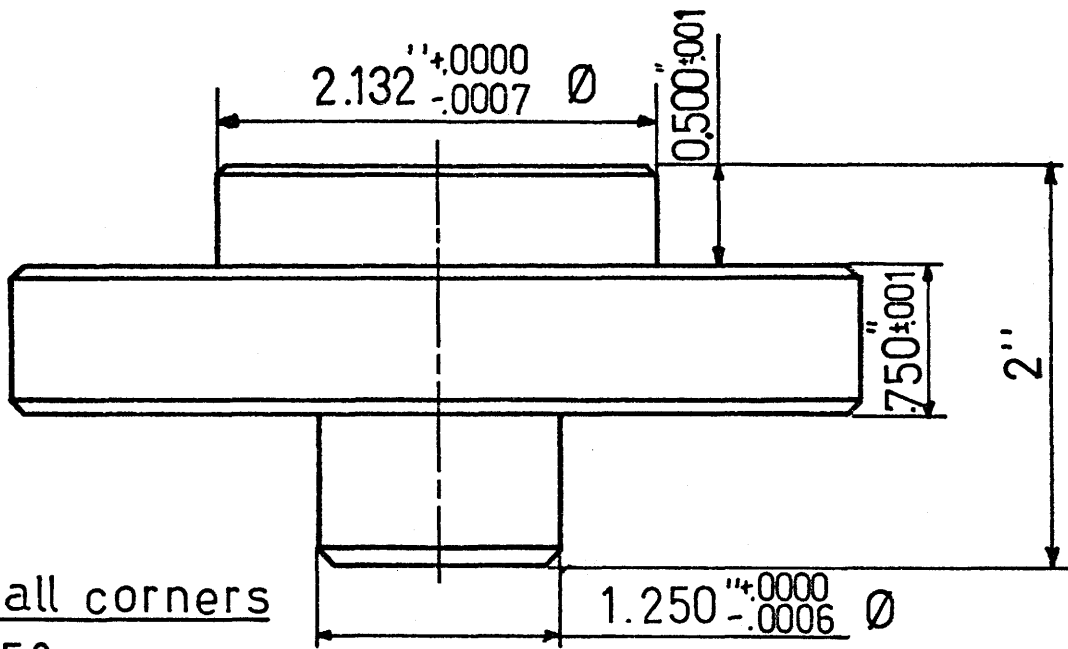
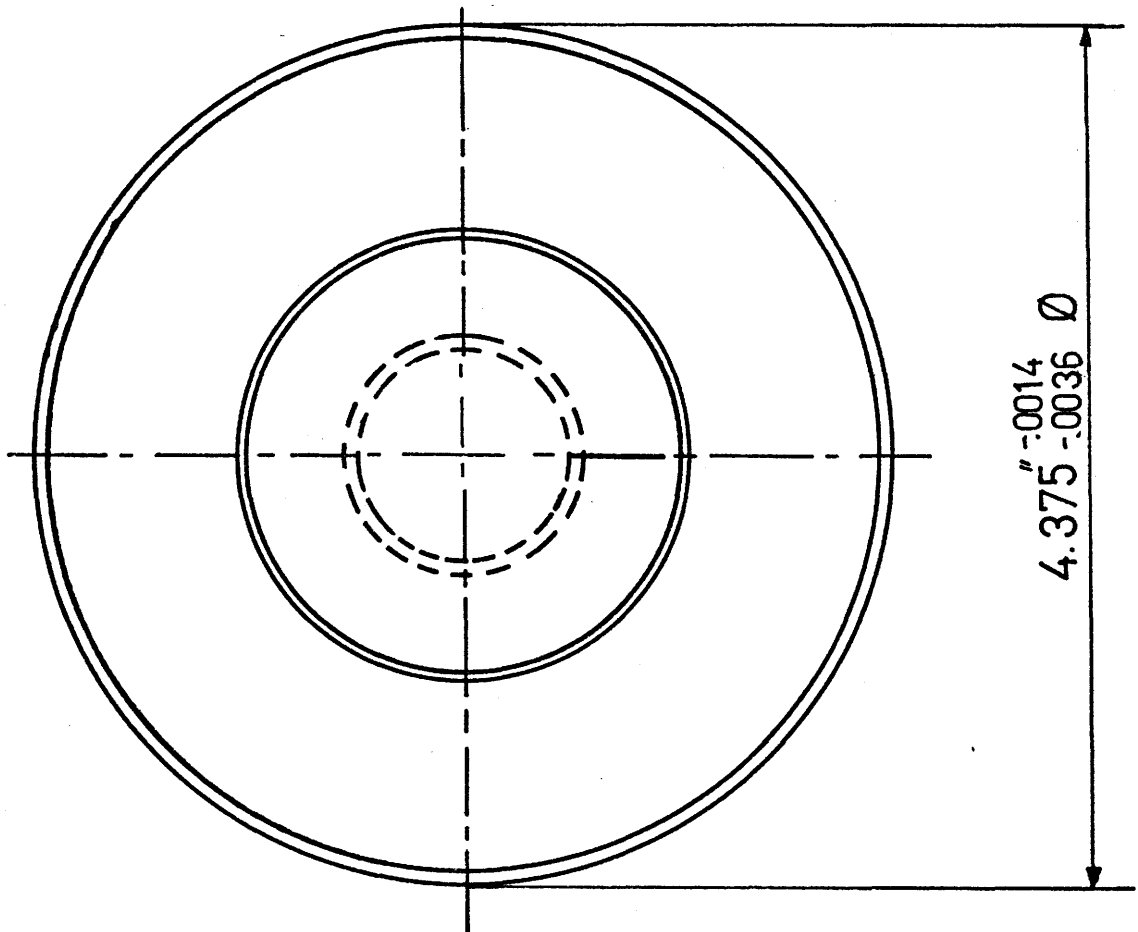


Fig. 15(b)

Split Die	Drg.No. 0002
Mech. Engg.	Scale 1:1
McMaster U.	KKJain
Hamilton, ONT.	June 10, 1971



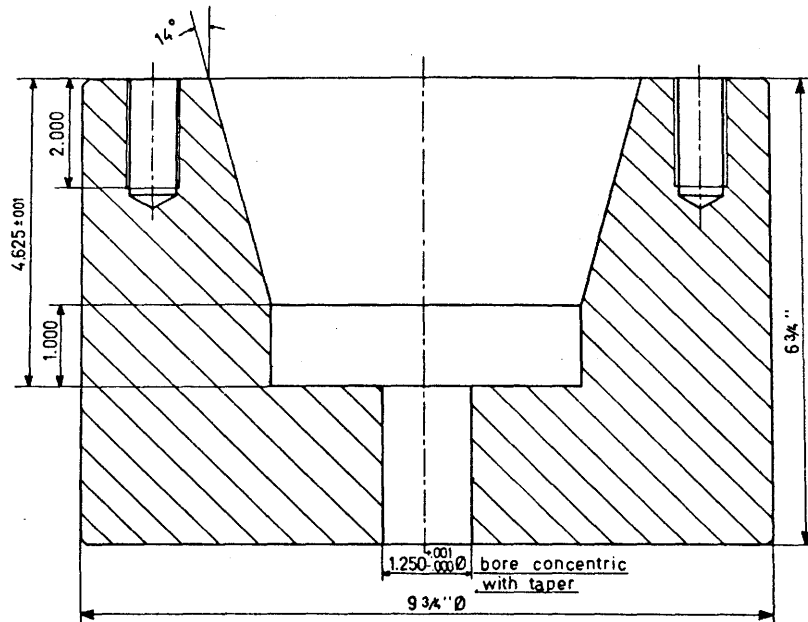
Chamfer all corners
1/16 at 45°



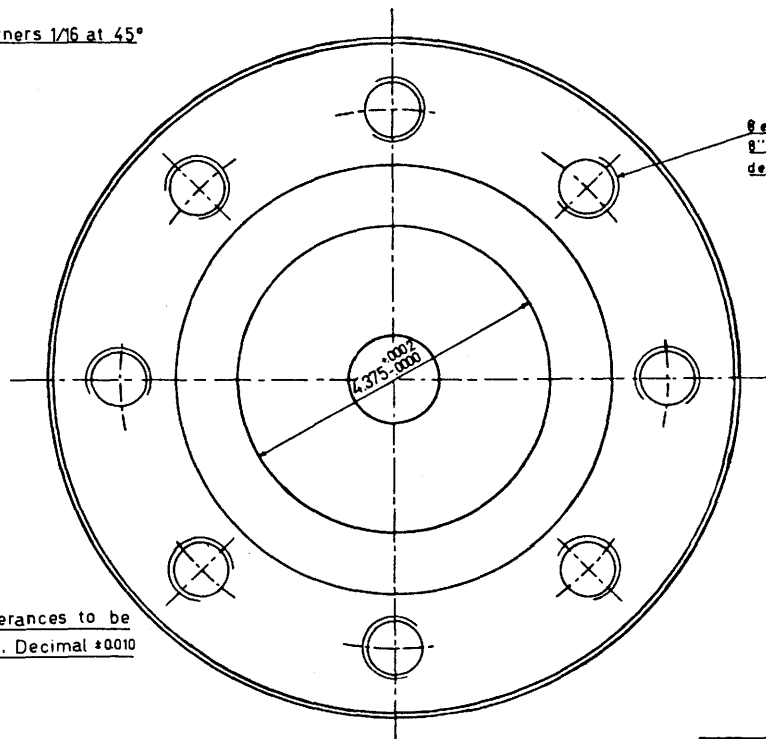
Unspecified tolerances
to be Fractional ±1/64",
Decimal ± 0.010

Fig 15(c)

Die Bottom	Drg.No.0003
Mech Engg	Scale 1:1
McMaster U.	K.K.Jain
Hamilton ONT	June 5 1971



Chamfer all corners 1/16 at 45°

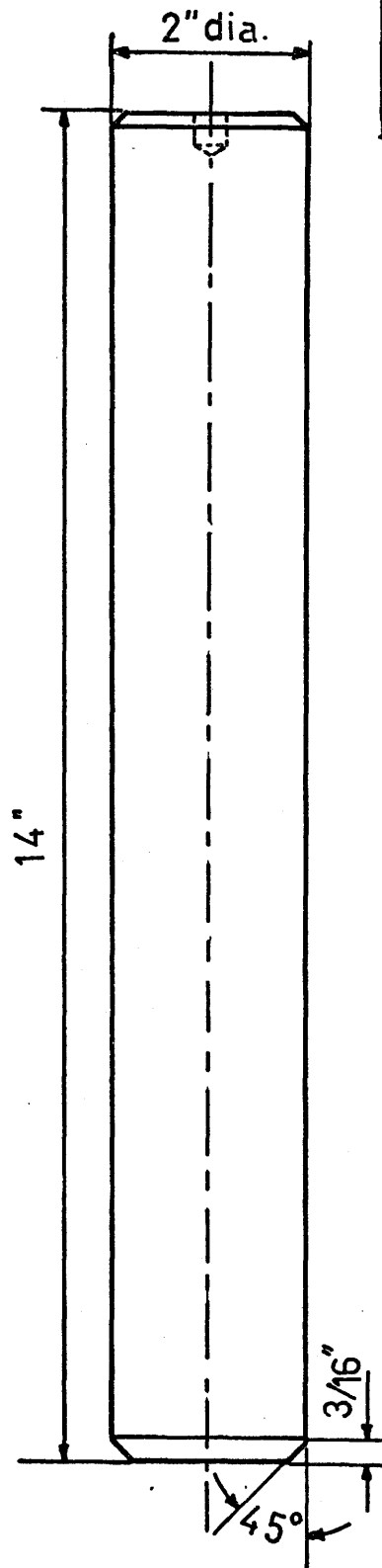


8 equally spaced holes on 8" PCD drilled and tapped 2" deep for 3/4" NC socket screws

Unspecified tolerances to be Fractional ±1/64, Decimal ±0.010

Die Holder	Drg. No. P0004
Mech. Engg.	Scale 1:1
McMaster University	KKJain
Hamilton, ONT.	June 1, 1971

Fig. 15 (d)

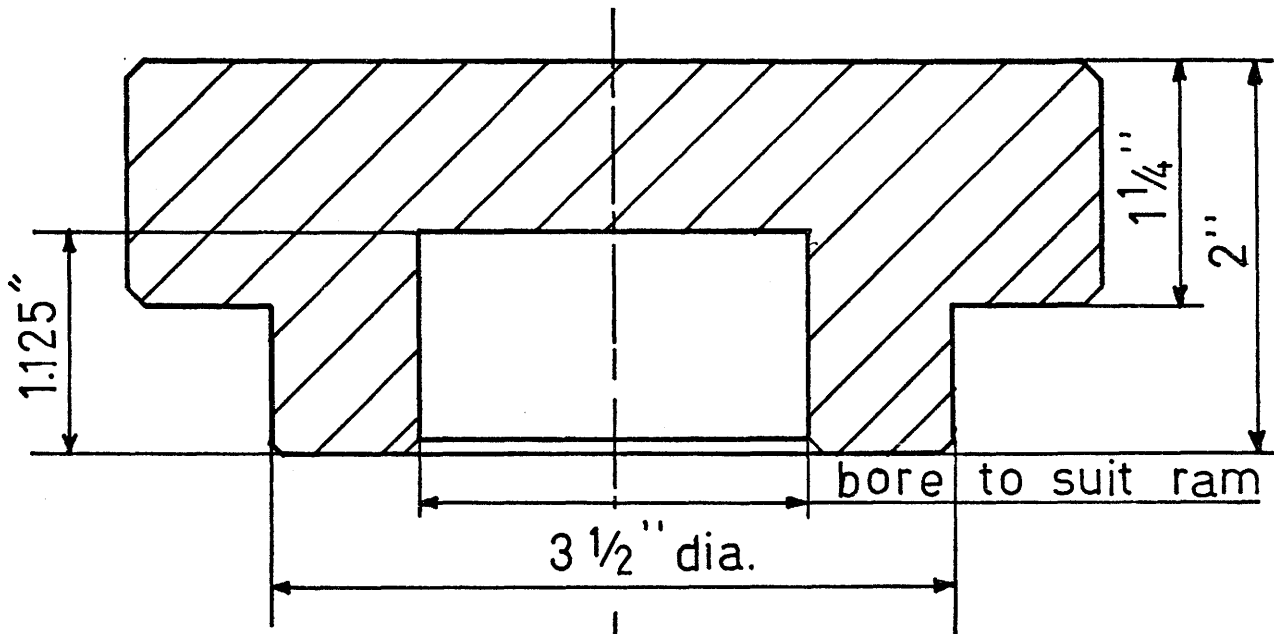


Tolerances $\pm 1/64$ "

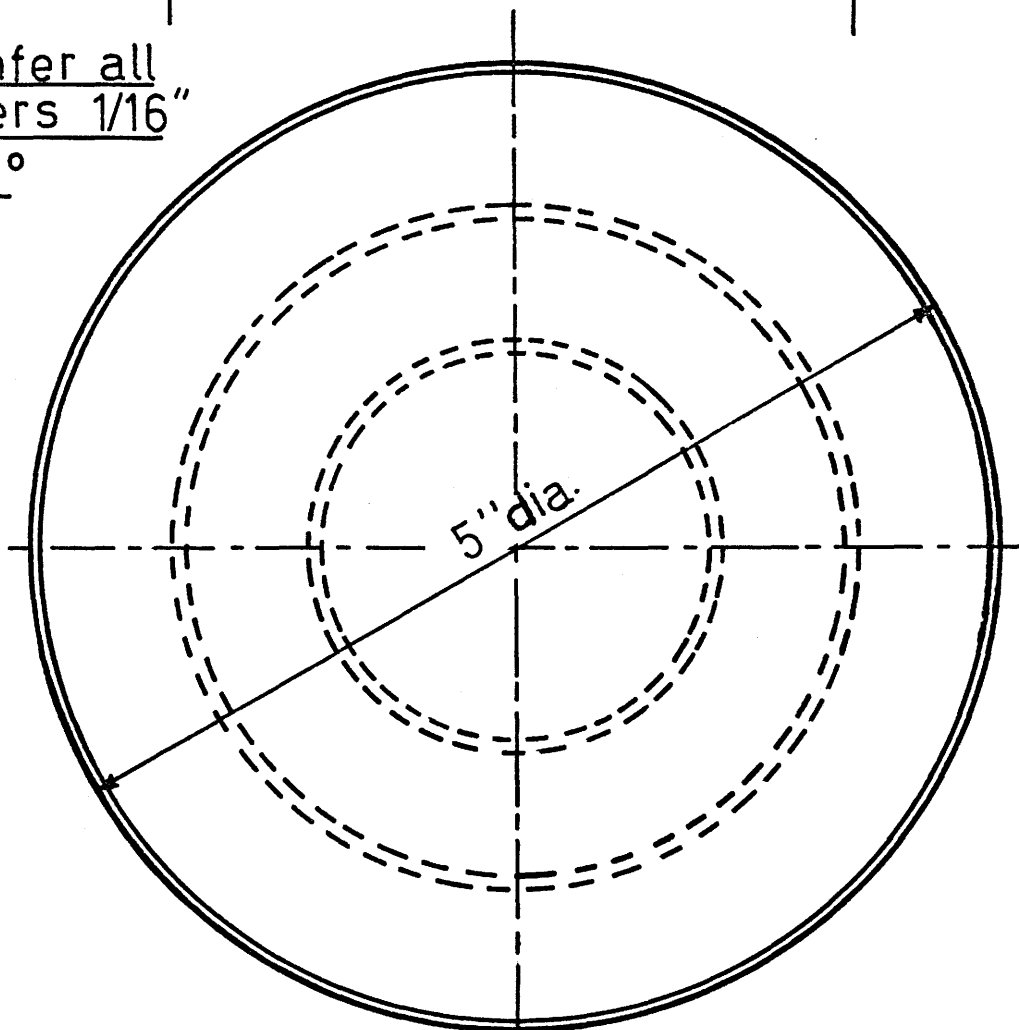
Date	Sym	Rev
Dec.1, 1971	A	7/32 rad.to 3/16 at 45°

Fig. 15 (e)

Punch	Drq.No. 0005
Mech. Engg.	Scale 1/2"
McMaster U.	K.K. Jain
Hamilton ONT.	June '71



Chamfer all corners 1/16"
at 45°

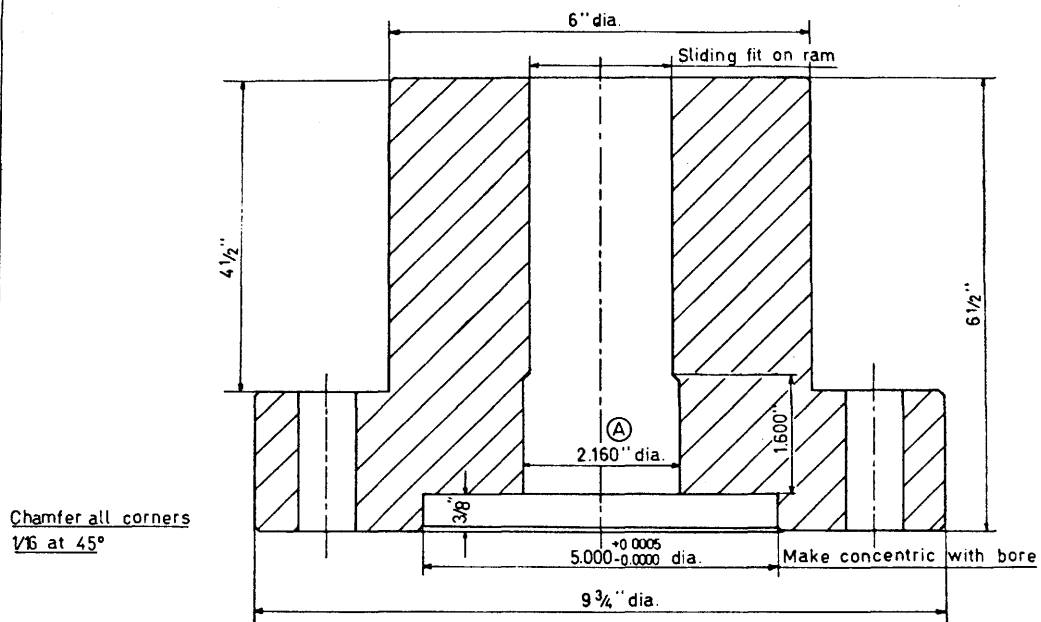


Unspecified tolerances
to be: Fractional $\pm 1/64$ ",
Decimal ± 0.010

Fig. 15 (f)

Cap	Drg.No. P 0006
Mech.Engg.	Scale 1:1
McMaster U.	K.K.Jain
Hamilton, ONT.	June 1'71

Date	Sym	Revision
Jan 172	A	Sliding fit changed to 2.60"



Unspecified tolerances to be
Fractional $\pm 1/64$ ", Decimal ± 0.00

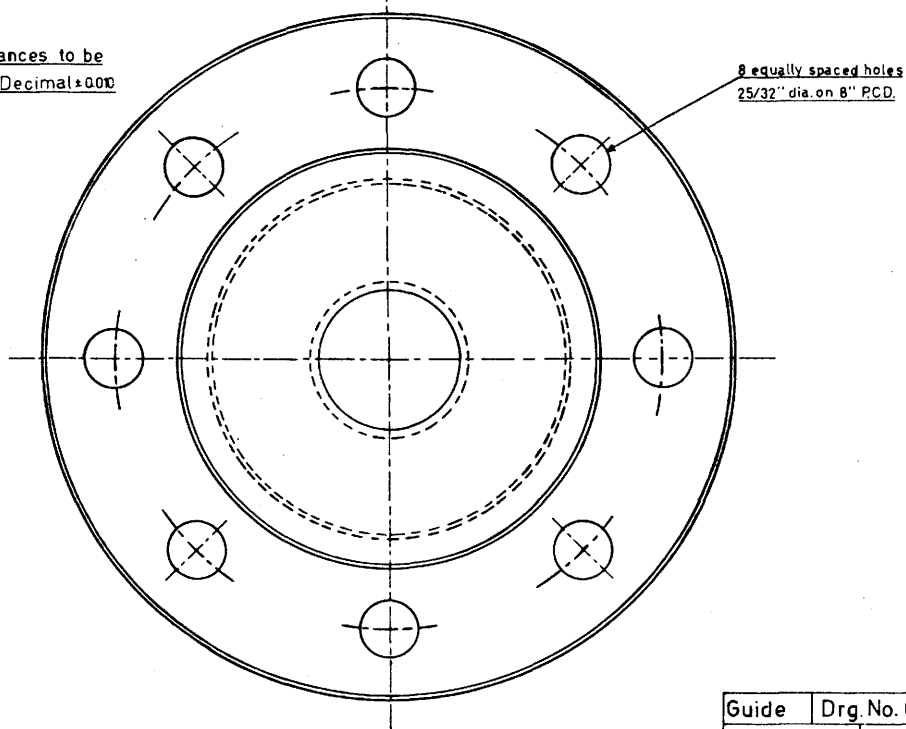


Fig 15 (g)

Guide	Drg. No. 0007
Mech. Engg.	Scale 1:1
McMaster U	KK.Jain
Hamilton, ONT	June 6, 1971

cup. It was made as one piece from four 4.8" x 3" x 3" blocks soft soldered together (fig. 15b). The sections were separated and the faces polished after completion of machining.

The bore, finally required to be 2.132" was made 0.002" bigger to make allowance for the thickness of the solder film between the segments.

A 14° self-locking taper was provided on the outside of the die. The top 1/2 inch was turned down to a diameter of $5.000 \begin{smallmatrix} + .0000 \\ - .0005 \end{smallmatrix}$ so that it could fit into a recess made in the guide.

The length of the die was maintained at $4.345 \pm .001$ ", designed such that face 'A' was flush with the top of the die holder and there was a 0.030" gap between the flange on the die bottom and the bottom of the die.

A recess $3.132 \pm .001$ " diameter and $0.040 \pm .001$ " deep was machined on the top of the die to form a flange on the cup.

b) Die Bottom This is shown in fig. 15c. The top of the die-bottom forms the bottom of the extrusion die. It was machined to $2.132 \begin{smallmatrix} +.0000 \\ -.0007 \end{smallmatrix}$ diameter in order that the split die fit snugly around it. The other end was turned to a diameter of 1.250" and fits into the die holder for location.

c) Die Holder (fig. 15 d). This is a cylinder block 9 3/4" dia. and 6 1/2" length. The cavity was machined to the same taper as the die without changing the machine setting, so that the mating surfaces could match exactly. The 1.250" hole, which locates the die bottom, was bored concentric with the taper--to ensure co-axial positioning of the die and die bottom. This hole was bored through so that the die and die

bottom assembly could be pushed up to facilitate removal of the formed specimen from the die, and also to permit forward extrusion if required in later developments.

d) Punch and Cap (fig 15e,f) The punch was made from polished 2.000 \pm .0005" dia. 'superior steel shafting' stock (Tensile strength 82,000 psi). A 7/32" radius was formed on one end and the other end was pressed into a soft cap. The nominal stress on the punch for 50 tons load is 32,000 /lbf/in².

e) Guide This is shown in Fig. 15(g). The guiding hole was bored to give a sliding fit on the ram. The top of the die fits into the recess on the bottom of the guide. This recess was machined concentric with the bore to ensure coaxiality of the ram and die. It was made 3/8" deep while the die extends 1/2" above the die holder. The guide thus rests solely on the die and when bolted to the die holder, pushes the die further into the holder, reducing the gap between the segments to minimum.

To facilitate lifting and hauling, a steel cable was fastened to two eyebolts fixed diametrically opposite on the top of the guide.

Assembly and exploded views of the rig are shown in fig. 16 and 17 respectively.

6.3.2 Expansion Rig

The expansion rig was similar to the extrusion equipment except that an internally contoured split die and a die bottom to suit were used (fig. 18a,b). Two V grooves were machined on the die to study the microforming characteristics of the material. The maximum internal

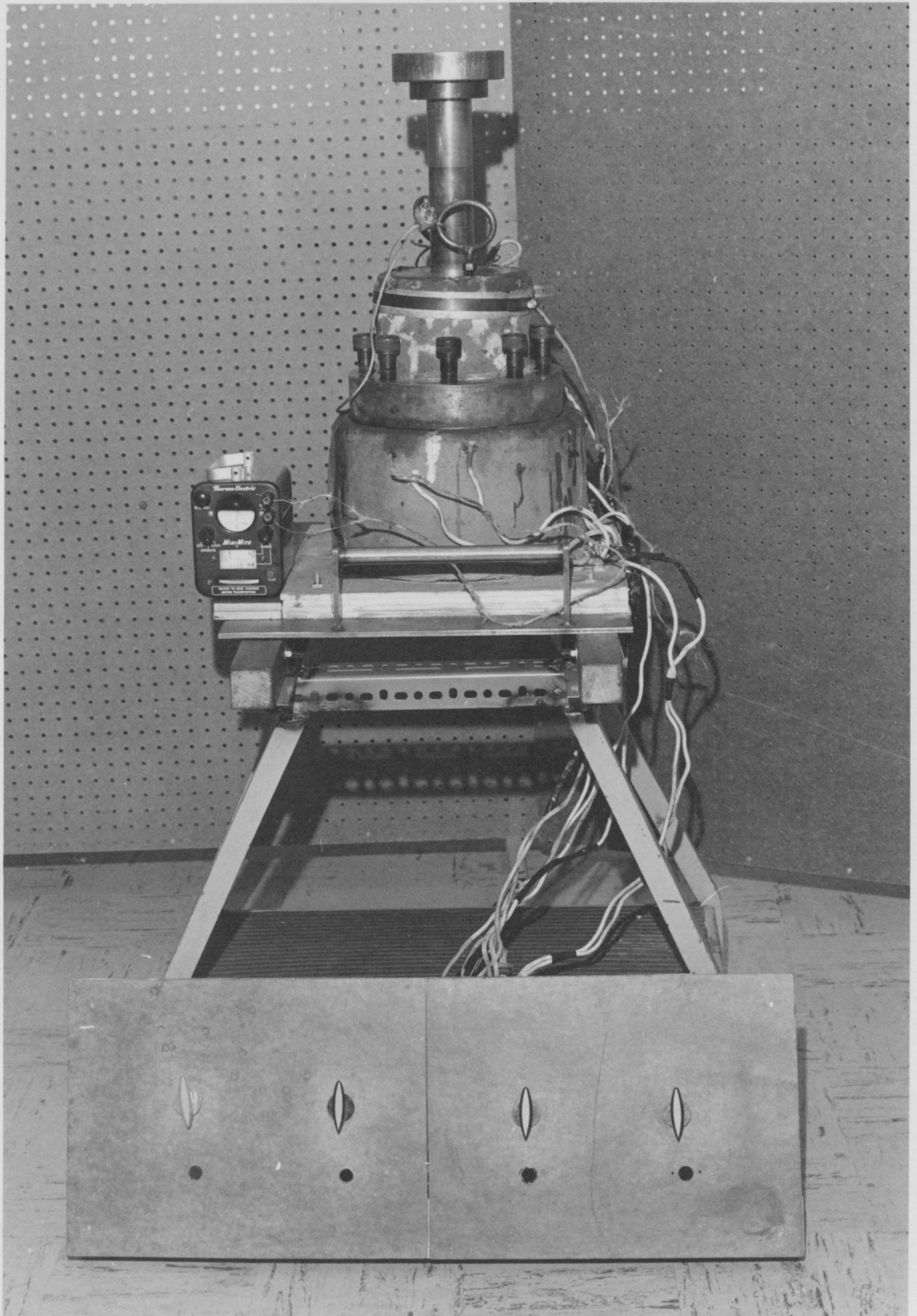


Figure 16- Backward extrusion equipment assembly

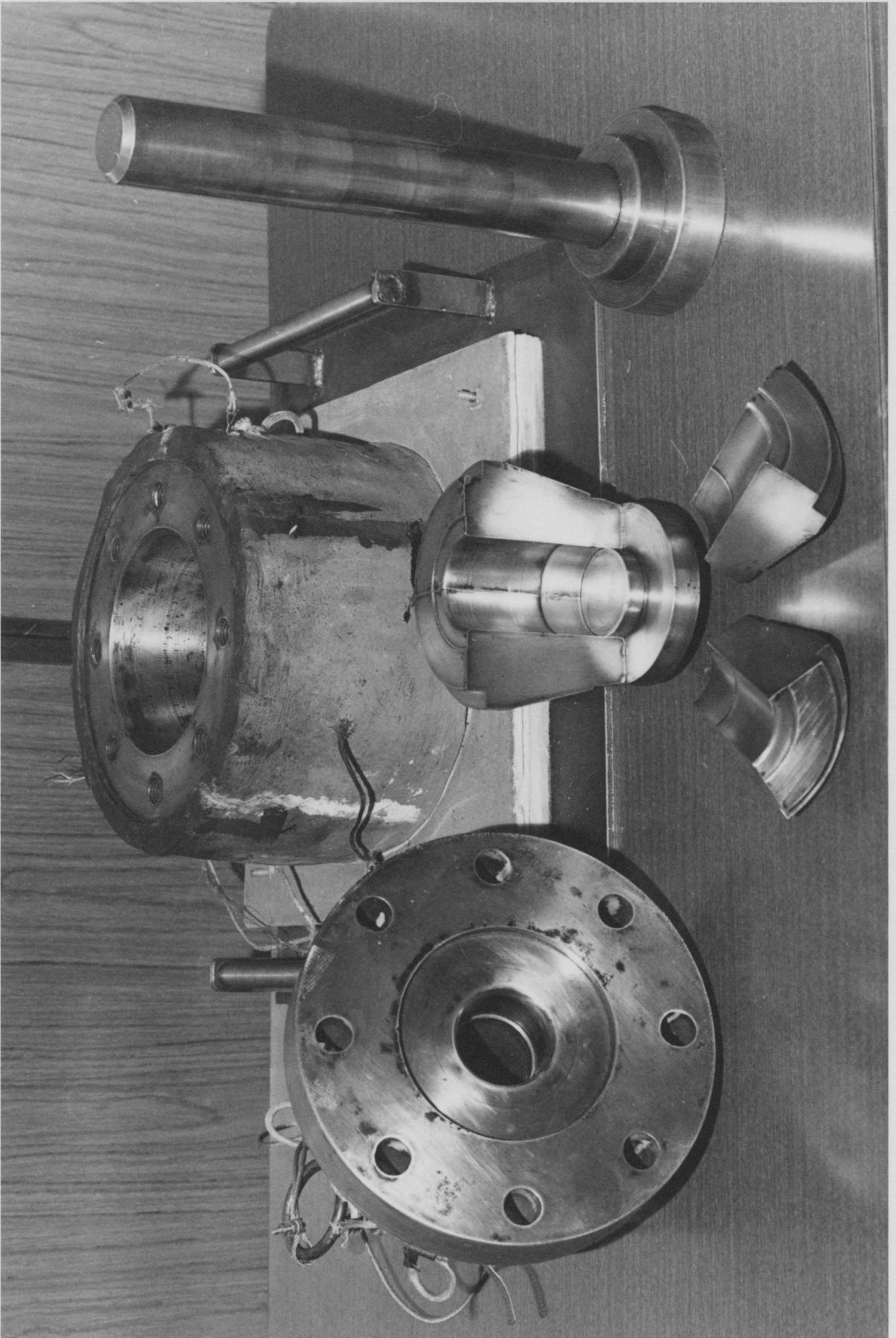
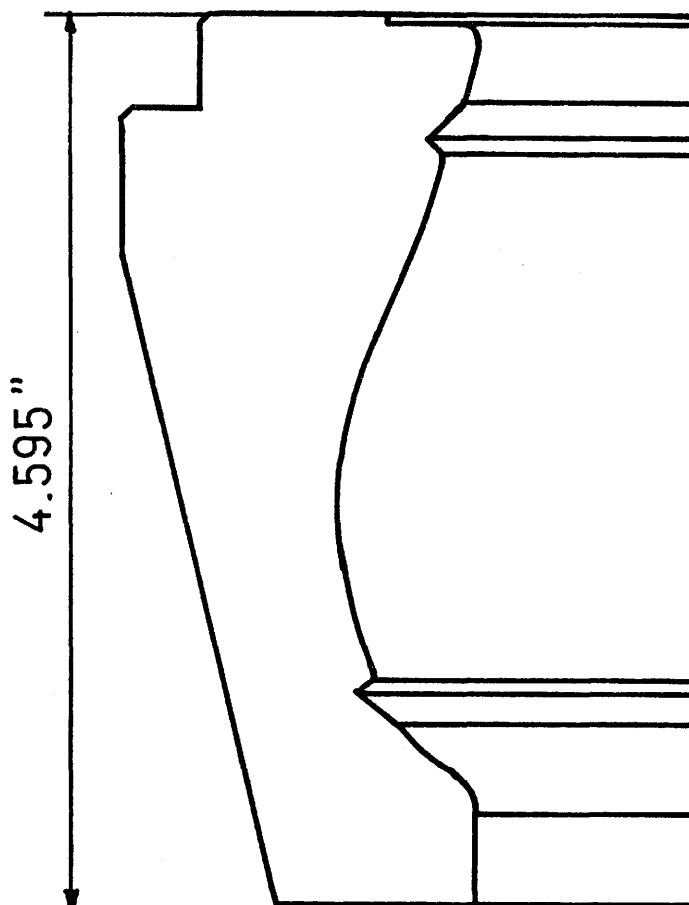


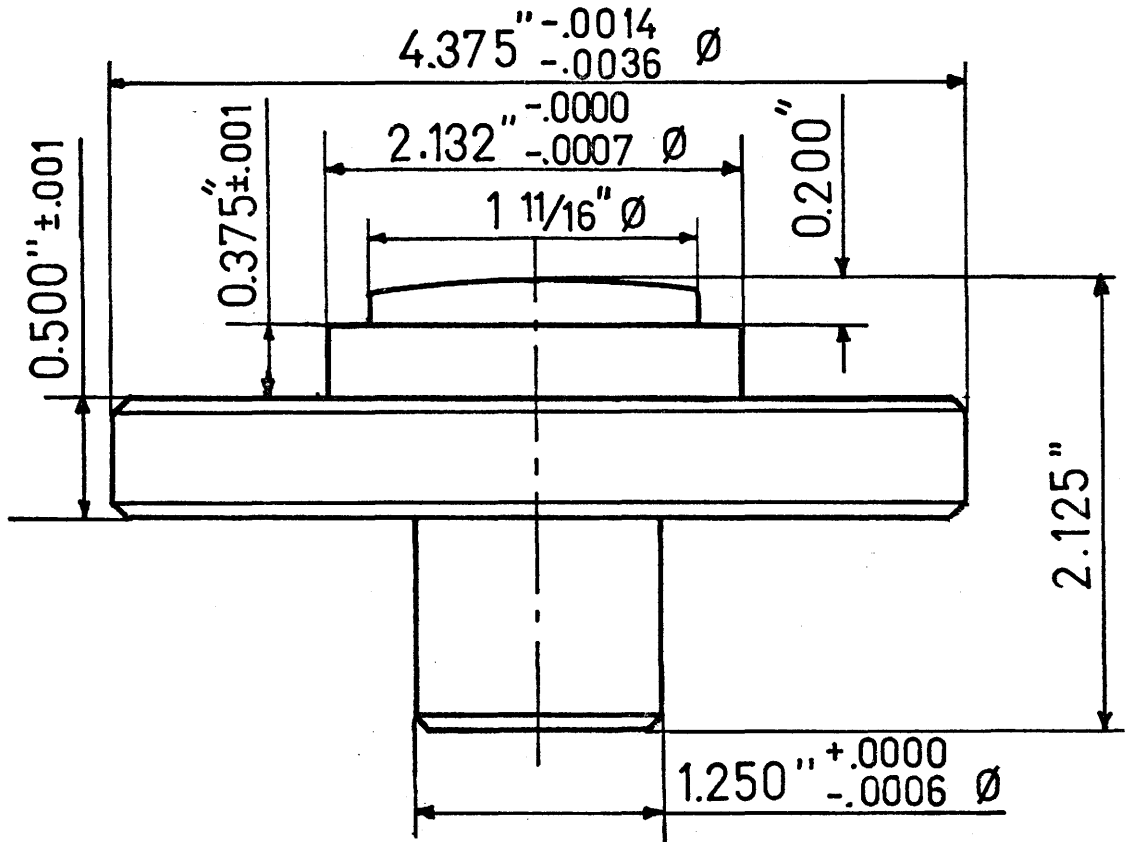
Figure 17- Exploded view of extrusion equipment



Other necessary dimensions same as
Extrusion split die

EXPANSION DIE PROFILE

Figure 18 (a) - Expansion split die segment.



Expansion Die Bottom

Figure 18 (b) - Expansion Die Bottom.

diameter of the die was 3.85".

A recess identical to the one on the extrusion die was provided on the top of the expansion die so that the flange on the extruded cup could be held rigidly by the pressure between the guide and the die.

6.3.3 Heating Arrangement

The dies were heated by means of nichrome resistance wire wound around the die holder. A 1/4" thick coat of 'Hi-Low insulating cement' was applied on the die holder for insulation and the wire was double wound on it. The wire was covered with another thick coat of cement to minimise heat loss to the atmosphere. Three separate heaters were provided (each drawing about 1.6 kw), one for each two inches of die holder length, so that heating in each section could be regulated if required. (Calculations regarding heater design are given in Appendix I).

A similar heater was built around the guide to preheat the ram.

Each heater was controlled through a 15A, 120V infinitely variable heat switch - similar to those used on household electric stoves.

Temperature along the length of the die was measured with three chromel-alumel thermocouples wedged into holes drilled into the die holder at a distance of 1", 3" and 5" respectively from the top. The depth of these holes was maintained such that the tips of the thermocouples were 1/2" from the cavity.

The die holder was screwed on to a 20" x 18" x 1/4" steel plate with 1" thick asbestos plate in between to minimise heat loss from the bottom.

6.3.4 Press

A 300 Ton Tinius Olsen hydraulic press was used for all extrusion tests.

6.3.5 Auxiliary Equipment

The open height of the press was just sufficient to accommodate the rig. A trolley was made such that it was the same height as the press table in its lowermost position. The equipment could thus be assembled on the trolley, slid on to the press for the test and then transferred back to the trolley for disassembly.

A fork lift trolley was used to lower the guide on the die holder.

A dial indicator was used to measure ram travel during extrusion.

6.3.6 Modifications

Some modifications and additions were made to the equipment during the experiments and these are described in subsequent chapters along with the tests.

CHAPTER 7

EXTRUSION TESTS

7.1 Preparation of Specimens

The material was received in the form of 2 1/4" diameter cast billets. About a foot length of the billet material was turned down to 2.128" diameter and sawed to lengths of 0.65". These pieces were faced to a length of 0.59" to obtain specimens for testing of as cast alloy. The calculation of billet size required is given in Appendix II.

To obtain superplastic material, half of these specimens were soaked for two hours in a furnace heated to 320°C and quenched in ice-cold water for 30 seconds.

7.2 Test Procedure

All extrusion tests were performed under the constant load condition.

The rig was assembled together on the trolley without the test specimen and heated up to about 220-230°C. This took approximately three hours. The guide and ram were then removed and the die, die bottom and ram were lubricated. The specimen was coated with lubricant, placed in the die, and the guide was positioned on the die and bolted down to the die holder. The ram was placed in position and the assembly was transferred to the press. The temperature was allowed to go up to 250°C, which took another 45 minutes to 1 hour. All tests were conducted at this temperature.

During the test duration, the heat was regulated so that the die temperature remained constant at 250° ± 2°C.

The travel of the ram was measured with a dial indicator fixed to the press frame with the tip of the plunger resting on the steel plate screwed to the die holder. The initial position of the ram was taken as the reading on the dial indicator at the moment the test load was reached and subsequent readings were taken at intervals of 10, 15 or 30 seconds, depending on the speed of travel of the ram. The load was released when ram speed dropped to less than 0.005"/minute.

After completion of the test, the equipment was transferred back to the trolley. The guide was unbolted and lifted from the die-holder using a fork-lift trolley and the cable hook provided on the guide. Due to the close locational fit between the recess on the guide and top of the die, the die segments sometimes got wedged in the recess, but these could easily be separated by a little tapping. Stripping of the formed cup from the ram was more difficult and involved manual pulling on the ram a number of times, thus hitting the top of the cup against the guide till it finally slid off the punch. This problem was caused by the absence of air between the cup and the punch. It was, however, later decided to make longer cups than originally planned by allowing them to extrude into the guide (this is discussed in greater detail in a subsequent section). It was virtually impossible to strip these cups from the punch manually because along with the afore-mentioned resistance the friction between the cup wall and guide bore also had to be countered now. The arrangement shown in fig. 19 was successfully used to eliminate this problem.

During the complete process of removal of the formed cup from the



Figure 19- Removal of extruded cup from ram

rig, the die only cooled down to approximately 225°C. This was used to advantage by performing a number of tests before allowing the die to cool to room temperature.

7.3 Lubricant

The choice of a proper lubricant presented considerable difficulty.

A colloidal suspension of fine graphite particles in water was tried initially as it has been successfully used in compression tests on Pb-Sn⁽⁴⁸⁾. This was applied to the die and ram when these had heated up to about 250°C so that the water evaporated leaving behind a thin film of graphite. However, this proved totally unsatisfactory as even at a load of 150,000 lbs cups of more than 1/2" wall length could not be obtained. Also, the material had a tendency to stick to the radius on the end of the ram. Further, the graphite imparted a dark skin to the metal, which was difficult to get rid of.

An aerosol spray of P.T.F.E. produced the same result, except that there were no surface-darkening effects.

The ram was modified to replace the radius by a 45° 3/16" taper and the same lubricants were tried again. This eliminated the sticking tendency of the material. Further, because of the reduction in the cross-sectional area at the indenting end of the ram, the extrusion pressure increased and longer wall lengths were obtained. Nevertheless, friction between the cup and die walls was still considerable and 150,000 lb load only produced cups 1 1/2" long.

To reduce friction, the die bore was increased from 2.132" to approximately 2.145" for a distance of 2.6" from the top so that the I.D.

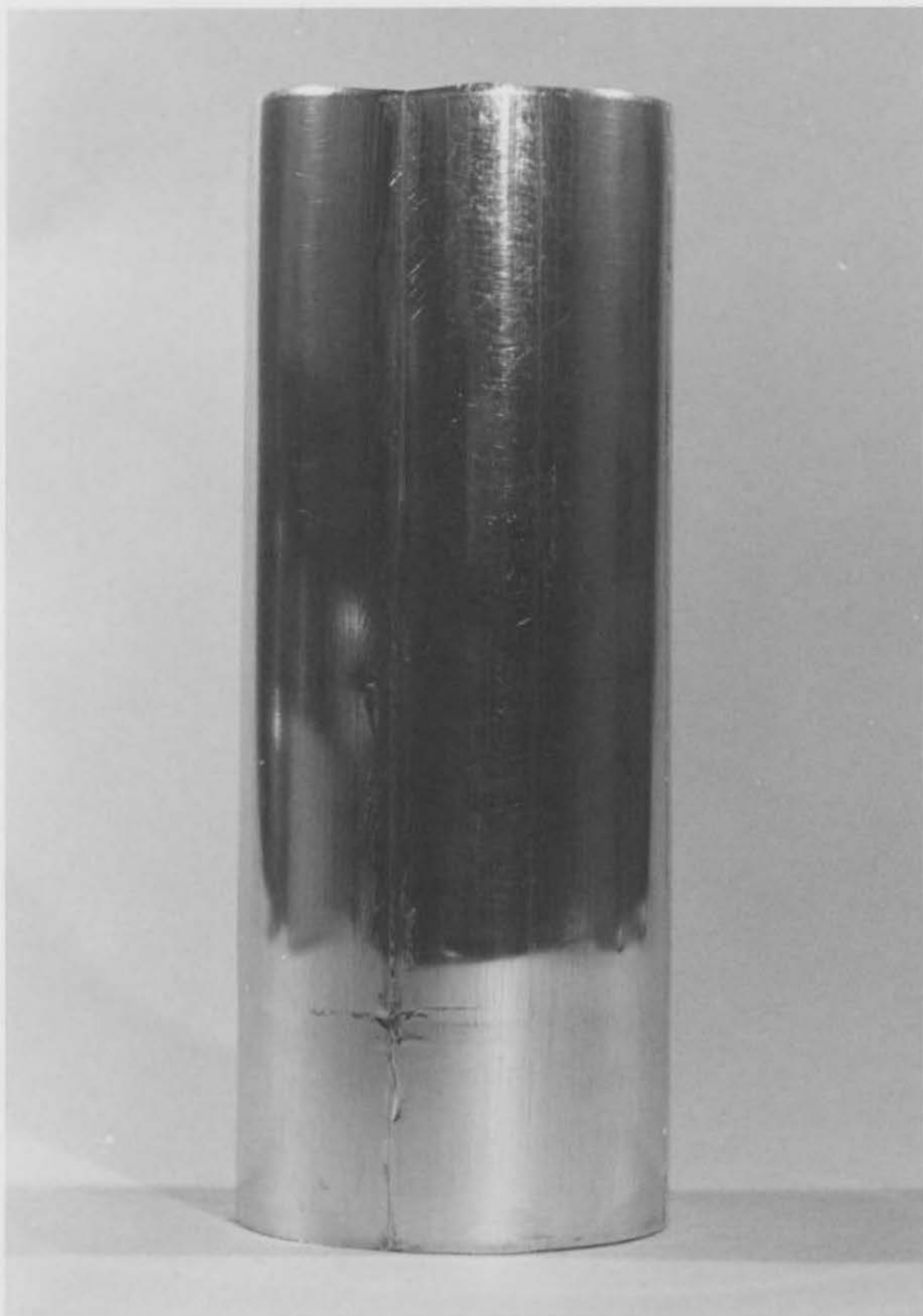


Figure 20- Backward extruded cup

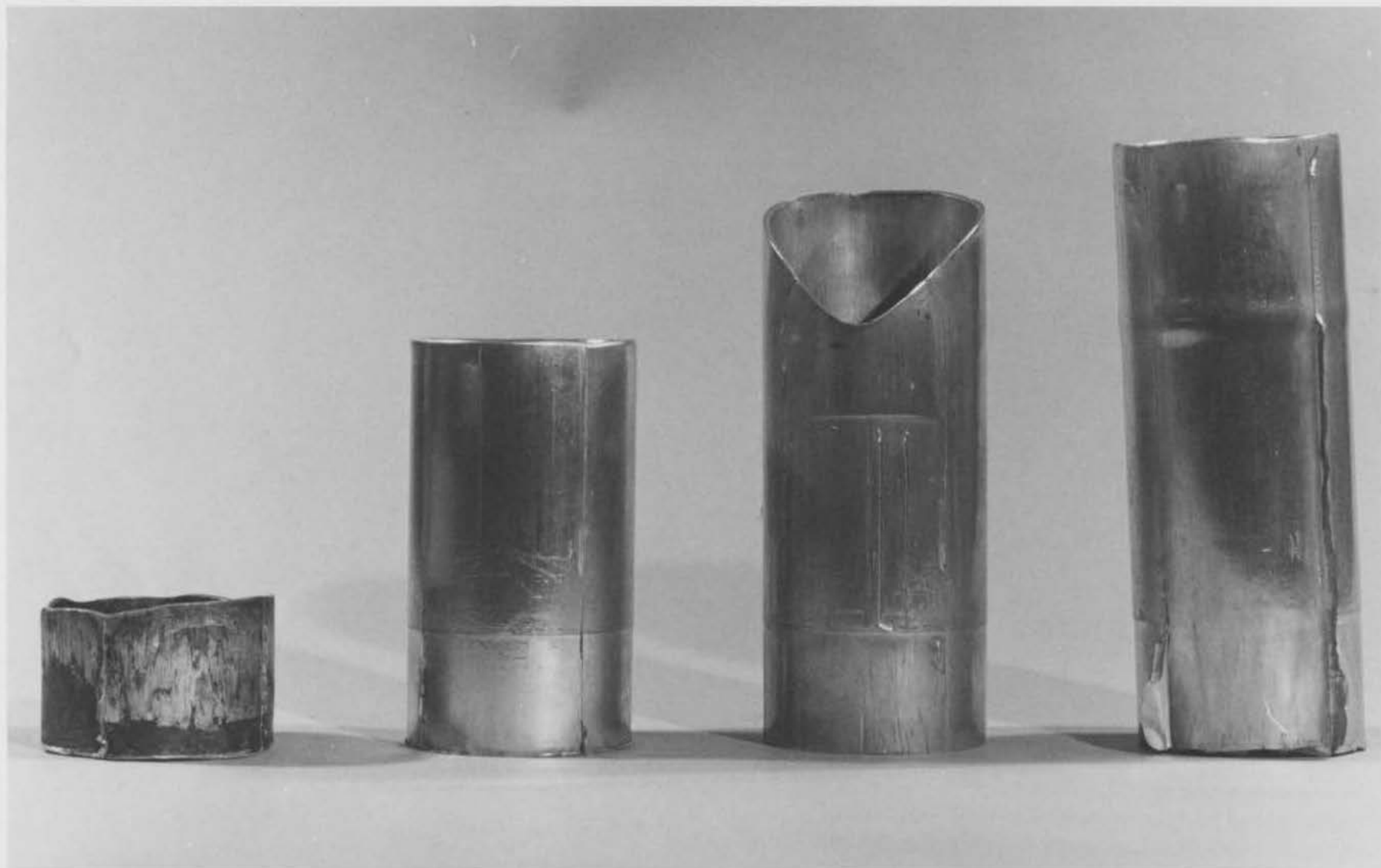


Figure 21-- L to R--(a) Cup extruded using graphite as lubricant. (b) Cup prior to modification of guide. (c) Effect of guide inclination. (d) Fully extruded cup with flash. (Sec. 7.4.2)

was still 2.132" to 1/2" above the undeformed slug. This was done with the expectation that after being reduced to the required thickness, the extruded material would follow the ram, staying clear of the die walls. Heavy duty gear box oil was used as a lubricant with this modification and this proved to be successful. A close-up of the final product is shown in fig. 20, whereas the various stages of development are shown in fig. 21.

7.4 Results and Discussion

7.4.1 Quantitative Results

The As-Cast material required a minimum load of 25,000 lbs (12,000 psi pressure) for extrusion to commence. Both the as cast and heat treated material were therefore tested at loads of 30,000, 50,000, 75,000 and 100,000 lbs load respectively. It was impossible to take readings at loads higher than 100,000 lbs as extrusion took less than 15 seconds.

Typical plots of the ram travel vs. time characteristics for both types of specimens are shown in fig. 22. A complete list of readings obtained is given in Appendix III.

Extrusion was found to proceed in three distinct stages represented by regions I, II and III on fig. 22 (a, b).

The first stage of extrusion is a non steady process in which the rate of extrusion is lower than in region II (as indicated by the smaller slope of the curve). In other words, higher pressures would be needed in region I if extrusion were to proceed at a constant rate. The extra pressure is required to compress the billet to fill out the die and induce the flow.

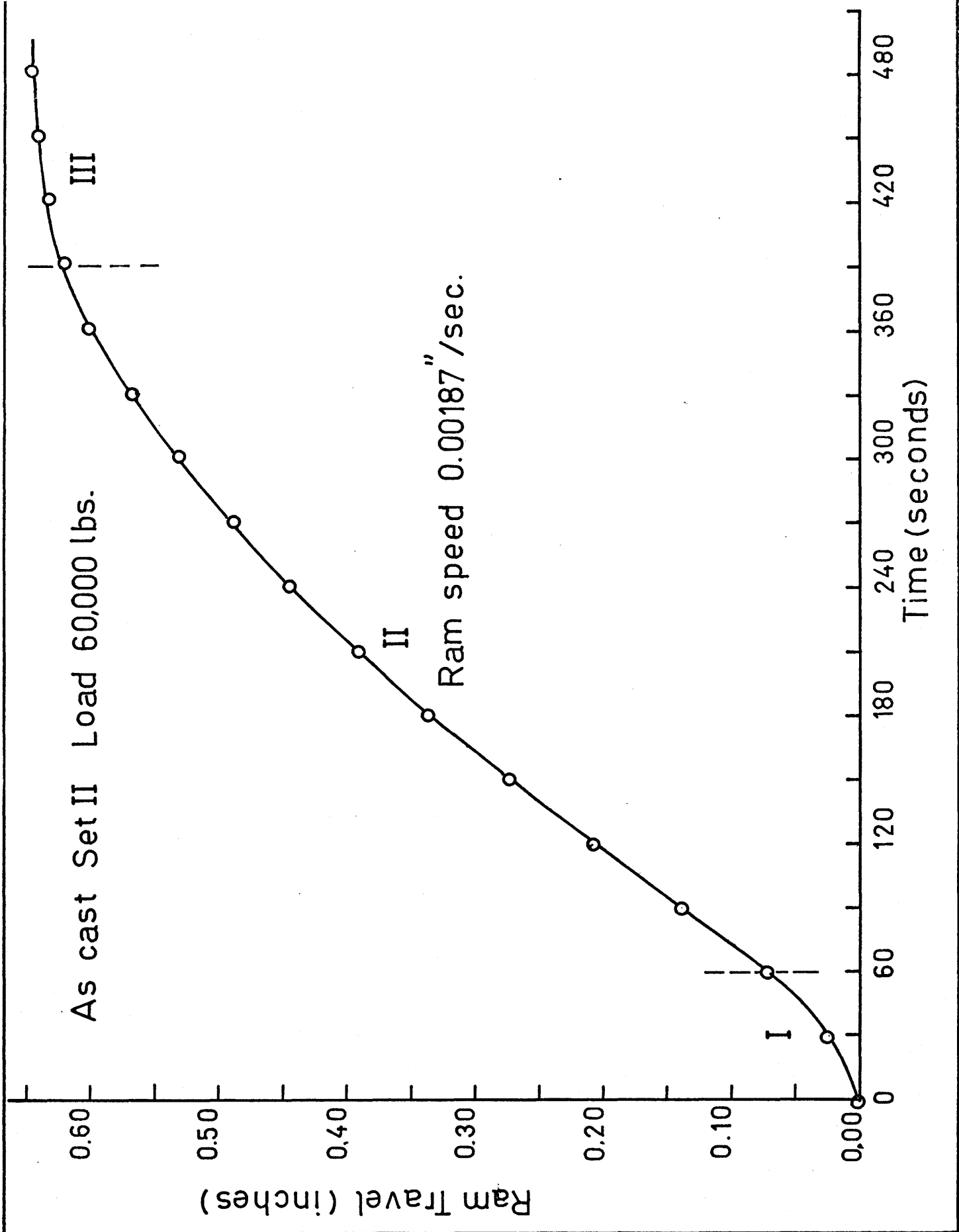


Figure 22 (a) - Ram Travel vs time for extrusion of as cast material.

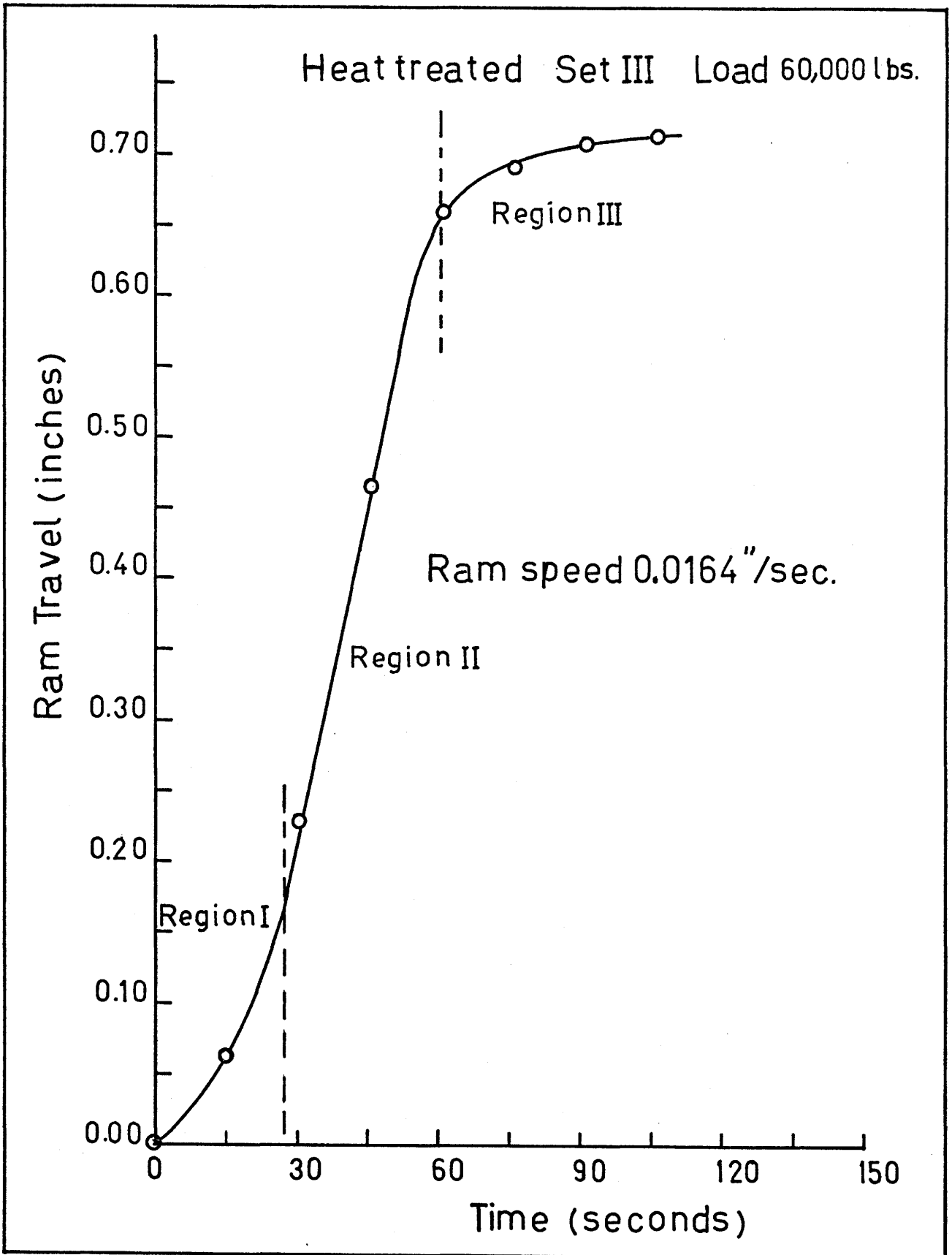


Figure 22 (b) - Ram Travel vs time for extrusion of heat treated Zn-Al.

Once the flow is established, extrusion proceeds at a steady rate (and hence constant pressure), as shown by the constant slope in region II.

The speed falls rapidly in region III as the compression effects and frictional resistance become more predominant as the thickness of the billet is reduced.

A second set of tests was performed in the same load range with specimens being taken from another section of the supplied billet to check the repeatability of the results. It was found that while the behaviour of the as cast specimens in the second set was in very good conformity with the first set, there was little similarity between the results for the heat treated material. The test results are again given in Appendix III.

In order to investigate this inconsistency further, the die was cleaned thoroughly and a third set of specimens was heat treated and tested. However, the ram speed-time characteristics again varied from those obtained in sets I and II (Appendix III).

A comparison of the steady state extrusion speeds for the various sets of tests on both as cast and heat treated materials is given in Table 4.

The wide discrepancy in the results on the heat treated material led to the suspicion that the specimens were only partially superplastic, and that the degree of superplasticity varied from set to set. A study of the microstructure of the undeformed specimens and extruded cups confirmed this suspicion. Some of these microstructures are shown in fig. 23. It was found that while the heat treated specimens had lost

TABLE 4
Loads and Extrusion Speeds

Load (lbs)	Steady State Ram Velocity (in./min.)					
	As Cast Set I	As Cast Set II	Heat Treated Set I	Heat Treated Set II	Heat Treated Set III	Heat Treated Set IV
30,000	0.018	+	0.014	—	—	0.209
40,000	—	—	—	—	0.070	—
50,000	0.070	0.090	0.040	0.120	0.240	1.280
60,000	—	0.112	—	0.207	0.980	—
70,000	—	—	—	—	1.100	—
75,000	0.320	—	0.247	—	—	—
80,000	—	—	—	—	*	—
100,000	0.900	0.900	0.572	1.710	—	—
125,000	*	—	—	*	—	—

— No Test Conducted.

* No readings could be taken as complete deformation took less than 10-15 seconds after test load was reached.

+ Test abandoned as ram speed was less than 0.010 inch/minute.



Figure 23(a)- As cast Zn-Al
billet X 1660

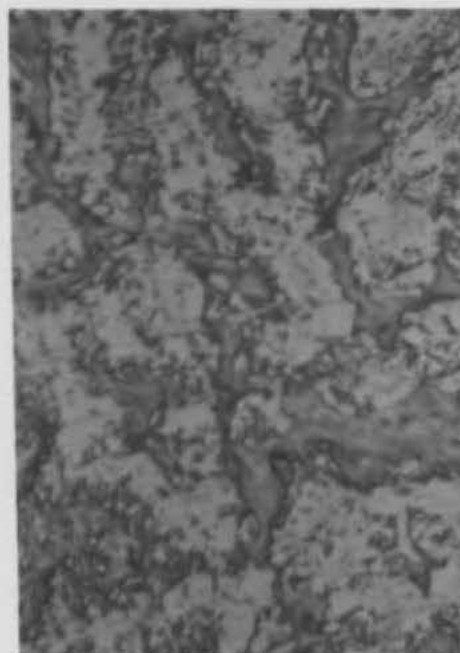


Figure 23(b)- Heat treated
billet (Set I)
X 1660

60μ

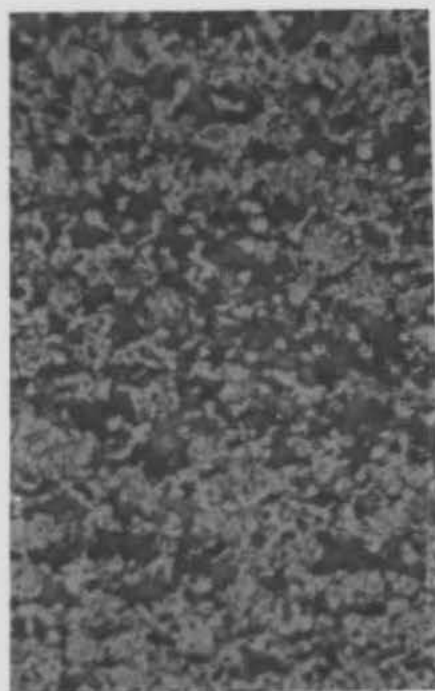


Figure 23(c)- Heat treated
Zn-Al after extrusion (Set III)
X 1660



Figure 23(d)- As cast Zn-Al
after extrusion X 1660

60μ

Figure 23- Microstructures of as cast and heat treated material

some of the preferred grain orientation characteristic of the non-superplastic state, the grain size ranged from 20 to 40 microns, far above the <10 micron requirement for superplasticity.

The fault was finally traced partially to the furnace and partially to the heat treatment given. A study of the temperature along the length of the furnace revealed that when the thermostat was set to 610°F (320°C), there was a temperature gradient of 175°F (95°C) from the back to the front of the furnace. Since the thermostat was controlled by a thermocouple connected to the back, the temperature at the front was only about 225°C while the indicator read 610°F (320°C). Since such a large gradient had not been expected, the specimens had been placed anywhere from the back to the middle of the furnace, which meant that the different sets (and in some cases even specimens within one set) had not been subjected to the same heat treatment.

Further, it was found that a soaking time of two hours at 320°C was not sufficient for the material to homogenise fully and become amenable to superplastic transformation. Through a process of trial and error, it was determined that the best microstructure was obtained by keeping the specimens in the furnace at 350°C for a period of 6-8 hours and quenching them in ice-cold water for 30 seconds. The superplastic transformation was accompanied by release of a large amount of heat--sufficient to raise the temperature of the specimen to approximately 80°C, and by a change in surface colour from silver-white to a dull grey.

A set of 8 slugs was subjected to the above-mentioned heat treatment and the microstructure of each was checked to ensure that they

were all superplastic. Fig. 24 shows the microstructure typical of this set. Only two specimens were tested from this set - at loads of 30,000 and 50,000 lbs. as the rig was damaged in an accident and would have required a few days to repair. Since it was felt that the data obtained from these two tests along with the information gained from the others was sufficient to complete the intended study of the extrusion process, no further investigation was made. The results of these tests are also presented in Table 4 and Appendix III.

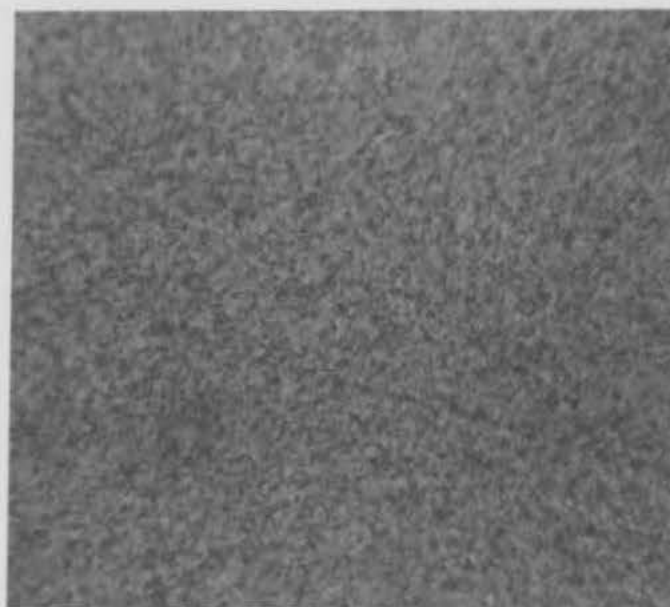
The data of Table 4 is plotted in fig. 25 on a log-log scale.

Since the load used is proportional to the extrusion pressure and the ram velocity is proportional to the strain rate, the slope of the log load vs. log velocity curve (fig. 25) represents the strain rate sensitivity for the material.

Both as cast and superplastic material were found to have a m value of .296, which is to be expected, as the tests on superplastic material were conducted in the high strain rate region. Nevertheless, considerable advantage may still be gained from the use of superplastic material in terms of load reduction. For instance, while the as cast material required 65,000 lbs load to achieve a ram velocity of .2"/minute only 30,000 lbs load was required to obtain the same strain rate in superplastic material (fig. 25c)

7.4.2 Qualitative Aspect

Co-axiality of the ram and die was essential to obtain cups of uniform wall thickness and length. Since the guide recess and die had been machined to maintain a close fit, some care had to be exercised to



60μ

Figure 24- Microstructure of superplastic
Zn-Al (Set IV) X 1660

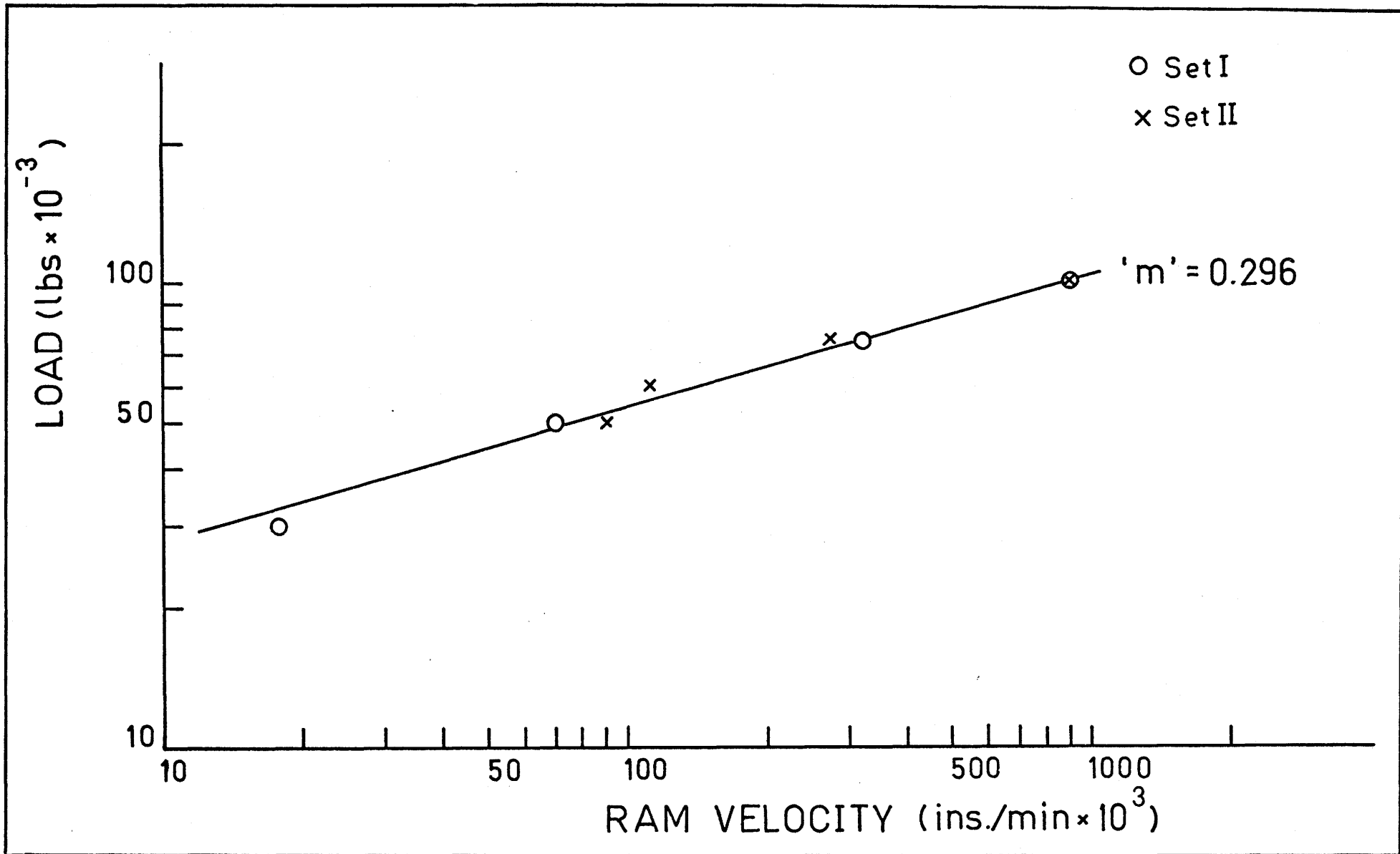


Figure 25 (a) - Load-Velocity characteristics for as cast material.

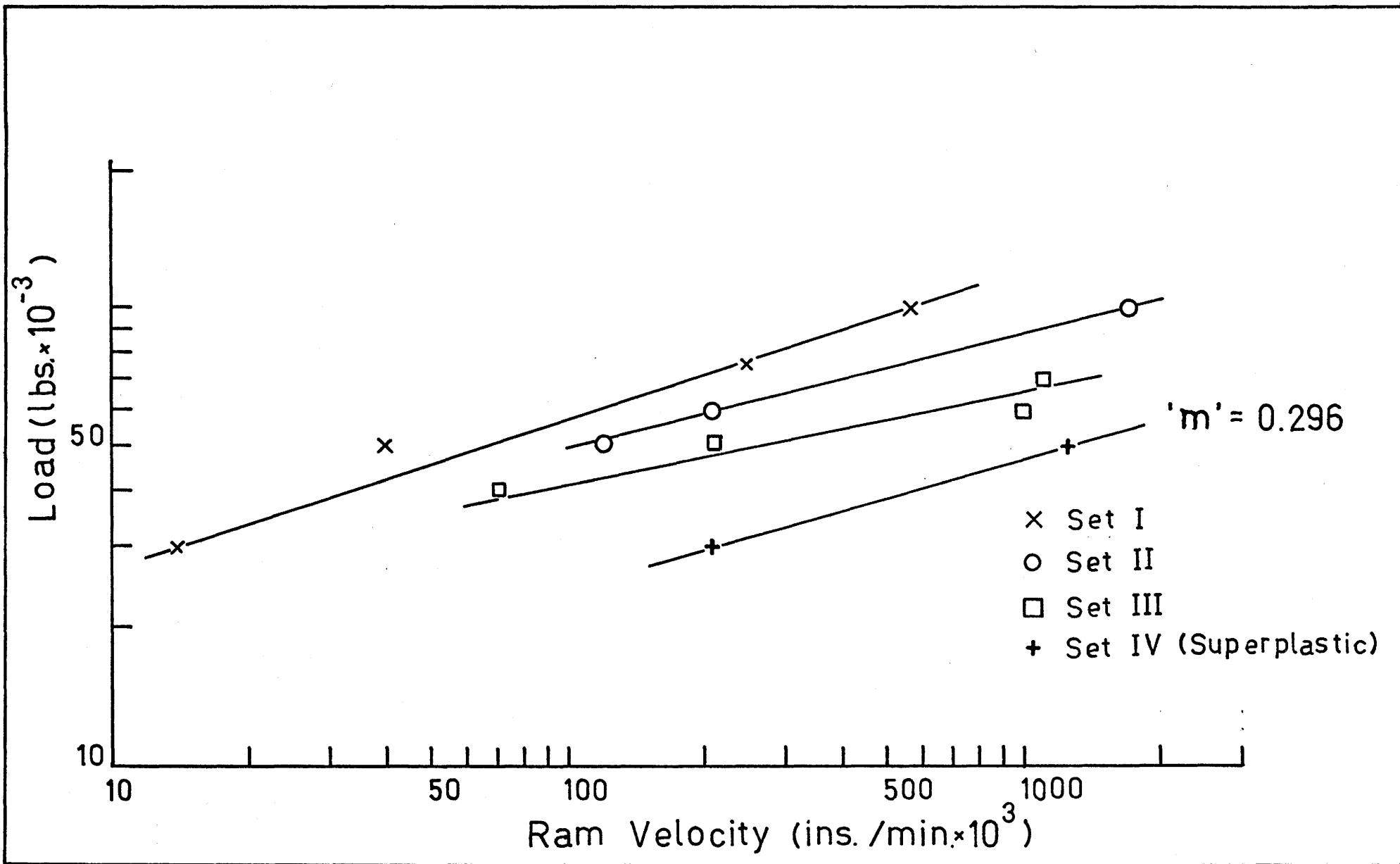


Figure 25 (b) - Load-Velocity characteristics for heat treated material.

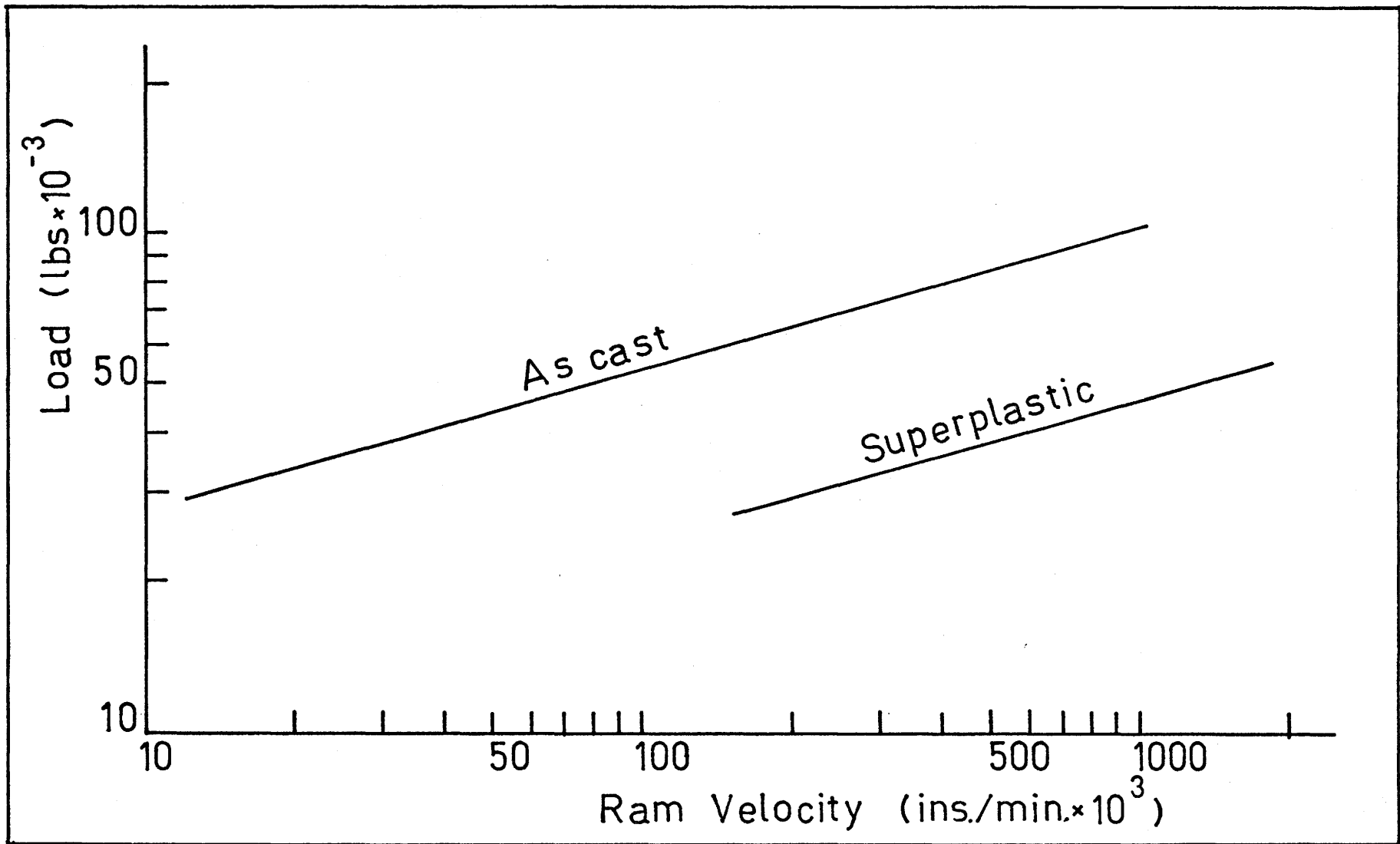


Figure 25 (c) - Load-Ram Velocity characteristics for as cast and superplastic Zn-Al reproduced for comparison.

to ensure proper positioning of the guide. Otherwise the guide (and hence the ram) sat at an angle, and cups of uneven wall thickness and length were formed (fig. 26).

The flange desired on the top of the cup could not be formed except by subjecting a fully extruded cup to a load of 100,000 lbs for about 5 minutes. For fear of excessive stressing of the die, the original plan of holding the cup in the expansion rig by the flange was abandoned and it was decided to use longer preforms in a process in which material would be drawn into the die and stretched out to shape. To obtain longer cups, the bottom 1.6" of the guide bore was increased to 2.160" and the extruded cup was allowed to continue into the space between the ram and guide thus created. The as cast material of Set II and the heat treated specimens of Sets II, III and IV were extruded with this modification. 0.85" thick slugs were used (Appendix II).

It was found that at low strain rates, the material in the wall did not move up the punch without deformation, but tended to thicken and fill the space between the punch and the relieved die wall. However, at higher loads, with strain rates approaching those in conventional extrusion, this problem was not encountered.

On the other hand, at high strain rates the material had a tendency to flow into the small gaps between the sections of the die and the die bottom, the amount of resultant flash increasing with load.

For the as cast material, loads between 60,000 to 75,000 lbs yielded a satisfactory compromise between these two defects. Cups produced in this load range had good surface finish except for a small degree

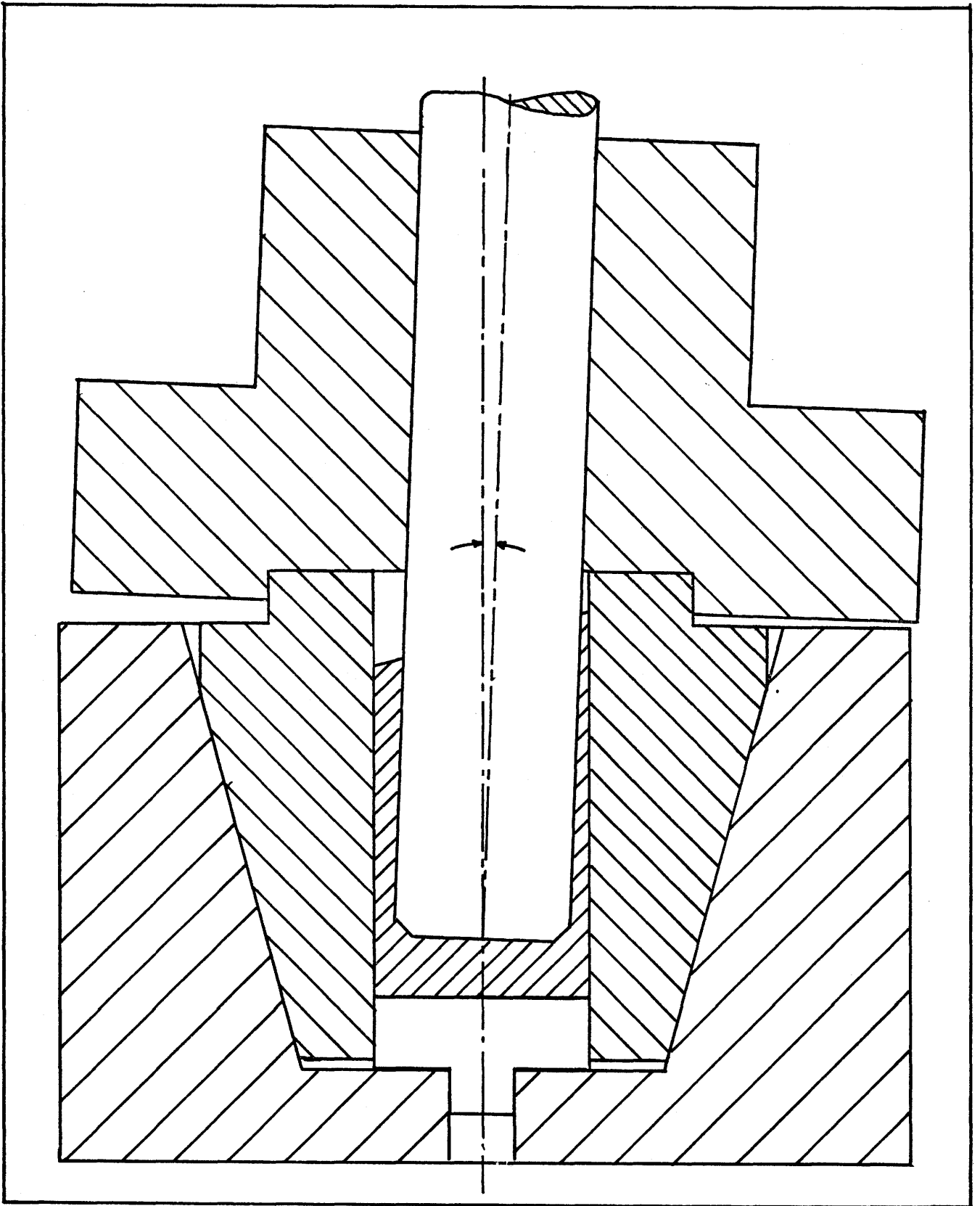


Figure 26 - Effect of misalignment of guide.

of flash. The wall thickness at the top was 0.0735" \pm .0025 and the inside diameter 2.000" \pm .002.

With the superplastic material, 30,000 lbs load yielded a cup totally free from both defects. Surface finish was excellent and there was no flash on the side or bottom. Measurements made on the internal and external diameters of the cup along its length showed that these two dimensions were 2.000" \pm .002 and 2.133" \pm .002 respectively - which compare very favourably with the designed values of 2.000" and 2.132".

7.5 Theoretical Analysis

Since superplastic materials are highly strain rate dependent, techniques such as the upper bound methods used to study extrusion of conventional metals cannot be applied directly to these materials.

It is suggested that a treatment similar to the semi-empirical technique now used to estimate extrusion pressures in strain-hardening materials is required. One such possible approach for extrusion through a conical orifice is developed below.

The extrusion pressure is given by

$$p = \bar{\gamma} \cdot \bar{\epsilon} \quad (16)$$

where $\bar{\epsilon}$ is the equivalent strain in the process and $\bar{\gamma}$ is the mean yield stress in uniaxial compression.

Johnson⁽⁵¹⁾ has shown that for the extrusion of a strain hardening material through a square die, the mean strain for the process may be calculated from the empirical relationship

$$\bar{\epsilon} = 0.8 + 1.5 \ln \frac{1}{1 - r} \quad (17)$$

where r is the reduction.

It is here assumed that this relation may also be used for conical dies without too much loss in accuracy.

Since the strain rate at different points along the orifice length varies, the yield stress is not constant and a mean value must be determined if Eqn. 15 is to be used to estimate the extrusion pressure. An assumption is here made that the mean flow stress for the process is the same as the flow stress at the mean strain rate.

The mean strain rate may be determined from consideration of flow rates and volume of the deformation zone.

If the steady state ram velocity is v and the cross-section area at the end of the punch is A_2 , then volume of material entering the deformation zone/time is

$$V_1 = A_2 \times v \quad (18)$$

Time required for the material to pass through the deformation zone is given by

$$t = \frac{V}{V_1} = \frac{V}{A_2 \times v} \quad (19)$$

where V is the volume of the deformation zone.

The mean strain rate will then be

$$\dot{\epsilon}_{av} = \frac{\bar{\epsilon}}{t} \quad (20)$$

The flow stress at this strain rate can be obtained from the compression test characteristics of the material and Eqn. 15 can be used to estimate the extrusion pressure.

At high and low strain rates, the strain rate dependence of flow

stress is lower than in the intermediate range. Hence the error introduced by making the assumption mentioned may be expected to be considerably lower in the high and low strain rate regions than in the intermediate range. If the superplastic properties of a material are to be industrially exploited in extrusion, the strain rates would have to be necessarily high and the approach outlined above may be effectively used to predict extrusion pressures.

In the present case (fig. 27)

$$r = 1 - \frac{\text{Area of extrusion orifice at exit}}{\text{Area of container}}$$

$$= 1 - \frac{.429}{3.570} = .88$$

$$\therefore \bar{\epsilon} = 0.8 + 1.5 \ln \frac{1}{1-.88}$$

$$= 3.8783$$

Volume of deformation zone, $V = .1838 \text{ in}^3$.

For extrusion of superplastic material at 30,000 load (Test 1, Heat treated set IV) .

Ram velocity $v = .2086 \text{ in/min}$.

\therefore Volume of material entering deformation zone/minute

$$V_1 = .4326 \text{ in}^3/\text{minute}$$

Hence $t = \frac{V}{V_1} = .4249 \text{ minutes}$

$$\therefore \bar{\dot{\epsilon}} = \frac{\bar{\epsilon}}{t} = 9.127/\text{minute}$$

Flow stress at this strain rate ^(1,20)

$$\bar{\gamma} = 3,600 \text{ psi.}$$

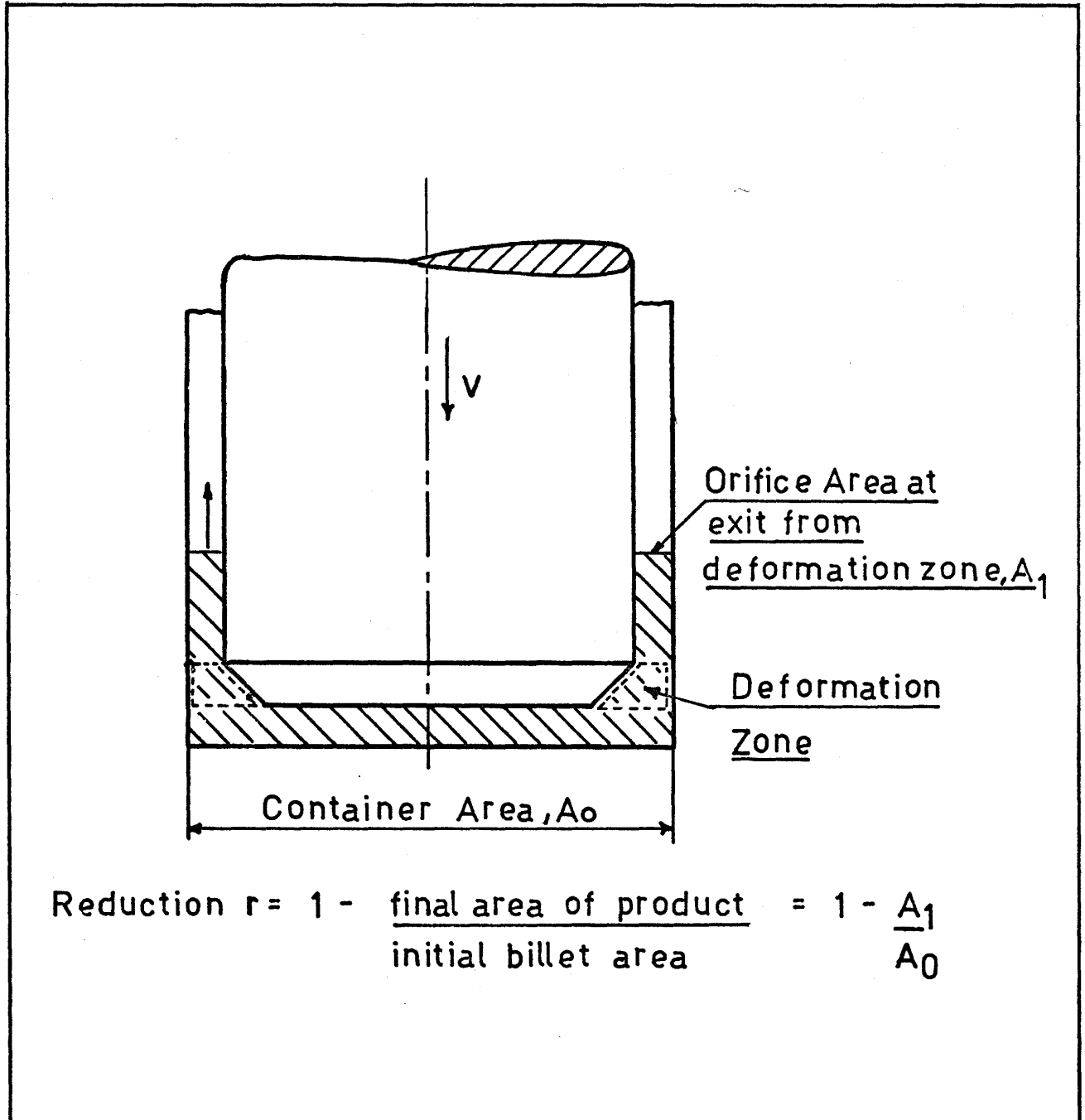


Figure 27 - 'Deformation zone' and 'reduction' defined for backward extrusion through a conical die.

$$\therefore p = \bar{\gamma} * \bar{\epsilon} = 13,962 \text{ psi.}$$

$$\begin{aligned} \text{Extrusion pressure used} &= \frac{\text{Load}}{\text{Area of ram at end}} \\ &= \frac{30,000}{2.074} = 14,464 \text{ psi.} \end{aligned}$$

Thus the extrusion pressure has been estimated to within 5% of the experimental value obtained.

Strain rates for various points on the load-velocity characteristics for as cast and superplastic material have been calculated as above and are presented in Table 5.

The theory could not be checked at the 50,000 lb load level as the yield stress value at the strain rate achieved was not available.

7.6 Conclusions

Some difficulty was experienced in the choice of proper lubricant for extrusion of Zn-Al eutectoid alloy. After experimentation with various lubricants, heavy duty gear box oil was found to be satisfactory, except that at the test temperature (250°C), it emitted fumes which had a rather unpleasant odour.

A fine grained equiaxed structure was achieved by quenching from above the invariant temperature of 275°C. Best results were obtained by holding at 350°C for 6 to 8 hours and quenching in ice-cold water for 30 seconds.

The tests showed that even at strain rates above an estimated value of 10/minutes (which are industrially viable but fall in the high strain rate region where the benefits to be derived from superplasticity

TABLE 5

Strain Rates for Extrusion of As Cast and Superplastic Zn-Al

Load (lbs)	Strain Rate (/min.)	
	As Cast	Superplastic
20,000	--	2.10
40,000	1.53	24.95
50,000	3.33	56.02
60,000	6.35	107.22
100,000	39.39	--

are minimum), considerable advantage could be gained from superplasticity in terms of load reduction.

A theoretical approach was developed to predict extrusion pressures for superplastic materials. It is concluded that while it may be used to estimate extrusion pressures at high strain rates with good accuracy, further refinement may be required for accurate estimation in the intermediate strain rate range.

CHAPTER 8

MACRO AND MICRO FORMING

8.1 Rubber Plug Forming

8.1.1 Choice of Rubber

The stringent requirement of a forming temperature of 250°C at once narrowed the choice to silicone rubbers since these seem to be the only rubbers that may be used at high temperatures. Silastic 601 RTV silicone rubber marketed by the Dow Corning Corporation was selected as the sales catalogue suggested that this material could be used for up to two weeks at 500°F (235°C).

8.1.2 Preparation of Plug

A steel plug 2" diameter, 1/2" length was made and a 3/8" hexagonal bolt was fixed in it so that the rubber plug could be cast over it. A 2" diameter cardboard mailing tube was lined with paper to reduce the I.D. to 1.95". This tube was placed over the steel plug, the rubber and its curing catalyst were thoroughly mixed in the prescribed proportions, and the mixture was poured into the tube. The rubber was de-aired in a vacuum chamber as required and allowed to cure for 48 hours at room temperature. The cardboard tube was stripped off the cured plug which was then cut to 9" length.

8.1.3 Test and Results

The extruded preform was placed in the expansion die and the equipment was assembled. The plug was placed in the guide and the rig was heated to 250°C.

A load of 2000 lbs was required before the rubber ram moved at all. The pressure was increased in small steps but at about 3,000 lbs load the ram suddenly collapsed, crumbling up into small pieces. The incompletely formed component is shown in fig 31.

Some silicone rubber foam (SILASTIC S-5270 RTV foam from Dow Corning) was added to the rubber and catalyst mix in an attempt to make a more flexible ram. However, a plug cast from this mixture failed to cure even after four days at room temperature and two days at 150°C.

This part of the project was abandoned as a more promising rubber could not be found. Nevertheless, it is evident from the results obtained that the process would definitely be feasible if suitable material becomes available. The degree of reproduction of surface detail would, of course, depend on the pliability of the rubber.

8.2 Internal Pressurisation

8.2.1 Additional Equipment

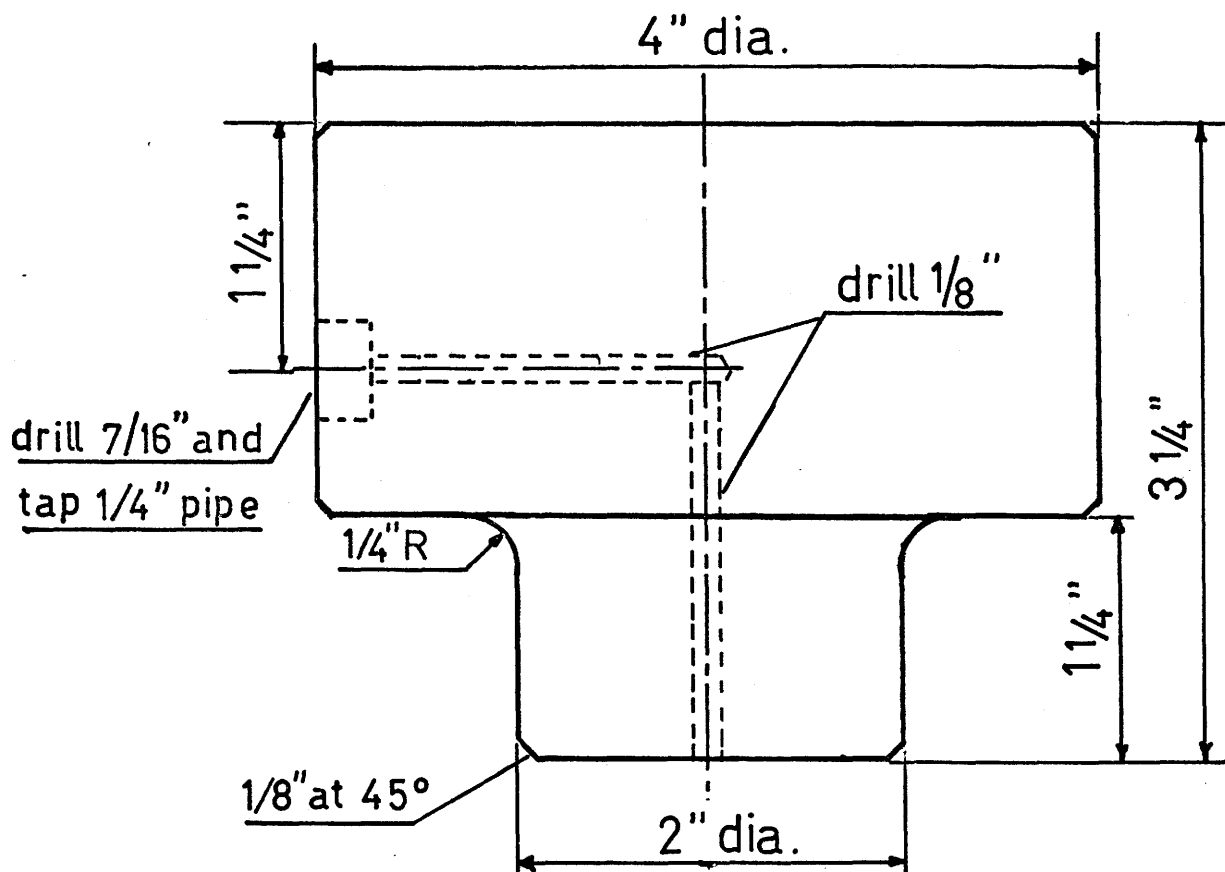
It had originally been planned to expand the tubular specimens by supplying air under pressure through the top of the guide. Since the cup could not be flanged in the extrusion process, this was not feasible as adequate sealing could not be provided.

The plug shown in fig. 28 was designed to apply air pressure and to prevent pressure loss from inside the cup.

A 60,000 lb capacity hydraulic press was used to supply the sealing pressure. Exploded view of the equipment is shown in fig. 29.

8.2.2 Test Procedure

The specimens were heat treated again and the microstructure



Tolerances: $\pm 1/64$ "

Plug	Drg.No.P0010
Mech Engg	Scale 1:1
McMaster U.	K.K.Jain
Hamilton,ONT.	Feb,172

Figure 28 - Plug for sealing and application of air-pressure in expansion experiments.



Figure 29- Pressure forming equipment

was checked to ensure that they were superplastic.

The specimen was placed in the die and the plug was pushed into it and connected to a bottle of compressed air through 1/8" copper tubing. The die was heated to 250°C. Heat loss from the top was minimized by completely covering with asbestos sheet and fibreglass wool.

A small load, about 200 lbf, was applied to the plug. This was sufficient to form the top of the cup along the radius on the plug and also to push the cup slightly into the die. The air-supply valve was opened and the air pressure increased in small steps. Even at 25 psi internal pressure, the cup started to expand laterally, drawing more material into the die. Air pressure was increased progressively and the load on the plug was simultaneously adjusted to provide just sufficient pressure to prevent air from leaking. This was continued till only about 3/8" of the cup remained above the die. The air pressure at this stage was approximately 75 psi and the sealing load 1,500 lbs. The load was then raised to 3,000 lbs to grip the edge of the cup between the plug and the die. The air pressure was quickly increased to the test value and maintained for the required time.

8.2.3 Results and Discussion

A number of combinations of pressure and holding time were tried- 100 psi for 3 minutes, 200 psi for 2 minutes, 250 psi for 1.5 minutes, 5 minutes, 20 minutes, etc. In all cases macroforming was found to be complete, though the degree of forming into the V grooves and reproduction of detail from coins attached to the outside surface of the cup depended strongly on the pressure and holding time. Best results were obtained by applying 250 psi pressure for five minutes.



Figure 30- Pressure formed cup--250 psi, 5 minutes



Figure 31- L to R -- (a) Rubber plug formed cup (b) Wrinkle produced due to excessive sealing load (c) Premature rupture due to localised thinning in semisuperplastic preform (d) As cast cup-- held at 250 psi for 20 minutes (e) Superplastic preform--250 psi for 1.5 minutes

The V-groove forming was complete and uniform around the circumference and reproduction of minute details was excellent. The surface finish on the formed part exactly matched the surface on the die.

Longer holding times at the same pressure failed to produce better results, showing that complete forming was obtained within 5 minutes.

Application of 250 psi pressure for 1.5 minutes produced good surface detail. V-groove forming, though almost complete, was not quite uniform around the circumference leading to the conclusion that about two minutes were required for complete microforming.

A cup extruded from as cast material was expanded under 250 psi pressure applied for 20 minutes. While the macroforming was good, microforming was extremely poor.

Some of the formed components are shown in figs. 30 and 31.

8.3 Conclusions

Rubber plug forming had to be abandoned for lack of availability of suitable material. The tests did show, however, that the process was feasible.

Air pressure forming was extremely successful. Complete macro and micro forming was achieved within 5 minutes at 250 psi.

CHAPTER 9

GENERAL CONCLUSIONS.

From the plethora of papers that have appeared in the literature in the past 3-4 years on various aspects of superplastic deformation, it is evident that interest in this field is spreading fast. Industrial exploitation of superplasticity is rather limited and only a few superplastic materials are commercially available. However, it is almost certain that industrial application of superplasticity will increase greatly as researchers discover techniques to impart superplasticity to more and more materials and to further reduce work loads at industrially viable strain rates.

In the present work, some insight has been gained into the pressures and time required and the problems associated with the production of hollow components from billet material using extrusion followed by pressure forming. It is concluded that superplasticity may be used to advantage in terms of load reductions in extrusion. The pressure forming process becomes specially attractive if components with minute surface detail are required.

One of the principal objectives of this work was to obtain sufficient information to permit an industrial process to be developed. This has been achieved but as the details of this process cannot be made public at the present time, it is described in a codicil to this dissertation.

SUPPLEMENT

A possible industrial process for producing hollow components from superplastic billet material is presented and discussed below.

A preliminary design for the suggested equipment is shown in fig. 32. A billet of the material, 3, is placed in the extrusion container, 1, and forward extruded over the mandrel, 6, through the extrusion die, 4. At the end of the extrusion process pressure is applied through the orifices 8, to expand the workpiece, 7, out to the shaped moulding die, 5, which is split to facilitate removal of the formed part. The end of the extruded workpiece is gripped by a sliding collet, 10, to prevent pressure loss and permit axial drawing of the workpiece into the mould during forming.

If the extrusion ram was, for example, 1 inch diameter, the load required would be as indicated in Table 6. This is calculated for extrusion of superplastic Zn-Al at 250°C using data from fig. 25. The time taken is that to produce a cup as shown in fig. 33.

The time to produce the overall shape (macroforming) is not long. If it is assumed that the circumference increases by 87% as in fig. 33 and that the superplastic properties are maintained up to a strain rate of 10/minute, then the forming time is 3.72 seconds. The subsequent time to complete forming of detail will depend on the particular die, but assuming that the case demonstrated is typical and that the forming was completed in 2 minutes at 250 lbf/in², then the microforming times should be as shown in Table 7.

It is therefore demonstrated that a total forming time of 52 seconds is possible in this process without requiring excessive forming

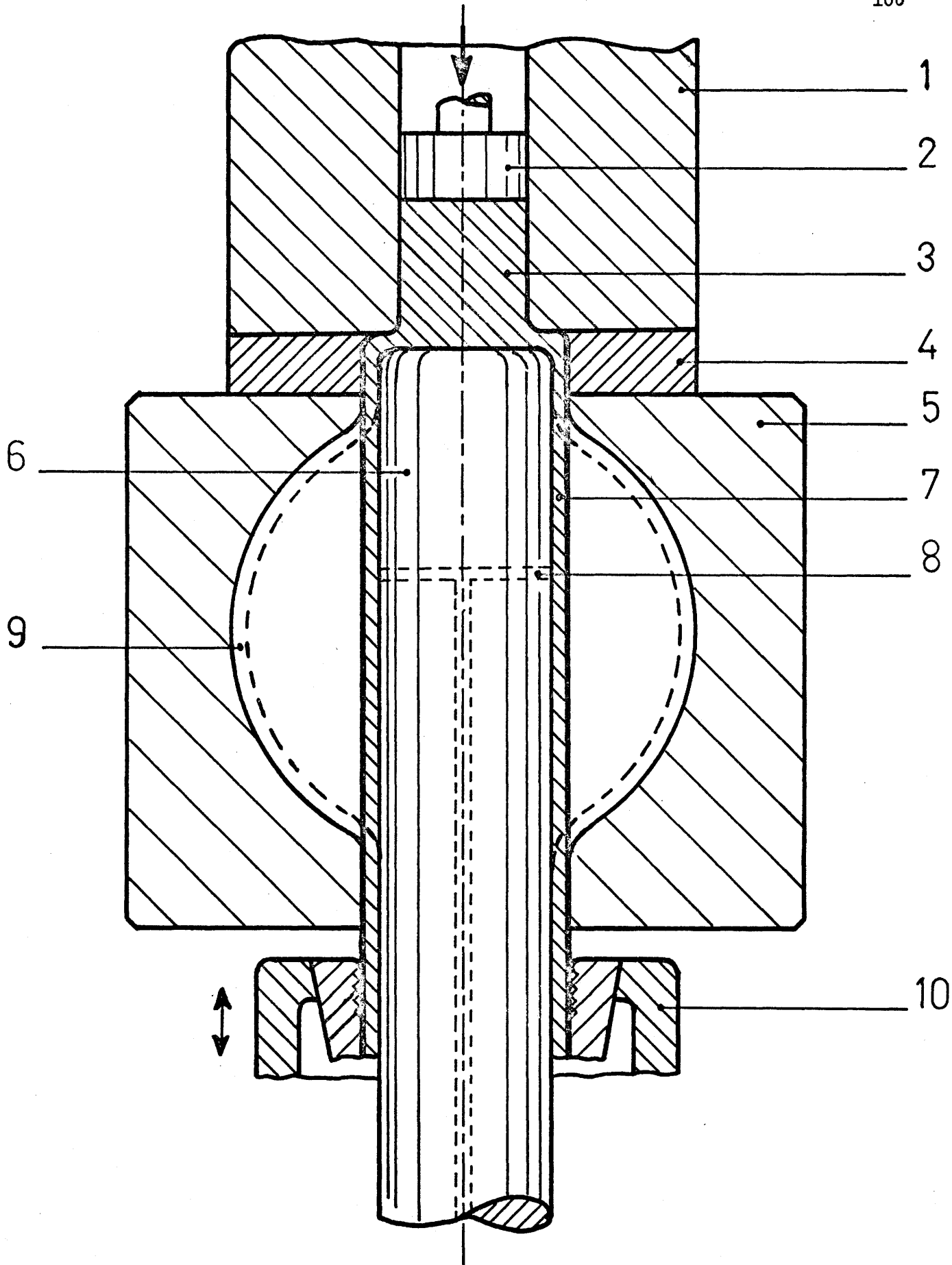


Figure 32 - Preliminary design of Production Machine.

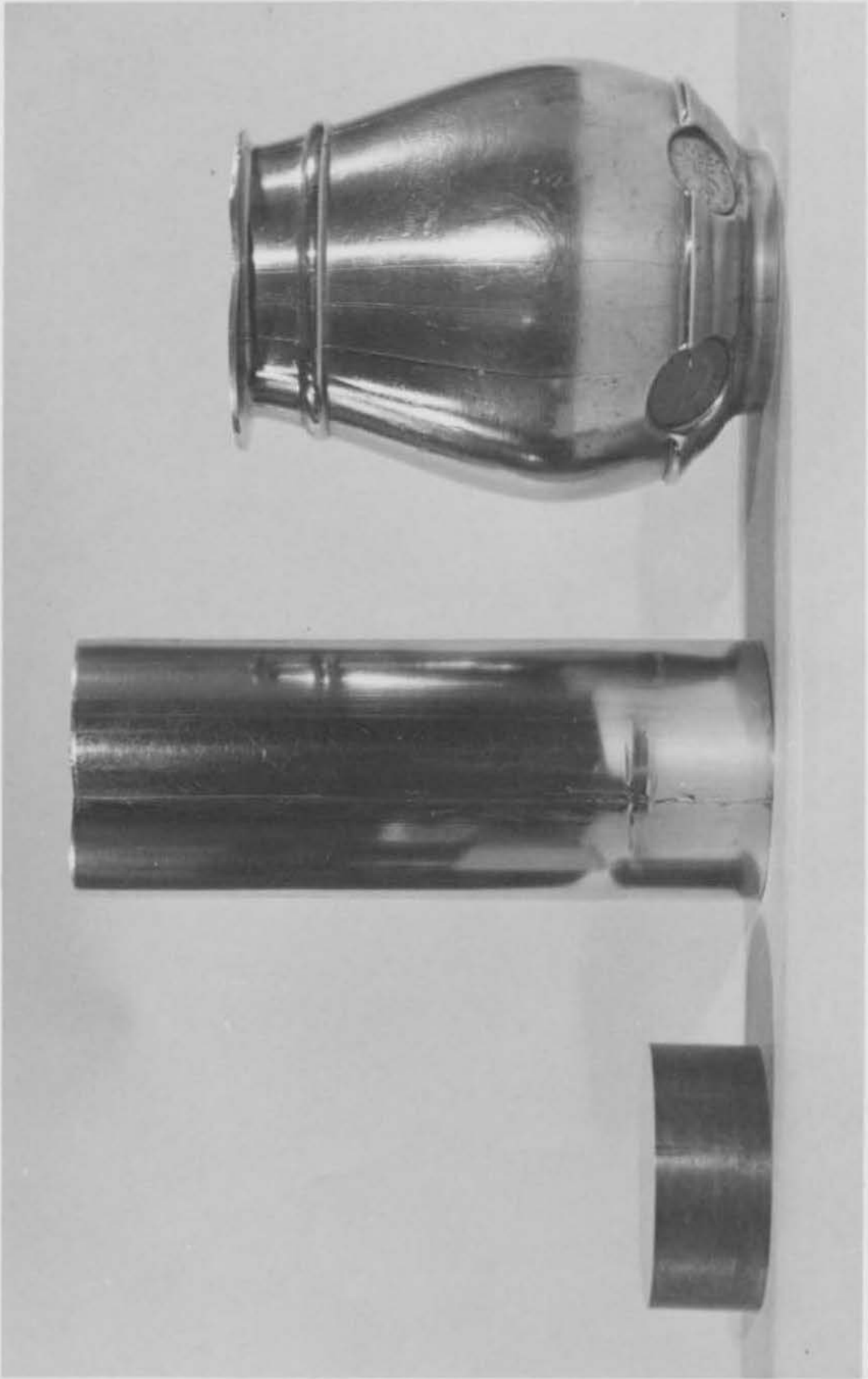


Figure 33- Development of a shaped hollow component from billet

TABLE 6

Ram Loads and Extrusion Time

Ram Load (lbs)	Ram Speed (in./sec.)	Extrusion Time (secs)
15,000	0.160	19
12,500	0.085	38
10,000	0.038	84
7,500	0.013	230
5,000	0.003	1,000

TABLE 7

Microforming Pressures and Time

Microforming pressure (lbf/in. ²)	Microforming time (secs.)
150	517
250	120
300	71
400	32

loads and pressures. Assuming a time of 15 seconds for loading and unloading the die in an automated machine, the output should be 54 pieces per hour.

The material for this process is an as cast Zn-Al billet. The raw material costs, based on metal prices of \$400/ton for .9999 Zn and \$550/ton for .995 Al ingots is 21.65 ¢/lb. An economic assessment of the product cost is not easy because the process is novel, but the following attempt is presented.

Material Cost

Raw material	14.38 ¢
Casting billet	}
Cleaning cast billet	
Heat treatment of billet	
	<u>15.38 ¢</u>

Tooling Cost

Estimated cost of tooling	\$2,000
Tool life estimate 10,000 parts	
∴ Tool Cost	20¢/part

Machine Cost

Estimated cost of production machine	\$9,000
Amortizing machine over 3 years, assuming	
1,500 hrs/year	\$2/hr

Labour Cost	\$6/hr
Overhead (50% of direct labour)	\$3/hr
∴ Machine, labour, overhead costs	\$11/hr
Power, heat cost	\$1/hr
∴ Machine, labour, power etc.	\$12/hr
	= 22.22¢/part
∴ Basic part cost	= 57.60¢/part

REFERENCES

1. W.A. Backofen, I.R. Turner and D.H. Avery, Trans. A.S.M. 57 (1964), 980.
2. W. Rosenhein, J.K. Haughton and K.E. Bingham, J. Inst. Metals, 23 (1920), 261.
3. C.E. Pearson, J. Inst. Metals, 54 (1934), 111.
4. A.A. Bochvar and Z.A. Sviderskaia, IZV Akad. Nauk, U.S.S.R. 9 (1945), 821.
5. A.A. Presnyakov and V.V. Chervyakova, Fiz. Metal, Metaloved, 8 (1959), 114.
6. A.A. Presnyakov and G.V. Starikova, Fiz. Metal, Metaloved, 12 (1961), 873.
7. E.E. Underwood, J. of Metals, 14 (1962), 914.
8. D.L. Holt and W.A. Backofen, Trans. A.S.M. 59 (1966), 755.
9. D.M. Avery and W.A. Backofen, Trans. A.S.M. 58 (1965), 551.
10. C. Rossard, Rev. Met., 63 (1966), 225.
11. J.L. Duncan, E. Shapiro, J. Crane and D.M.R. Taplin, "Applications of Solid Mechanics" symposium, U. of Waterloo, Waterloo, Ontario, June 1972.
12. A.R. Ragab and J.L. Duncan (to be presented at the International Conference of Plasticity, 1972, Poland).
13. D. Oelschlagel and W. Veiss, Trans. A.S.M., 58 (1966), 143.
14. R.H. Johnson and E.C. Sykes, Nature, 209 (1966), 192.
15. D.M.R. Taplin, P. Rama Rao and V.V.P.K. Rao, Proc. Silver Jubilee Conference, Indian Institute of Metals, Delhi, February 1972.

16. C.M. Packer and O.D. Sherby, Trans. A.S.M., 60 (1967), 21.
17. D. Lee and W.A. Backofen, Trans. Met. Soc. AIME, 236 (1966), 1637.
18. N.J. Petch, J.I.S.I. 174 (1953), 25.
19. S.W. Zehr and W.A. Backofen, Trans. A.S.M., 61 (1968), 300.
20. H. Naziri and R. Pearce, Int. J. Mech. Sci., 12 (1970), 513.
21. M. Hansen, Constitution of Binary Alloys, McGraw-Hill, Second Edition.
22. R.H. Johnson, Met. Rev., 146 (1970), 115.
23. G.J. Davies, Edington, J.W., Cutler, C.P. and Padmanabhan, K.A., J. Mat. Sci. 5 (1970), 1091.
24. K. Nuttall and R.B. Nicholson, Phil. Mag., 17 (1968), 1087.
25. W.A. Backofen, F.J. Azzarto, G.S. Murty and S.W. Zehr, "Ductility", A.S.M. (Cleveland), (1968), 279.
26. D. Lee, Acta. Met. 17 (1969), 1057.
27. T.H. Alden, Acta. Met. 15 (1967), 468.
28. D.L. Holt, Trans. A.I.M.E. 242 (1968), 25.
29. C.M. Packer, R.H. Johnson and O.D. Sherby, Trans. A.I.M.E. 242 (1968), 2485.
30. C. Herring, J. App. Phys. 21 (1950), 437.
31. R.F. Coble, J. App. Phys. 34 (1963), 1679.
32. A Karim, Scripta Met. 3 (1969) 887.
33. M.F. Ashby, Scripta Met. 3 (1969), 837.
34. Burton, B., Scripta Met. 5 (1971), 669.
35. A. Karim and W.A. Backofen, Met. Trans. 3 (1972), 709.
36. D. Lee, Scripta Met. 3 (1969), 893.
37. E. Orawan, Reports Prog. Phys., 12 (1948-49), 185.

38. G.L. Dunlop and D.M.R. Taplin, J. Aus. Ins. Met. 16 (1971), 195.
39. W.A. Backofen, G.S. Murty and S.W. Zehr, Trans. TMS-AIME, 242 (1968), 195.
40. A. Ball and M.M. Hutchinson, Metal Sci. J., 3 (1969) 1.
41. P.J. Martin and W.A. Backofen, Trans. A.S.M., 60 (1967), 352.
42. R.B. Nicholson, Inst. of Metallurgists Review Course (1969), 19.
43. R.H. Johnson, Design Engineering, March 1969.
44. R. Pearce and C.J. Swanson, Sheet Metal Industries, July 1970.
45. E. Gervais, P. Chollet, R. Ranger, Conference of Metallurgists, Hamilton, Ont., 1970.
46. 'Superplastic Metal', The New Jersey Zinc Company.
47. R.A. Saller and J.L. Duncan, J. Inst. Met. 99 (1971), 173.
48. T.Y.M. Al-Naib and J.L. Duncan, Int. J. Mech. Sci., 12 (1970), 463.
49. G.C. Cornfield and R.H. Johnson, Int. J. Mech. Sci., 12 (1970), 479.
50. J.F. Hubert and R.C. Kay, Design Eng. Conference, ASME, April 1971.
51. W. Johnson, J. Inst. Met. 85 (1957), 403.

A P P E N D I X I

The heaters were designed to give approximately 1.6 KW energy for every two inches of die holder length.

∴ If Mains voltage = 120 V,

Total heater resistance has to be 9 ohms.

$$\text{(Power } P = \frac{E^2}{R}$$

$$\therefore R = \frac{E^2}{P} = \frac{120^2}{1,600} = 9 \text{ ohms).}$$

This was achieved by double winding 0.020 inch dia., 1.49 ohm/ft. nichrome resistance wire around the die holder.

O.D. of the holder after first coat of insulating cement

= 10 inches.

∴ Circumference = 2.68 ft.

4.5 turns (pitch .49 inch per turn) require 12 ft. wire with a total resistance of 18 ohms.

Two such windings connected in parallel yield the desired resistance of 9 ohms.

A P P E N D I X II

Billet size required for smaller cups

Length of cup	=	3.875 in.
Thickness of base	=	0.100 in.
I.D.	=	2.000 in.
O.D.	=	2.132 in.
Flange	=	0.5 in. wide, 0.040 in. thick

Volume of material required =

$$\frac{\pi \times 0.100^2}{4} + \frac{\pi \times 3.775}{4} (2.132^2 - 2.000^2) +$$

(base) (walls)

$$\frac{\pi \times 0.040}{4} (3.132^2 - 2.132^2)$$

(flange)

$$= 2.121 \text{ cu. in.}$$

Billet dia. = 2.125 in.

$$\therefore \text{ Cross-section area } = 3.5461 \text{ sq. in.}$$

$$\therefore \text{ Billet length required } = \frac{2.121}{3.546} = \underline{0.59 \text{ in.}}$$

Billet size for longer cups

$$\text{Additional 1.6 in. length requires } \frac{\pi \times 1.6}{4} (2.132^2 - 2.000^2)$$

$$= 0.921 \text{ cu.in.}$$

$$\text{Additional billet length} = 0.26 \text{ in.}$$

$$\therefore \text{ Total billet length} = \underline{0.85 \text{ in.}}$$

A P P E N D I X III

As Cast, Set 1 (All Tests At 250°C)

Test 1, Load 30,000 lbs.

Time (sec.)	Displacement (thousandths of inch)	Time	Displacement
0	0	900	307
60	27	960	325
120	59	1020	342
180	71	1080	359
240	86	1140	375
300	104	1200	391
360	123	1260	406
420	144	1320	420
480	166	1380	435
540	188	1440	449
600	209	1500	462
660	231	1560	469
720	251	1620	475
780	270	1680	480
840	289		

Test 2, Load 50,000 lbs.

Time	Displacement	Time	Displacement
0	0	390	363
30	36	420	379
60	57	450	412
90	67	480	453
120	82	510	469
150	100	540	478
180	123	570	488
210	153	600	497
240	184	630	506
270	221	660	511
300	258	690	516
330	293	720	520
360	329	750	522

Test 3, Load 75,000 lbs.

Time	Displacement	Time	Displacement
0	0	105	455
15	40	120	467
30	100	135	472
45	187	150	475
60	270	165	478
75	345	180	480
90	430		

Test 4, Load 100,000 lbs.

Time	Displacement	Time	Displacement
0	0	75	480
15	230	90	483
30	450	105	485
45	470	120	487
60	476	135	489
		150	490

Test 5, Load 125,000 lbs.

No readings could be taken as extrusion took less than 15 seconds after the required load was reached.

As Cast, Set 2 (All Tests At 50°c)

Test 1, Load 60,000 lbs.

Time (secs.)	Displacement (thousandths of inch)	Time	Displacement
0	0	270	488
15	9	285	510
30	23	300	532
45	44	315	548
60	71	330	569
75	103	345	585
90	137	360	601
105	171	375	613
120	209	390	620
135	240	405	626
150	274	420	631
165	306	435	635
180	337	450	639
195	364	465	643
210	391	480	646
225	418	495	649
240	442	510	651
255	466		

Test 2, Load 50,000 lbs.

Time	Displacement	Time	Displacement
0	0	300	372
30	15	330	412
60	32	360	447
90	60	390	480
120	105	420	508
150	150	450	534
180	194	480	550
210	238	510	555
240	283	540	559
270	328		

Test 3, Load 75,000 lbs.

Time	Displacement	Time	Displacement
0	0	210	610
60	200	240	616
90	340	270	621
120	475	300	624
150	545		

Test 4, Load 100,000 lbs.

Time	Displacement	Time	Displacement
0	0	105	704
15	230	120	708
30	447	135	711
45	630	150	714
60	672	165	717
75	689	180	719
90	698	195	720

Test 5, Load 30,000 lbs.

Test abandoned as the initial deformation was too low --
less than 0.010 inch per minute.

Heat Treated, Set 1 (All tests at 250°C)

Test 1, Load 30,000 lbs.

Time	Displacement	Time	Displacement
0	0	1200	268
60	18	1320	298
120	41	1440	326
240	60	1560	353
360	78	1680	381
480	99	1800	407
600	122	1920	432
720	148	2040	456
840	177	2160	470
960	208	2280	483
1080	238	2400	492

Test 2, Load 50,000 lbs.

Time	Displacement	Time	Displacement
0	0	390	286
30	44	420	306
60	58	450	325
90	74	480	342
120	92	510	360
150	113	540	377
180	136	570	395
210	160	600	411
240	181	630	425
270	204	660	435
300	226	690	444
330	247	720	451
360	267	750	456

Test 3, Load 75,000 lbs.

Time	Displacement	Time	Displacement
0	0	180	581
30	180	210	586
60	290	240	590
90	430	270	594
120	540	300	596
150	573		

Test 4, 100,000 lbs. load

Time	Displacement	Time	Displacement
0	0	75	478
15	140	90	482
30	283	105	484
45	363	120	486
60	475	135	485

Heat Treated, Set 2 (All Tests At 250°C)

Test 1, Load 50,000 lbs.

Time (secs.)	Displacement (thousandths of inch)	Time	Displacement
0	0	225	310
15	47	240	340
30	59	255	371
45	65	270	398
60	71	285	427
75	80	300	453
90	90	315	482
105	104	330	506
120	120	345	522
135	141	360	536
150	167	375	548
165	184	390	559
180	222	405	564
195	252	420	567
210	283	435	570

Test 2, Load 60,000 lbs.

Time	Displacement	Time	Displacement
0	0	150	372
15	43	165	424
30	53	180	473
45	70	195	503
60	87	210	521
75	133	225	530
90	173	240	536
105	220	255	539
120	271	270	542
135	328		

Test 3, Load 100,000 lbs.

Time	Displacement	Time	Displacement
0	0	60	655
10	280	75	660
20	570	90	663
30	635	105	665
40	647	120	666
50	651		

Test 4, Load 125,000 lbs

No readings could be taken. Deformation took less than 15 seconds.

Heat Treated Set 3 (All Tests At 250°C)

Test 1, Load 40,000 lbs

Time (secs.)	Displacement (thousandths of inch)	Time	Displacement
0	0	390	409
30	15	420	444
60	36	450	478
90	60	480	512
120	92	510	544
150	127	540	572
180	163	570	595
210	197	600	618
240	233	630	631
270	271	660	640
300	307	690	646
330	342	720	651
360	376	750	654

Test 2, Load 50,000 lbs

Time	Displacement	Time	Displacement
0	0	135	625
15	40	150	679
30	74	165	704
45	135	180	720
60	215	195	732
75	303	210	739
90	385	225	745
105	472	240	750
120	550	255	754

Test 3, Load 60,000

Time	Displacement	Time	Displacement
0	0	105	714
15	60	120	718
30	220	135	721
45	465	150	724
60	660	165	727
90	692	180	728

Test 4, Load 70,000 lbs.

Time	Displacement	Time	Displacement
0	0	75	723
15	130	90	729
30	410	105	734
45	680	120	737
60	712		

Test 5, Load 80,000 lbs.

Complete deformation took less than 10 seconds and hence no readings could be taken.

Heat Treated Set 4 (All Tests At 250°C)

Test 1, Load 30,000 lbs.

Time (secs.)	Displacement (thousandths of inch)	Time	Displacement
0	0	180	496
15	65	195	515
30	130	210	532
45	192	225	547
60	245	240	561
75	290	255	575
90	329	270	589
105	365	285	601
120	398	300	612
135	425	315	622
150	450	330	628
165	475	345	632

Test 2, Load 50,000 lbs.

Time	Displacement	Time	Displacement
0	0	40	880
10	110	50	1015
20	410	60	1055
30	610		
